ENHANCEMENT OF TURBIDIMETER PERFORMANCE WITH OPTICAL FIBER, GRIN LENSES, AND DIODE LASERS

by

Berthold Heinrich Habicher

A thesis

presented to the University of Waterloo

in fulfilment of the

thesis requirement for the degree of

Master of Applied Science

in

Mechanical Engineering

Waterloo, Ontario, Canada, 1996

Borrower's page

The University of Waterloo requires the signature of all persons using or photocopying this thesis. Please sign below, and give address and date.

Abstract

A commercial turbidimeter, the Claritek Model SM8830 was updated by the utilization of more modern electro-optical components. Various diode lasers were tested as incident light sources with and without fiber optic collimators. These sources were tested in combination with phototransistor, photodiode and a light intensity-to-frequency converter integrated circuit detectors. The integrated circuit detector and photodiode were tested with and without a multiple fiber light guide. Testing consisted of correlating the detector response to an incrementally changing concentration of diatomaceous earth slurry. Results are presented as graphs of detector response vs. slurry concentration. The best performance was realized with a 10 mW diode laser fitted with a multimode fiber collimator in combination with the light intensity-to-frequency converter I.C. fitted with a multiple fiber light guide. These component subassemblies were used in constructing a prototype sensing head suitable for adaptation to the model SM8830 suspended solids monitor.

Acknowledgements

I would like to acknowledge my supervisors Professors Hugh Martin and Professor Peter Silveston for their support and assistance. Ms. Marguarite Knechtel for her assistance in compiling this work. Mr. Wolfgang Habicher for his critique and editing. My loving wife, Elizabeth, for her steadfast support and relentless encouragement.

This work was supported by a contract from B&P Silveston, Engineers, using funds granted to Arjay Instrument Company by the Industrial Research Assistance Program of the National Research Council of Canada.

Dedication

This work is dedicated to the father of my wife, John Suggitt, whose ability to remain technologically current is an inspiration to me.

TABLE OF CONTENTS

List of Tables

List of Figures

continued...

CHAPTER 1

Introduction

The current climate of environmental awareness has resulted in an unprecedented demand for instrumentation to monitor the performance of pollution control equipment. Turbidimeters and nephelometers have often been used to quantify the behaviour of sewage treatment plants and other clarifying operations. To satisfy this demand, Claritek Instrument Co. was established to develop and manufacture an optical suspended solids measuring device, the Claritek monitor.

There are two distinct, although related, techniques used for the optical determination of liquid-borne suspended solids: turbidimetry and nephelometry (1,2,3). Turbidimetry provides a measure of the suspended solids concentration by the degree of extinction of a beam of light projected through a sample or stream. Nephelometry measures the suspended solids concentration as a function of the intensity of the light scattered from the incident beam by particles in the sample or stream.

In their simplest forms, these instruments consist of a light source, a sample, a series of standards, and a detector. The Jackson Turbidimeter (4) used a candle as a light source, and a human observer as a detector. The Claritek monitor (5,6) used a light emitting diode (LED) as a light source and a phototransistor as a detector. This instrument was microprocessor-controlled, used a stored, programmable calibration curve, had compensation for ambient illumination, and data-logging capability.

The focus of this development project was to identify and correct opto-mechanical deficiencies of the Claritek monitor while increasing its nephelo-turbidometric range. The program consisted of identifying optical components which would provide the desired performance, isolate those which would be cost-effective, and designing and constructing a prototype.

Secondary objectives were to identify other applications to which the instrument could be adapted, and to consider other instrument configurations for the current application.

1.1 Claritek SM-8830 Suspended Solids Monitor

The Claritek suspended solids monitor was designed to measure suspended solids concentrations in water-based process streams. The instrument was made up of the transmitter enclosure, and the sensor assembly. The transmitter enclosure contained all of the control, signal processing, and data-logging circuitry. The sensor assembly contained the incident light source, detectors, and lens flushing system (see Fig. 1.1). The incident light source, contained within a waterproof enclosure in the sensing head, was a 100 mA, 940 nm infrared light emitting diode (LED) (7).

The detectors, mounted within similar enclosures, were photo transistors fitted with infrared-pass filters, Skanamatic part P33014. The LED and extinction (turbidimetric) detector were mounted facing each other on a horizontal axis transverse to the monitored flow direction, giving an optical path length of 100 mm. The nephelometric detector was mounted 25 mm above, and its axis perpendicular to, the midpoint of the turbidimetric

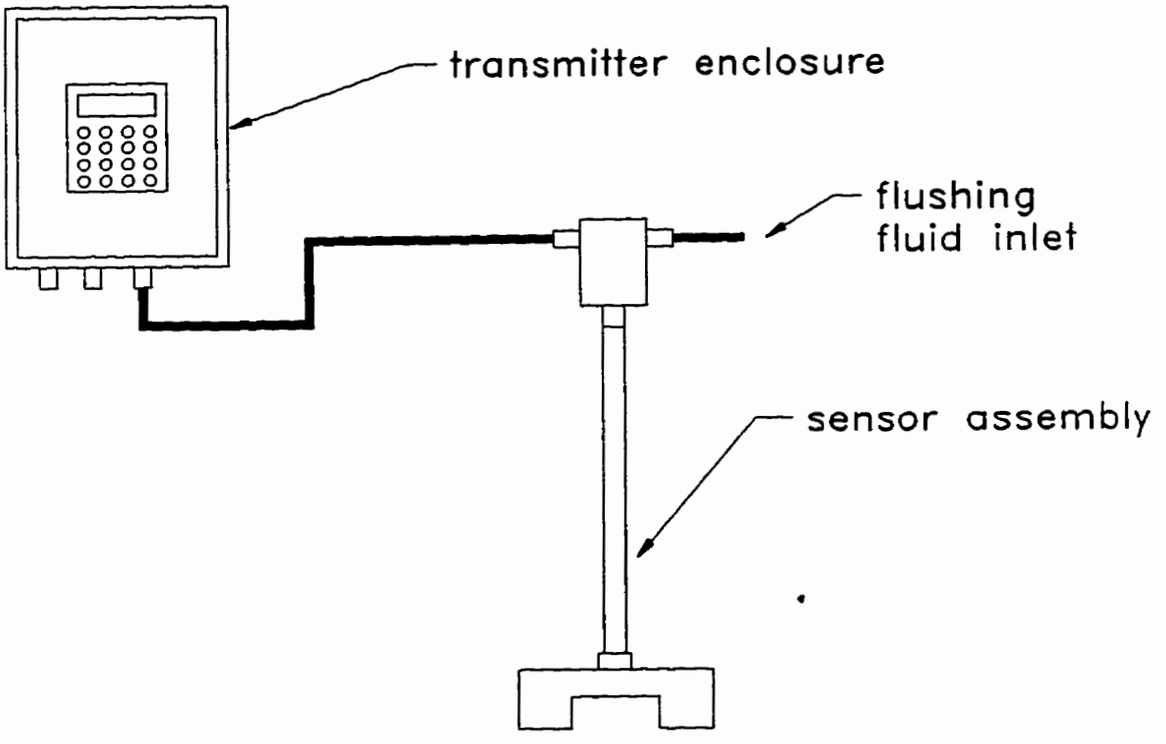

Figure 1.1: Block Diagram of SM8830 Suspended Solids Monitor

optical path. The windows to the component enclosures were kept clean by the action of flushing jets of clear water or process fluid directed downstream across the faces of the windows (see Fig.1.2).

Typically, the instrument was operated from a membrane keypad with a four line, twenty characters per line, liquid crystal display. Other outputs were a serial port, a scalable 4-20 mA output, and a variable setpoint relay closure.

To begin operation of the instrument, calibration was required. If the specific application used the 4-20 mA output, the desired zero and span could be programmed. Similarly, the conditions for the relay closure could be programmed. The instrument could be calibrated by immersing the sensing head in process fluids of known solids concentration. Alternatively, with the sensing head installed in the process, the instrument could be calibrated by sampling the process stream.

The marketing effort for the device was directed toward industries which produced, monitored, or consumed water containing suspended solids. These potential applications occurred in the metals sector (mining, ore beneficiation, smelting, and forming), water-, and waste-water treatment, pulp and paper, food and beverage, petroleum, and chemical industries.

1.2 Opto-mechanical Shortcomings of the Claritek Monitor

The performance and service life of the Claritek Monitor did not live up to expectations. In service, the nephelometric function was unusable. Furthermore, the range of the instrument was considerably smaller than expected (0 to 400 Jackson Turbidity Units).

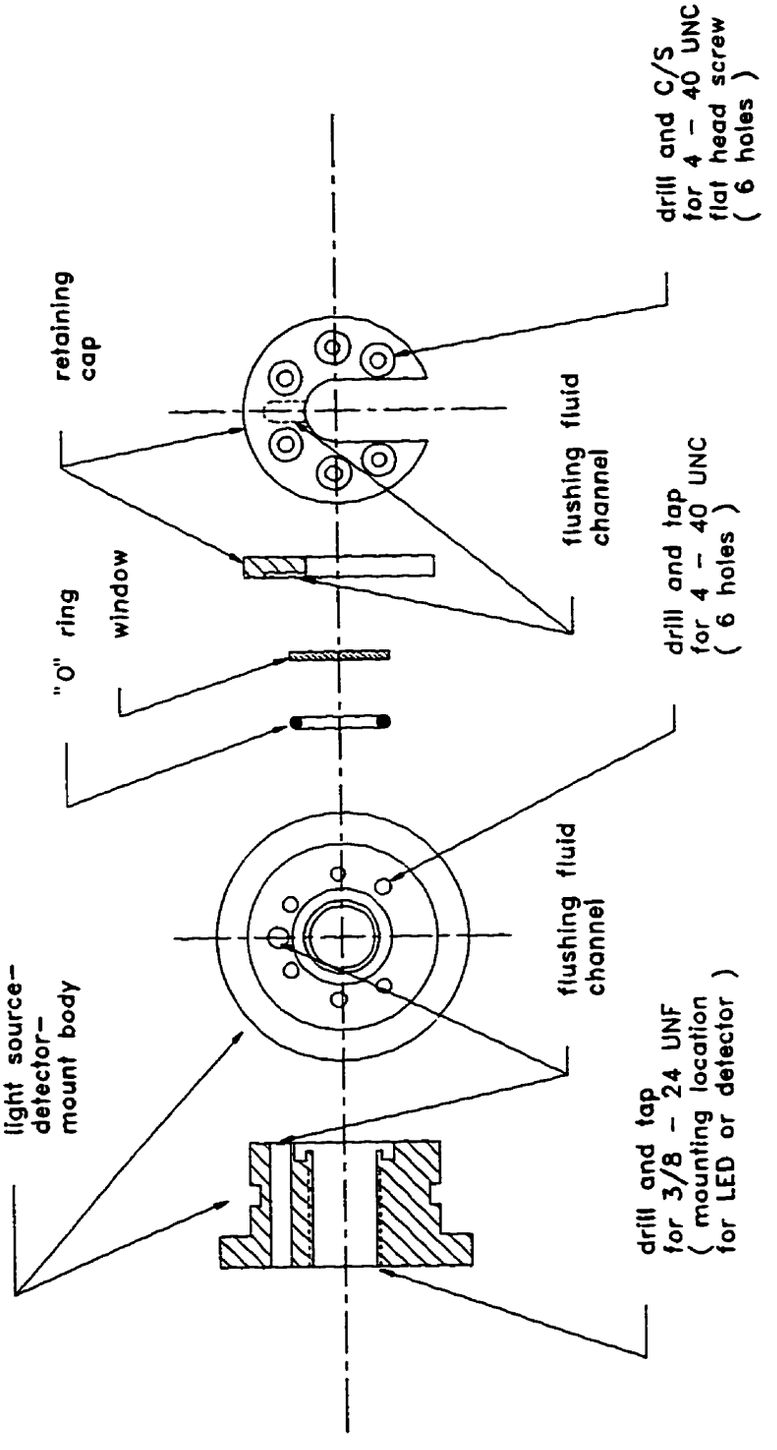

Figure 1.2a: Flushing Insert Components

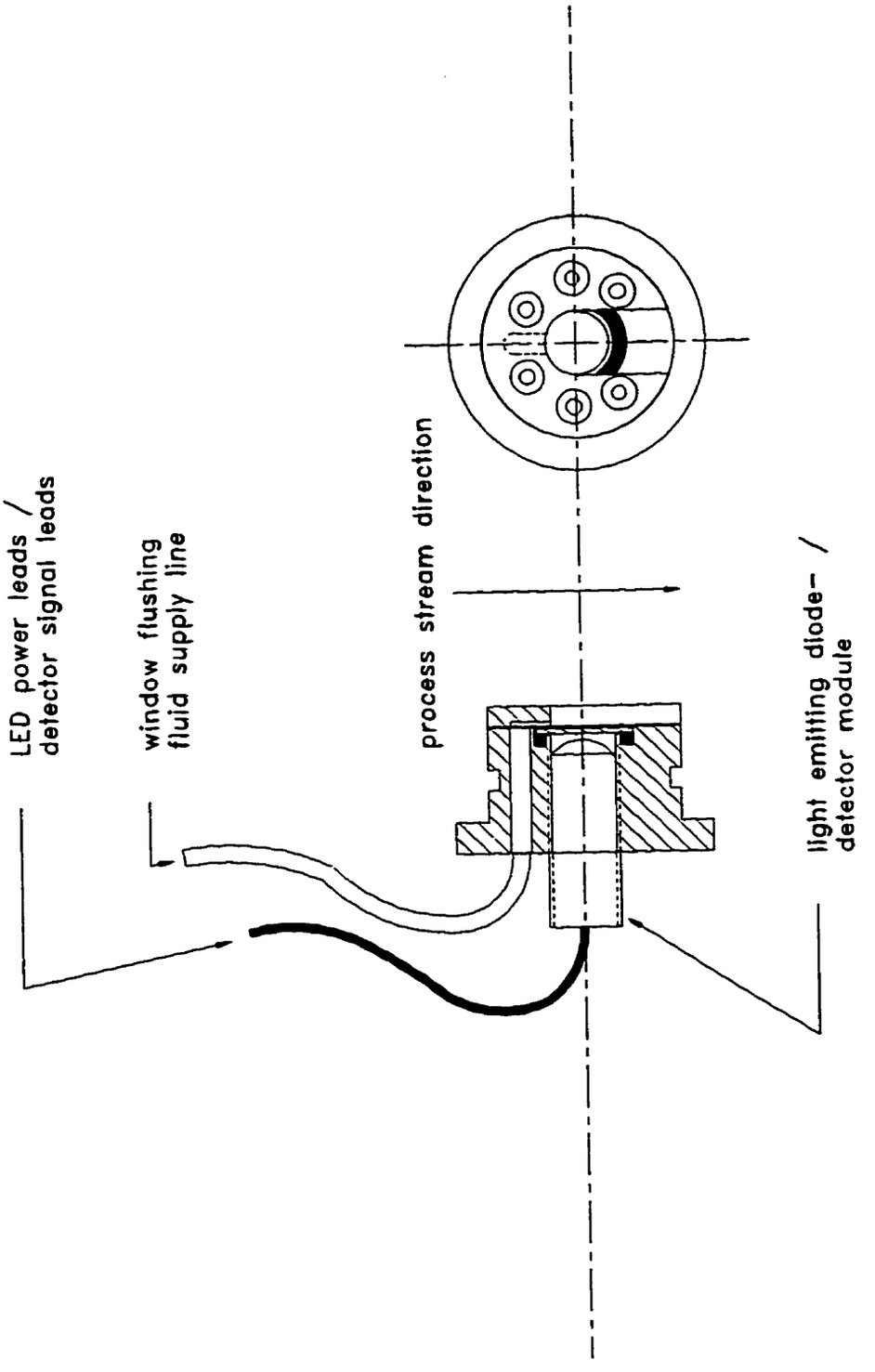

Figure 1.2b: Flushing Insert Assembly

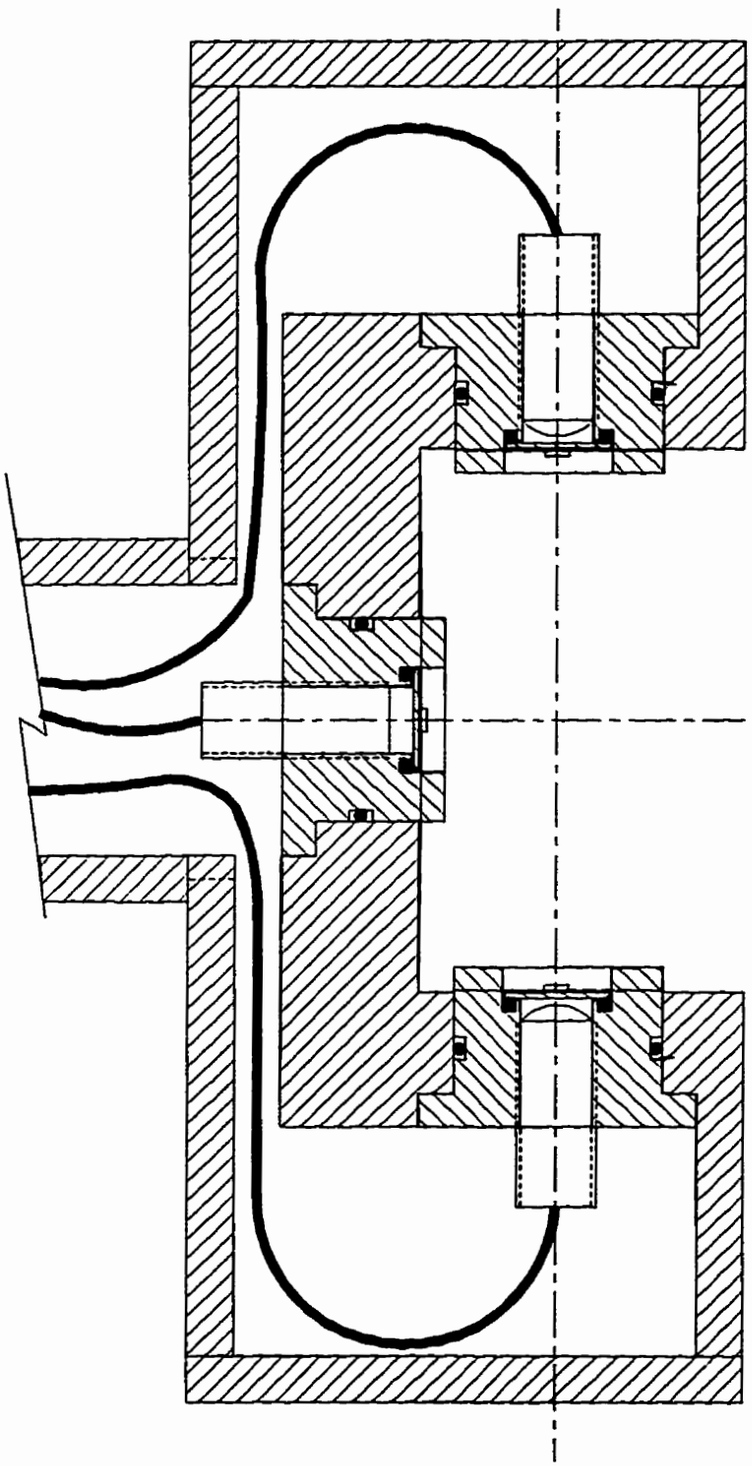

Figure 1.2c: Sectioned View of Sensing Head (showing location of inserts; fluid supply line omitted for clarity)

Frequent repairs were required for the effects of moisture on the incident light source and detector. Although the opto-electronic components were contained within water tight enclosures, small amounts of moisture still accumulated in these cavities. The moisture damage manifested itself in three ways: corrosion of the component housing, short circuiting of the components, and impairment of the component lenses by condensation and deposition of corrosion products. Although the corrosion and electrical problems could be resolved by sealing the components, the impairment of the optics by condensation was a more intractable problem.

The cause of the reduction in operating range of the instrument was not determined until the components were evaluated for performance characteristics as part of the redevelopment process. At that time it was determined that the optical system of the opto-electronic components suffered from a form of "tunnel vision" which reduced both the incident beam intensity and detector sensitivity. The cause of loss of the nephelometric function was not specifically determined, but could be the result of any of the above- mentioned phenomena.

1.3 Problem Statement

To overcome the deficiencies in the Claritek Monitor, a program to re-engineer the sensing head was instituted. *The mandate of this program was to redesign the opto-electronics of the sensing head for reliability and ease of service, and to incorporate any technological advancements which were cost-effective. The specific technical objectives (8) were to: 1) increase the range of the instrument from 5 - 200 Jackson Turbidity Units*

to 0 - 2000 Jackson Turbidity Units; 2) improve the accuracy of the instrument from 5% of the calibrated range to 1%; 3) use a semiconductor laser of wavelength less than 750 nanometers as the incident light source; and 4) use optical fiber to transmit the signal to and from the sensing head. The major design constraint on this program was the requirement that modifications to the sensing head envelope be minimized.

The proposed solution consisted of three phases of development. Initially, the consideration and testing of brighter incident light sources and more responsive photodetectors; subsequently, the use of more robust and technically superior optical components; and finally, the adaptation of the opto-electronic subassemblies to the sensing head.

For the initial stage of development, the use of laser diodes and silicon photodiodes would be investigated. Diode lasers are not only more intense than LEDs, they generally incorporate sensing components which, in conjunction with most common drive circuits, allow the laser to be operated at constant optical output. The net result would be an incident light source with an increased useful life. Silicon photodiodes have a more linear response with regard to illumination than phototransistors.

The second phase of development would be concerned with improving the performance of the optical components. The use of fiber optic components and gradient index lenses would be considered. The primary electronic weakness and service problem of having submerged electronic components could be eliminated by removing them from the detector head and routing the optical signal with fiber optics. Transmitting the incident beam, and attenuated light signal via optical fiber would allow the light source and

detector to be mounted on the signal processing board, thus reducing the source of electro-magnetic interference. In addition, the optical fiber subassemblies should be maintenance-free when installed, and would allow servicing of the incident light source and detector at the signal processing board with the unit in place.

The primary optical/mechanical weakness could be eliminated by replacing conventional spherical lenses with gradient index (GRIN) lenses. Conventional spherical lenses depend upon differences in refractive index between two media to function. Generally the two media are air and glass. The required air gap with a conventional lens creates an intrinsic water vapour sink which becomes a source of condensation if the optical assembly is cooled. Gradient index (GRIN) lenses (9), as their name implies, have a refractive index which has a radial gradient (see Fig. 1.3); thus, the bending of light occurs within the lens, eliminating the need for a void or air space.

In the final stage of the program, the incident source and detector subassemblies developed previously would be adapted to the sensing head of the instrument to produce the prototype. This would consist of designing inserts to support the terminal optics of the source and detector subassemblies within the sensing head.

Therefore, this work documents the method and result of a program to update an instrument made obsolete by encroaching technologies. The evaluation of likely photo-electronic components, the design and testing of photo-electronic subassemblies, and the adaptation of the selected subassemblies to the existing envelope, are detailed herein.

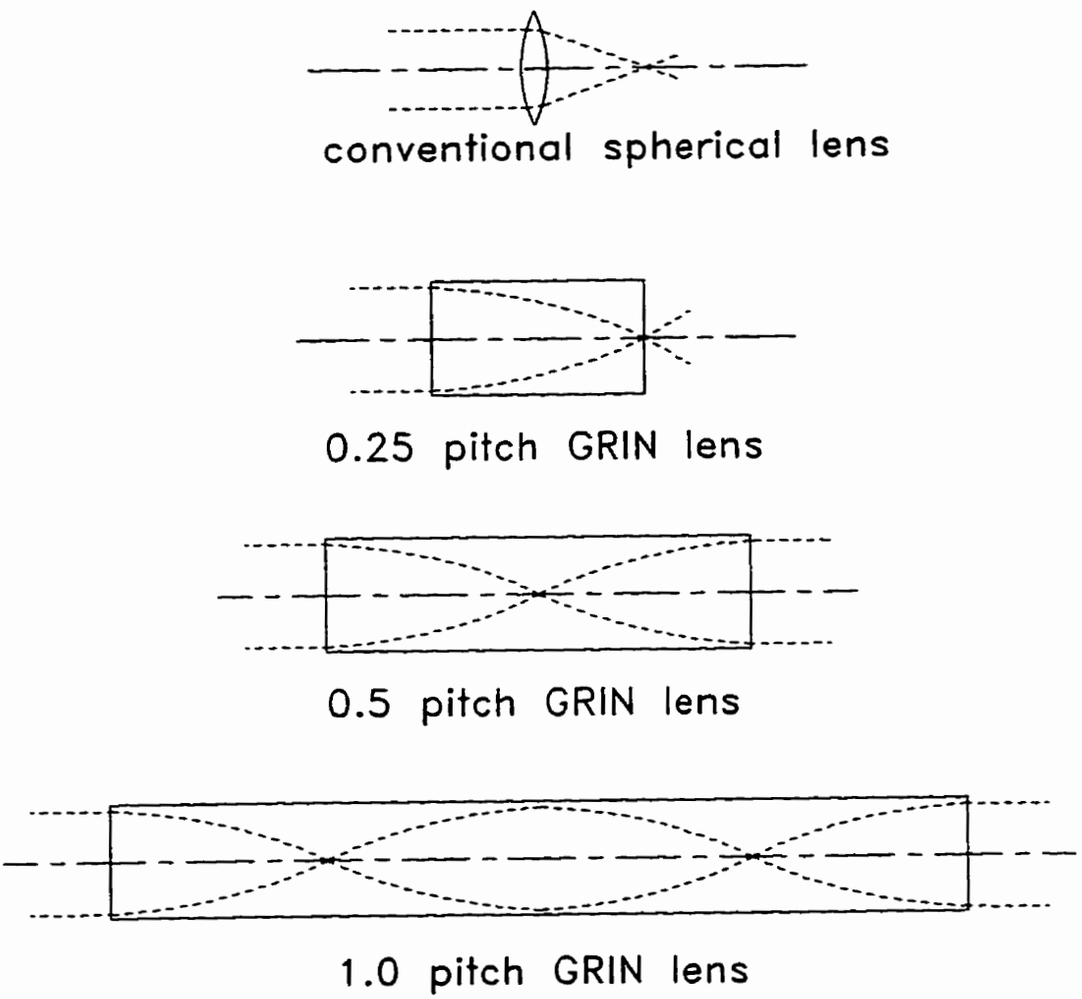

Figure 1.3: Ray Trace Through Spherical Lens and Gradient Index Lens

CHAPTER 2

Theoretical Considerations and Historical Perspective

This chapter provides an overview of the mechanisms involved in, and historical applications of, optical turbidimetry.

2.1 The Principle of Operation of Optical Components

2.1.1 Diode Lasers

LASER : Light Amplification by Stimulated Emission of Radiation (10, 11, 12)

Matter is made up of discrete particles: molecules, atoms and fragments thereof. The theory of quantum mechanics dictates that these particles exist at discrete energy levels related to the vibrational state of the electrons and nuclei of the particles. The lowest energy level is referred to as the ground state, all others are excited states.

Transitions between energy levels are accompanied by the absorption or release of energy. Certain electron energy transitions, termed optical transitions, are accompanied by the absorption or emission of light. There are three types of optical transitions: absorption, in which a passing photon of the correct frequency excites an electron to a higher energy level, thereby annihilating the photon; spontaneous emission, where an excited electron reverts to a lower energy state, thereby emitting a photon; stimulated emission, which results from a passing photon of the correct frequency perturbing an excited electron, causing it to revert to a lower energy state while emitting a photon with the same frequency, phase, and polarization as the perturbing photon. Stimulated emission is the fundamental process utilized in all laser action.

An additional requirement for laser action is the "population inversion". This unstable condition occurs in a medium involving electron transitions when the population of excited electrons exceeds those in the ground state. The effect of this condition is to dramatically increase the probability of a stimulated emission and reduced probability of absorption resulting in light amplification. A continuous wave laser would place the laser media in a resonant cavity, for example, between two mirrors such that the multiple reflections would increase the probability of stimulated emissions. A pulsed laser may have a separate source for the "stimulating" photons, or alternatively, be constructed similarly to a continuous wave laser but contain a switchable absorptive element between the laser medium and mirror to trap spontaneous emissions.

In a semiconductor, a crystalline solid, the electrons can be considerably more delocalized than in a discrete atom or small molecule. As a result a large population of electrons exists with very similar energy levels. These energy levels may be grouped as pseudo-continuous energy bands, and may be treated as a bulk property of the material. The electron population of a solid may be distributed over three energy bands: the "filled" band, the valence band, and the conduction band. The "filled" band electrons have the lowest energy and are the inner electrons of the constituent atoms. The valence band electrons are those associated with the inter-atomic bonds and as such are somewhat delocalized with respect to specific atoms. The conduction band electrons may be considered to be in an excited, or higher energy, state than the valence band electrons, and are highly delocalized. The energy difference between the valence band and conduction band is the band gap. Insulators have large band gaps, conductors have zero

band gaps, and semi-conductors have small band gaps.

The band gap of a simple semiconductor, for example silicon, can be modified by the inclusion of impurities from the group IIIa and group Va elements of the periodic table. This process, referred to as doping, produces a surplus of vacant electron sites or holes when doped with group IIIa elements. If the semiconductor is doped with a group Va element, the lattice contains a surplus of electrons. Semiconductors with a surplus of holes are called p-type; those with a surplus of electrons are called n-type. These electrons and holes are quite mobile at normal temperatures and act as negative and positive charge carriers, respectively. The more important photoactive semiconductors are generally ternary or quaternary compounds of aluminum, gallium, indium, nitrogen, phosphorus, arsenic, and antimony.

The joining of a p-type semiconductor to an n-type semiconductor produces the ubiquitous semiconductor p-n junction, the basis of all semiconductor devices such as diodes and transistors. At the p-n junction, the electrons from the n-type material combine with "holes" from the p-type material, creating a depletion zone of charge carriers in the immediate vicinity of the junction. Applying a voltage (forward biased: p-type, positive; n-type, negative) across the p-n junction supplies electrons and "holes" to the depletion zone where the electrons relax from the excited state (i.e., the electrons combine with the "holes") accompanied by the spontaneous emission of a photon. This is the operating principle of a light emitting diode (LED).

To construct a semiconductor laser, two other criteria must be satisfied: the requirement for a population inversion, and a resonant cavity. To achieve a population

inversion in the junction requires a current in excess of that capable of being consumed by the spontaneous emission process. This relatively high current requires that the semiconductor material be sufficiently well-doped to provide the requisite concentration of charge carriers. To produce a resonant cavity would require two parallel mirrors normal to one axis of the plane of the p-n junction. In the case of semiconductors, their refractive index is high enough to form reflective surfaces at air/semiconductor interfaces. In many cases the cleaved surface of the semiconductor wafer is smooth enough to produce an effective resonant cavity.

The band gap of the semiconductor will determine the frequency of the laser by the relationship

$$\nu = \Delta E/h$$

where ν = frequency of light

ΔE = energy of band gap

h = Planck's constant

Many low-power diode lasers are packaged with a diode photodetector. This device uses the light radiating from the back facet (light radiates from both mirrors of the laser diode, but only one is normally used as a light source) of the laser to produce a signal in proportion to the laser output. This signal is commonly used to provide a feedback signal to the power supply for controlling the optical output of the laser.

The predominant failure mechanisms for diode lasers are thermal in nature. Two

heat sources operate in the diode laser, resistive heating and reabsorption of the light. Degradation of performance results from gradual accumulation of crystalline defects in the junction region. These defects tend to produce internal heat instead of emitted photons. The principal cause of catastrophic failure is current spikes which create thermal pulses in excess of the heat dissipation capability of the semiconductor material. Therefore, temperature and current control are the critical factors which determine the life of diode lasers.

The output of a diode laser suffers from a number of optical aberrations not found in other types of lasers. These aberrations must be corrected to generate the circular, collimated beam typically expected of a "laser beam". The output of a diode laser is asymmetrically divergent and astigmatic. The asymmetry of the output is a direct result of the comparable asymmetry of the junction area of the diode, which is typically 0.1 micrometer thick versus 5 micrometers wide. In the plane of the junction the half angle of divergence may range from 2 to 15 degrees. In the plane normal to the active layer the divergence may be as great as 45 degrees. The astigmatism of the output beam manifests itself as a difference in the apparent point of origin of that beam component normal to the plane of the junction relative to the component in the plane of the junction. In the plane of the junction, the point of origin appears to be 5 to 50 micrometers inside the surface of the diode. In the plane normal to the plane of the junction, the point of origin appears to be on the end facet of the diode. Astigmatism can be corrected by a weak cylindrical lens, and the asymmetry by an aspherical lens.

2.1.2 Photodetectors

Photodetectors are opto-electronic devices which respond in a predictable fashion to light intensity by producing an electrical signal (13, 14, 15).

In a manner analogous to the LED, a photodetector consists of a p-n junction in which the band gap of the semiconductors used corresponds to the wave-length of light to be detected. The detector will then respond to photons with energy levels greater than that required to excite electrons from the valence band to the conduction band.

Recall from the previous section that the construction of a p-n junction results in a zone depleted of charge carriers immediately adjacent to the junction. The application of a reverse-bias (n-type: positive; p-type: negative) voltage to the junction further depletes the semiconductor of charge carriers. In the absence of light, the lack of charge carriers prevents current from passing through the junction. Light of suitable wavelength striking the junction region excites electrons to the conduction band, creating an electron/hole pair which separates, with each charge carrier migrating into its respective respective region, causing a current to flow. The magnitude of the current is directly proportional to the number of photons, ie. the light intensity impinging on the p-n junction.

2.1.3 Optical Fiber

The principle underlying the light-guiding function of optical fiber is total internal reflection (11, 16, 17). It has been demonstrated that the speed of light in vacuum is approximately 300,000 kilometers per second. In any other medium, the speed of light is

reduced. This change in speed is responsible for the bending of non-perpendicular light rays at the interface between two transmissive media (the ray normal to the plane of the interface is not bent). This phenomenon is known as refraction. The refractive index of a material is defined as the ratio of the speed of light in vacuum to the speed of light in that material.

Table 1: Representative Indices of Refraction (11, 18)

	n_D
vacuum	1.0
air	1.003
water	1.333
fused quartz	1.458
rock salt (NaCl)	1.516
crown glass	1.520
heavy flint glass	1.650
diamond	2.417

The relationship between the angles of refraction and refractive indices is expressed by Snell's Law:

$$n_1 \sin \theta_1 = n_2 \sin \theta_2$$

where

n_x = respective refractive index

θ_x = respective angle relative to normal of interface plane

Due to this phenomenon, a light ray passing through an interface between two media will have a greater angle in the medium of the lower refractive index as shown in Figure 2.1. Specifically, if the ray originates in the material of lower refractive index, the ray will be bent closer to the normal on entering the higher refractive index material. Conversely, if the ray originates in the higher index material, it will be bent away from the normal on entering the lower index material.

If the incident angle in the higher index material is increased to a certain value (dependent on the relative refractive indices of the materials involved), as shown in Figure 2.2, the refracted ray will form an angle of 90 degrees to the interface normal. This angle of incidence is the critical angle for this interface. Any light with an incident angle greater than the critical angle as shown in Figure 2.3 is reflected back into the higher index medium.

An optical fiber consists of a central "core" surrounded by a layer of lower index material referred to as "cladding", which in turn is covered with a protective material called the "jacket". The most common core and cladding combinations are: glass core and cladding, glass core and plastic cladding, and plastic core and cladding.

As shown in Figure 2.4, any light ray entering the fiber core at an angle less than $\theta_{in(max)}$ will be propagated along the core by the process of "perfect internal reflection". The light acceptance half-angle of an optical fiber is generally quantified as its "numerical aperture" and is defined as:

$$N.A.= \sin \theta_{in(max)} = (n_1^2 - n_2^2)^{1/2}/n_0$$

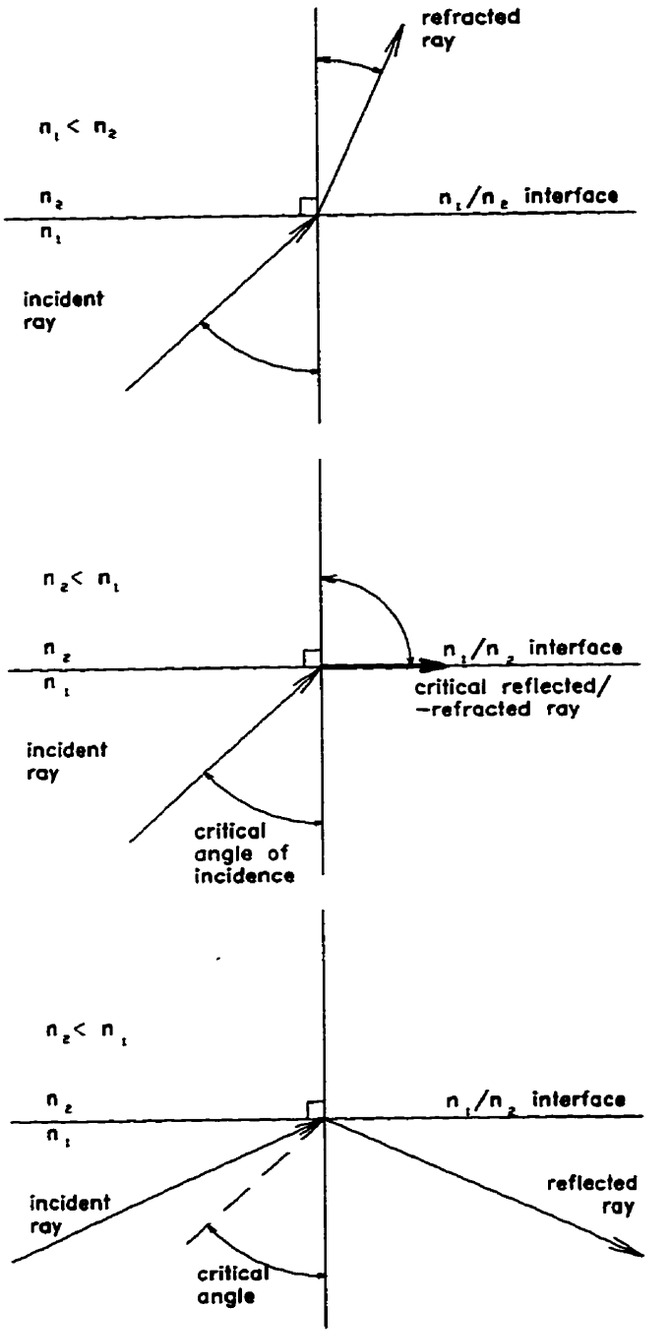

Figure 2.1: Refracted Ray

Figure 2.2: Critically Refracted Ray

Figure 2.3: Reflected Ray

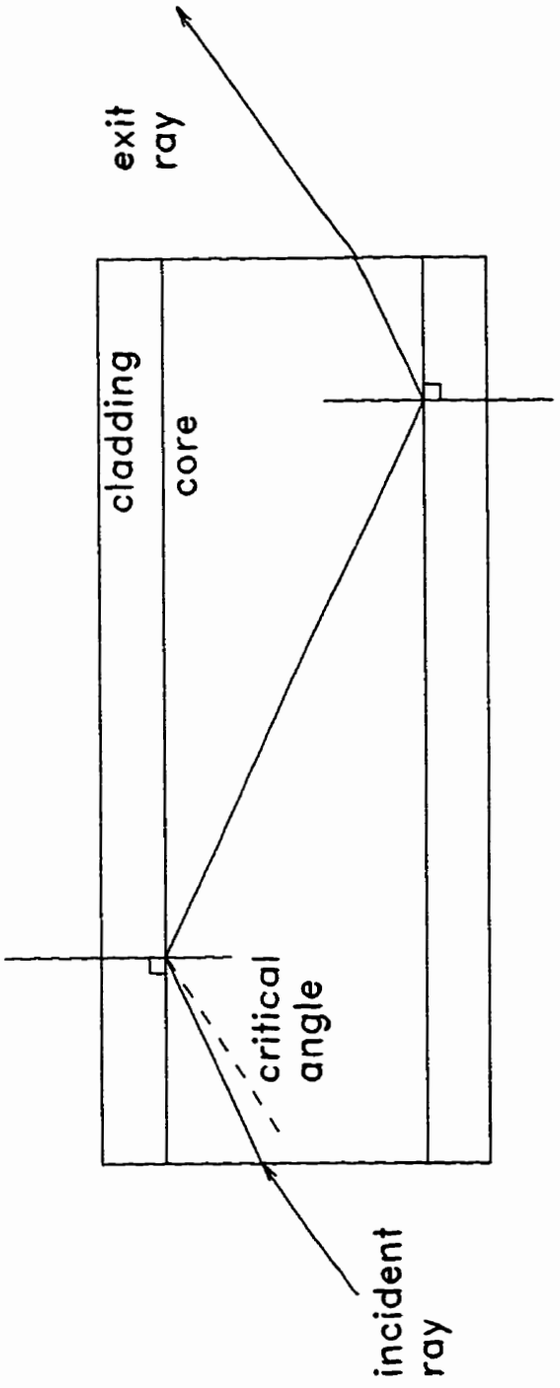

Figure 2.4: Light Propagation in Optical Fiber by Internal Reflection

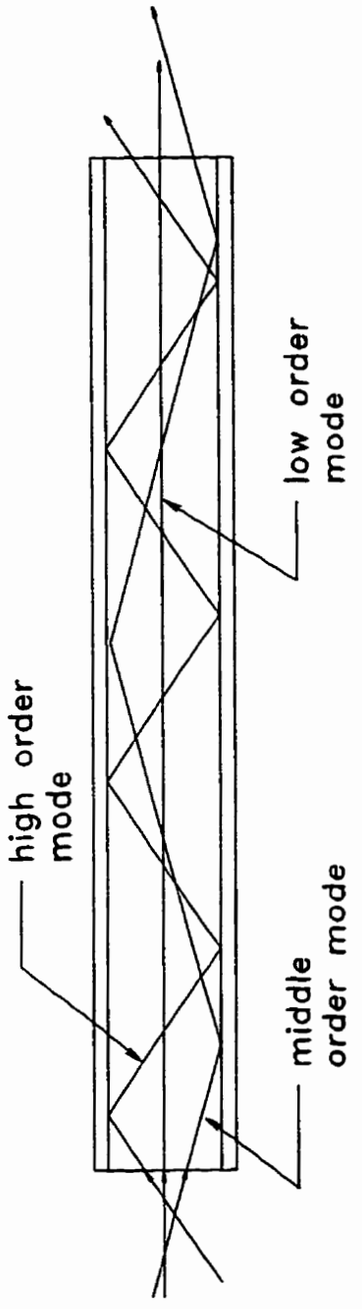

Figure 2.5: Propagation Modes in Multimode, Step Index Fiber

where

n_0 = index of launch media (= 1.000 if air)

n_1 = index of core

n_2 = index of cladding

In examining Figure 2.5, showing the two extremes and a nominal mode of propagation in a "multimode, step index" fiber, it is apparent that the path length of the higher order propagation modes is substantially greater than that of the lower order modes. As a result, the higher order modes are much more likely to be affected, or "attenuated", by surface imperfections or impurities in the fiber. If the diameter of the fiber core is extremely small (less than about ten micrometers, depending on the wave length of light), only the lowest order modes are propagated. This is referred to as "singlemode, step index fiber".

A further development is "multimode, graded index" fiber. This fiber has a parabolic index gradient which is of significance to communications applications. It can be seen in Figure 2.6 that although the high order propagation modes travel a greater distance along the core, these modes travel in regions of generally lower refractive index, where the speed of light is greater. As a result, a light pulse spread over most of the modes available will still arrive at the end of the fiber with less dispersion, or pulse spreading, than a pulse transmitted through a multimode, step index fiber.

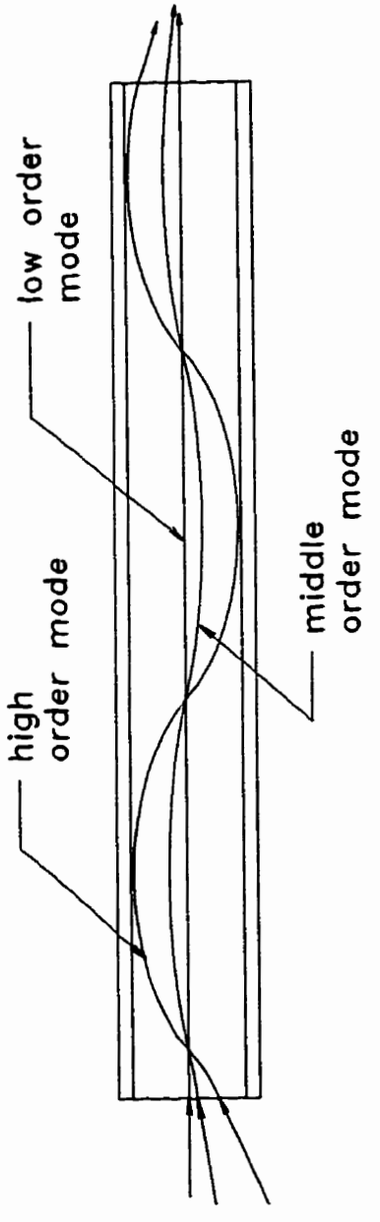

Figure 2.6: Propagation Modes in Multimode, Graded Index Fiber

2.1.4 Gradient Index Lenses

Gradient index (GRIN) lenses (9, 19) are a departure from conventional spherical lenses. Whereas conventional lenses reshape light beams by varying the angle of incidence of the constituent rays as shown in Figure 2.7, GRIN lenses reshape light beams by varying the refractive index of the medium. As shown in Figure 2.8, the index profile of a GRIN lens has a parabolic shape. A ray parallel to optical axis, striking near the lens's periphery will follow a sinusoidal path as shown in Figure 2.9.

Although the concept of focal length may be applied to GRIN lenses, the beam shaping property of these lenses is governed by their length and degree of index gradient. The beam shaping property is expressed as the "pitch" of the lens. A lens of 1.0 pitch is one of sufficient length to allow a light ray to describe one complete sinusoidal waveform. Figure 2.10 shows the effect of fractional pitch length in collimated and point source applications. Since both refractive index and the relative index gradient are wavelength-dependent, the pitch length of a lens will vary with the wavelength of light used.

2.2 An Overview of the Optical Quantitative Determination of Suspended Solids

2.2.1 Review of Turbidimeter Technology

Beginning with the standardization of the Jackson Candle Turbidimeter prior to 1900 (4) the state of Turbidimeter development has been one of constant advance.

The Jackson Candle Turbidimeter consisted of a calibrated glass tube, a standard beeswax and spermaceti candle, and a support fixture. The candle and tube were aligned

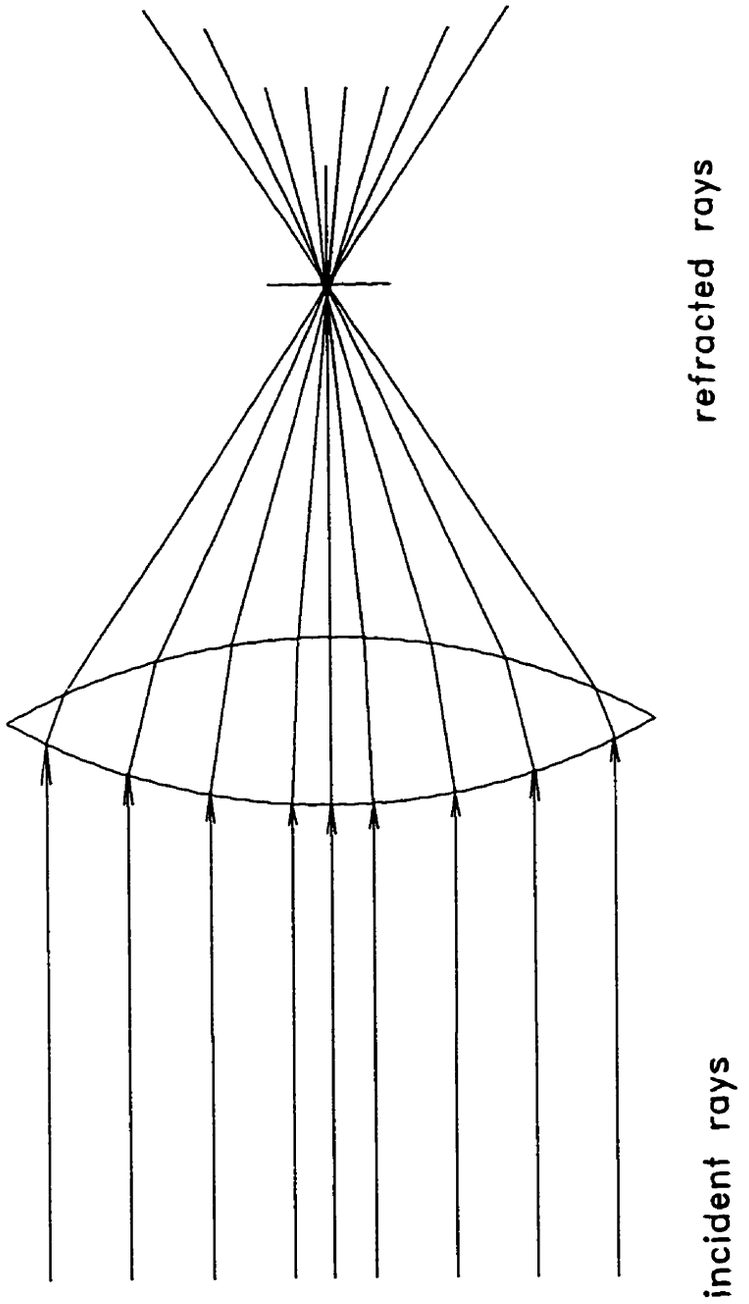

Figure 2.7: Ray Trace Through Spherical Lens

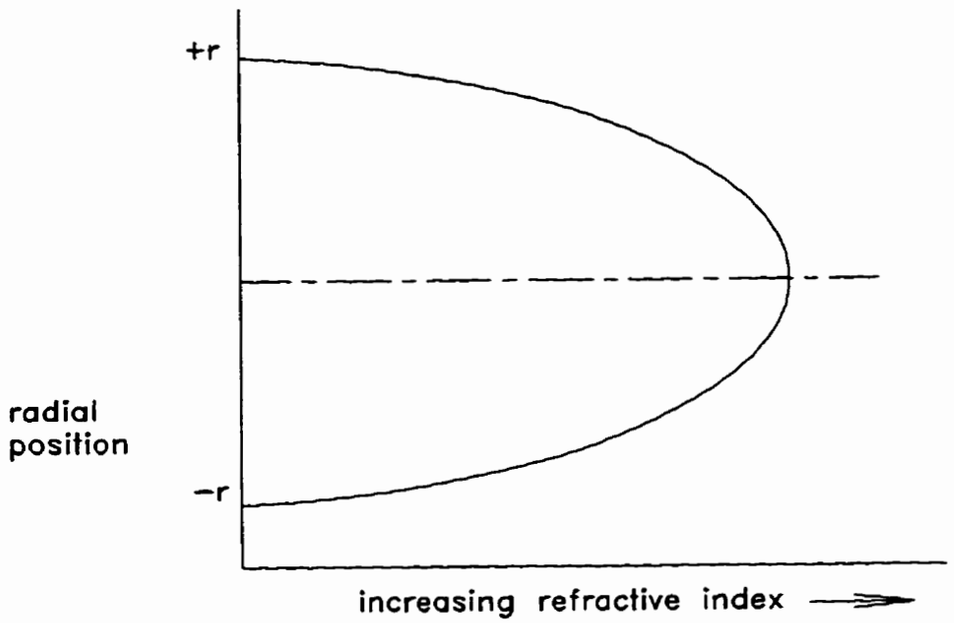

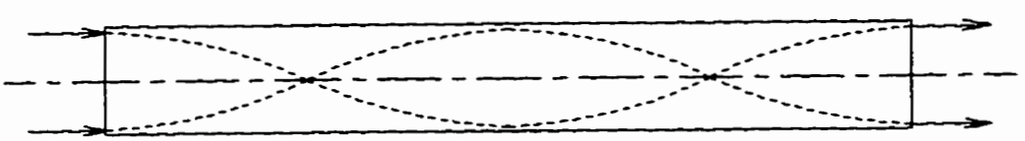

Figure 2.8: Refractive Index Profile of GRIN Lens

Figure 2.9: Ray Trace Through Grin Lens

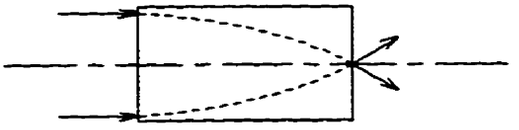

0.25 pitch GRIN lens

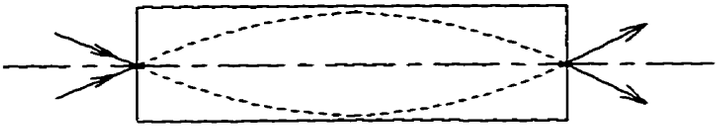

0.5 pitch GRIN lens

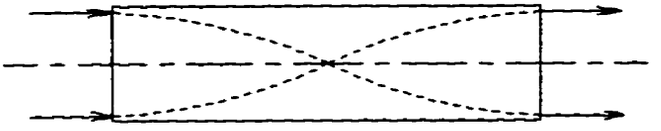

0.5 pitch GRIN lens

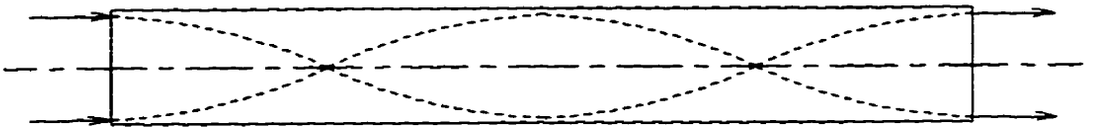

1.0 pitch GRIN lens

Figure 2.10: Ray Trace Through Fractional Pitch GRIN Lenses

on centre, with the closed bottom of the tube located 7.6 cm above the candle flame. Turbidity is determined visually by the depth of sample at which the image of the candle flame disappears from view.

The availability of fiber optics for communications purposes has led to their adaptation to suspended solids measuring instruments. Perlicki et al. (20) describe two turbidimeters for measuring suspended solids continuously and on discrete samples. These devices use He-Ne laser sources and relatively large diameter fibers. The incident light fiber, and signal collection fiber, are affixed directly onto a glass flow cell or sample cell. There are no other optical components used. There appears to be no provision for cleaning the optical surfaces. The use of optical fiber is not uncommon, Jamstnon et al. (21) and Fent et al. (22) use fibers for bringing incident light to the attenuating medium. Crowther and Dalrymple (23) describe a method of mechanically cleaning optical surfaces.

A current trend is the development of much more sophisticated instrumentation which measures light scattered from suspended particles at various angles (24, 25, 26)). This technique, more properly termed nephelometry, attempts to derive particle size data from the relationship between particle size and angle of scatter. Further attempts at refinement include the use of polarized laser light (27) and variable path length (28).

There are always conservative die-hards though: Brown et al. (29) determined the time to nucleation of calcium oxalate monohydrate in their crystallization kinetics studies by "turbidity measurement using the unaided eye". As the advance of technology makes more sophisticated materials and data analysis capability available, the mechanisms

associated with the measurement of suspended solids by attenuated (turbidity) and scattered (nephelometry) light will certainly keep pace.

2.2.2 Turbidimetric Applications

The most common applications of turbidimetry are associated with water and wastewater treatment. Aside from aesthetic considerations, Roebeck et al. (30) make a strong case relating turbidity to the presence of coliform bacteria even in heavily chlorinated waters. They suggest that these micro organisms are embedded inside suspended particles and are shielded from the sanitizer.

In this context, turbidity is used to characterize the performance of potable water treatment plants (31, 32, 33). Similarly, the performance of wastewater treatment operations is also characterized (34, 35). A related application is the monitoring of surface and coastal water quality to assess the environmental impact of human activity (36, 37, 38, 39). Turbidity has also been used to monitor and control microbial culture growth (24, 40, 41)), and the characterization of polymer solutions and reactions (42, 43, 44, 45, 46). Many reactions which result in a dispersed phase of different color or refractive index from the suspending medium are candidates for monitoring by turbidimetry.

2.2.3 Turbidimetric Standards

There are three commonly accepted turbidity standards: Formazin (47), diatomaceous earth, and more recently approved by US EPA are AMCO AEPA-1 polymer spheres (48).

Work by Pickering (49) and confirmed by Ronald et al. (50) determines that Jackson Turbidity Units (JTU) as calibrated by Formazin, are equivalent to concentration of diatomaceous earth in ppm. However, Mack (51) and several other researchers (52, 53) show that using "standards" with turbidity measurement to determine suspended solids concentration is problematic. If the nature of the particles remains constant, i.e., if the particle size distribution and particle density remain the same, determinations of suspended solids concentration by turbidimetry are valid. However, if the source, or nature, of the particulates should change, recalibration with the new material would likely be necessary.

CHAPTER 3

Experimental Methodology

The redesign of the Claritek Monitor proceeded through a series of steps. These can be described as: conceptualization of testing method, design and construction of test rig, test and evaluation of electro-optic components relative to current Claritek monitor components, development of incident light source subassembly, development of detector subassembly, and fabrication of prototype.

3.1 Testing Method

The redesign process entailed the replacement of components in the Claritek sensing head with components selected for improved performance. In most cases, the increased cost of these components had to be justified by their performance. To evaluate the performance of the component subassemblies, they would have to be tested under conditions which simulate the normal operation of the Claritek Monitor.

The attenuating medium used throughout the tests was diatomaceous earth dispersed in deionized water. Throughout all the tests, the change in attenuation of the incident beam was affected by increasing the density of the suspension by the addition of weighed portions of diatomaceous earth.

In order to evaluate the impact of component variations, the testing apparatus would have to simulate the working environment of the turbidimeter while maintaining ease of use and reproducibility. Testing consisted of the generation of calibration curves correlating the detector response to a variable attenuating medium, with a given incident

light source. Beginning with only water, the response of the detector to the relatively unattenuated incident beam was noted. The degree of attenuation of the water was then increased by the addition of weighed portions of diatomaceous earth. The amounts of diatomaceous earth added varied with state of the test: initial additions were determined by the sensitivity of the particular source/detector combination under test, and were typically in the one to two milligram range; in the latter stages of extended tests, additions of several hundred milligrams were used.

Three parameters were measured and used to define the viability of any incident source-detector assembly: maximum detector signal, maximum linear measurable concentration and maximum nonlinear measurable concentration. The maximum detector signal was measured with the incident light source and detector installed on the test cell. The test cell was filled with deionized water, and the source and detector aligned for strongest signal. The maximum linear measurable concentration was determined from a graph of LOG (detector signal) vs concentration of diatomaceous earth. The point at which the LOG (detector signal) vs. concentration curve deviated by more than 2% of concentration from the linear was taken as the "maximum linear measurable concentration". The highest concentration measured with a resolution better than 5% of total concentration was taken as the "maximum nonlinear measurable concentration".

3.2 Experimental Equipment

The apparatus used to test the viability of incident source and detection components consisted of a test cell to simulate the operation of the Claritek monitor sensing head,

along with an arrangement of power supplies and multimeters.

3.2.1 Test Cell

The sensing head of the Claritek monitor was normally mounted in a flowing channel or pipe in the feed and/or product stream of some process. Although a very close approximation of this arrangement could have been built, the uncertainty of the solids concentration caused by the required pumps, piping, and tanks far outweighed any benefit derived. A test cell patterned after a constantly stirred tank reactor was adopted.

The test cell was a small rectangular tank, with interior dimensions of 100 mm width, 200 mm length, 200 mm height. The dimensions were derived from certain system requirements: the optical path in the sensing head was 100 mm long; the volume of the cell would need to be at least one liter for ease of setting the concentration of the attenuating medium; the cell surfaces parallel to the incident beam would need to be at least 25 mm from the optical path to minimize the effect of reflections. The cell was fabricated of 2 mm glass sheeting with silicone rubber as the adhesive/sealant. The use of glass simplified the alignment of the incident beam with the detector and permitted viewing of the optical path from any angle.

To simulate the flow condition in which the turbidimeter would normally operate, the cell was continuously mixed with a magnetic stirrer during tests. The magnetic stirrer allowed the mixing to occur unobtrusively with the further advantage of mechanical simplicity. The optical components were supported by simple, heavy-based laboratory stands and clamps which allowed for the alignment of the source with detector optics.

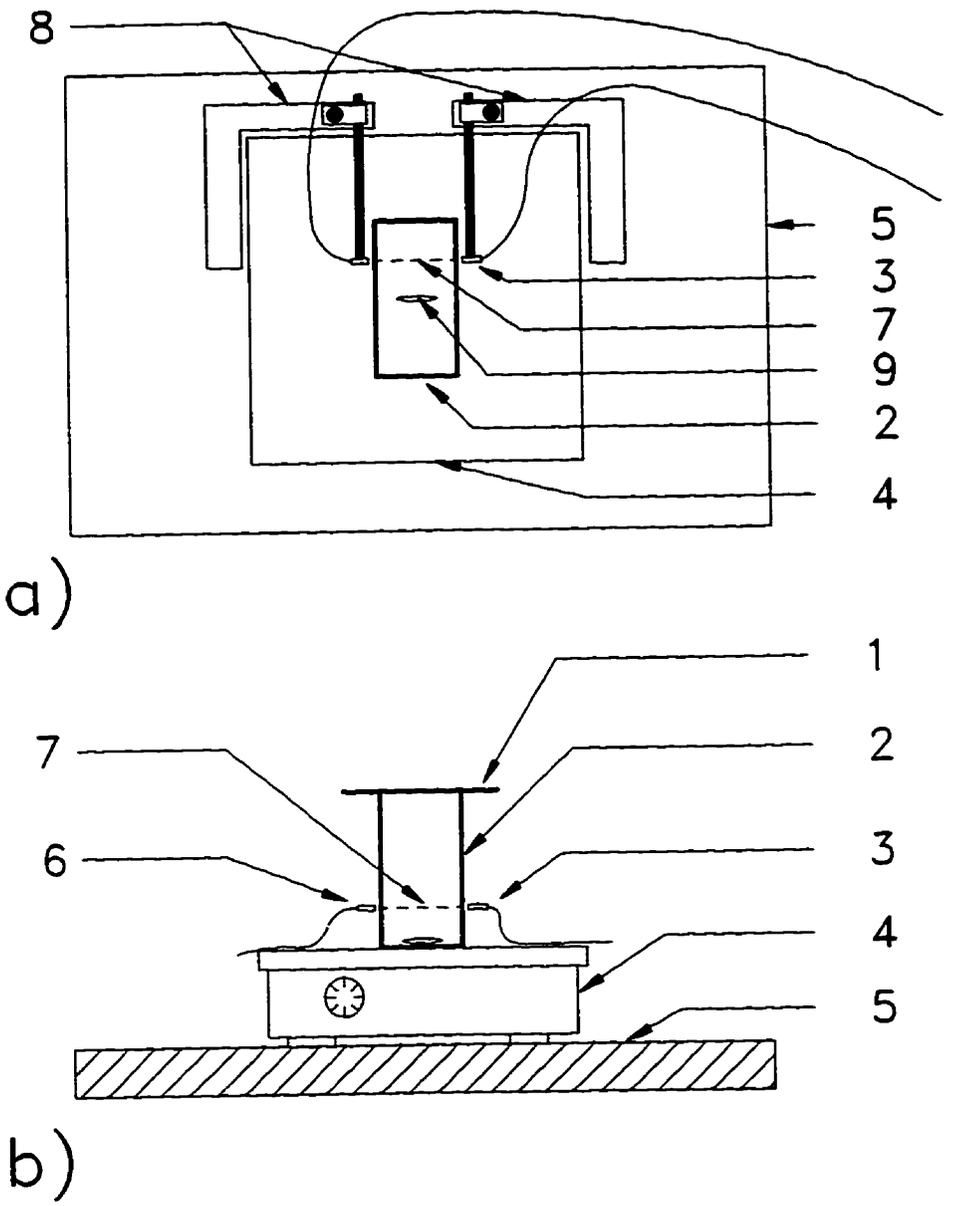

1. Cell Cover
2. Cell
3. Detector Optic/ Module
4. Magnetic Stirrer
5. Optical Table
6. Incident light Source-Optic/ Module
7. Optical Path
8. Lab Stand
9. Stirring Bar

Figure 3.1 Test Apparatus Layout: a) Top View, Cell Cover Omitted for Clarity
b) Front View, Lab Stands Omitted for Clarity

The complete test cell and optical apparatus was supported on an optical table. The optical table provided a flat, stable surface which simplified the optical alignment of the incident light source with the detector (see Fig. 3.1).

3.2.2 Power and Measurement

A number of power supply arrangements were used to drive the various incident light sources tested. The light emitting diode (LED) and modular visible laser diode (VLD) sources were powered by constant voltage-constant current (CV/CC) power supplies (this was possible since the VLD modules contain the necessary power conditioning circuitry). To drive bare laser diodes required an additional power conditioning module. The power condition of these light sources was monitored with digital multimeters (see Fig. 3.2).

The detectors used were reverse-biased using a CV/CC power supply and the signal current monitored with a digital multimeter. The integrated light-intensity-to-frequency converter was powered and controlled by a simple, task-specific circuit. The frequency output of the integrated detector was monitored with a pulse counter (see Fig. 3.3).

3.3 Opto-Electronic Components Tested

3.3.1 Incident Light Sources

The incident illumination in the original Claritek monitor was provided by a Skanamatic L33007 (7). This device was a commercially available module consisting of a light emitting diode (LED) with collimating lens sealed inside a threaded aluminum body.

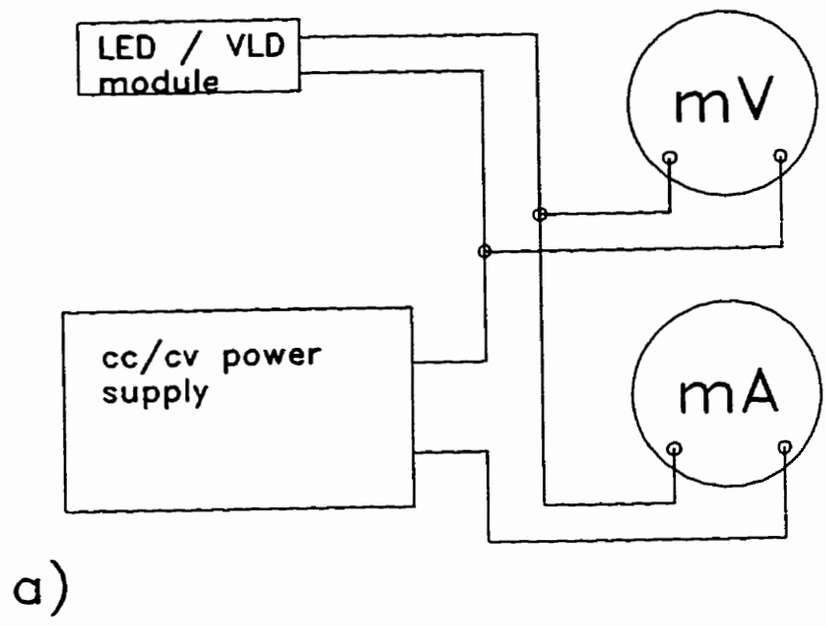

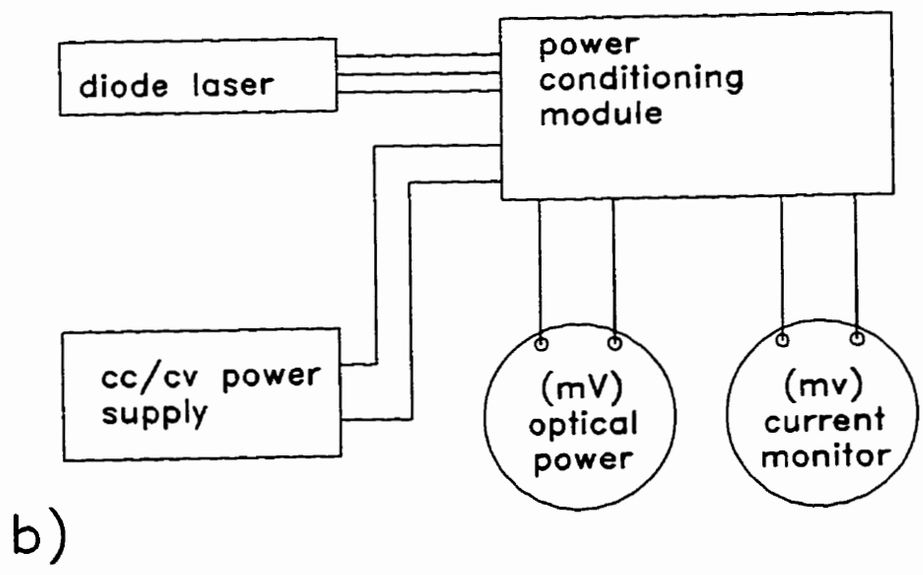

Figure 3.2: Block Diagrams for Incident Light Source Control Circuits

a) Light Emitting Diode / Modular Laser Diode Sources

b) "Bare" Diode Laser Sources

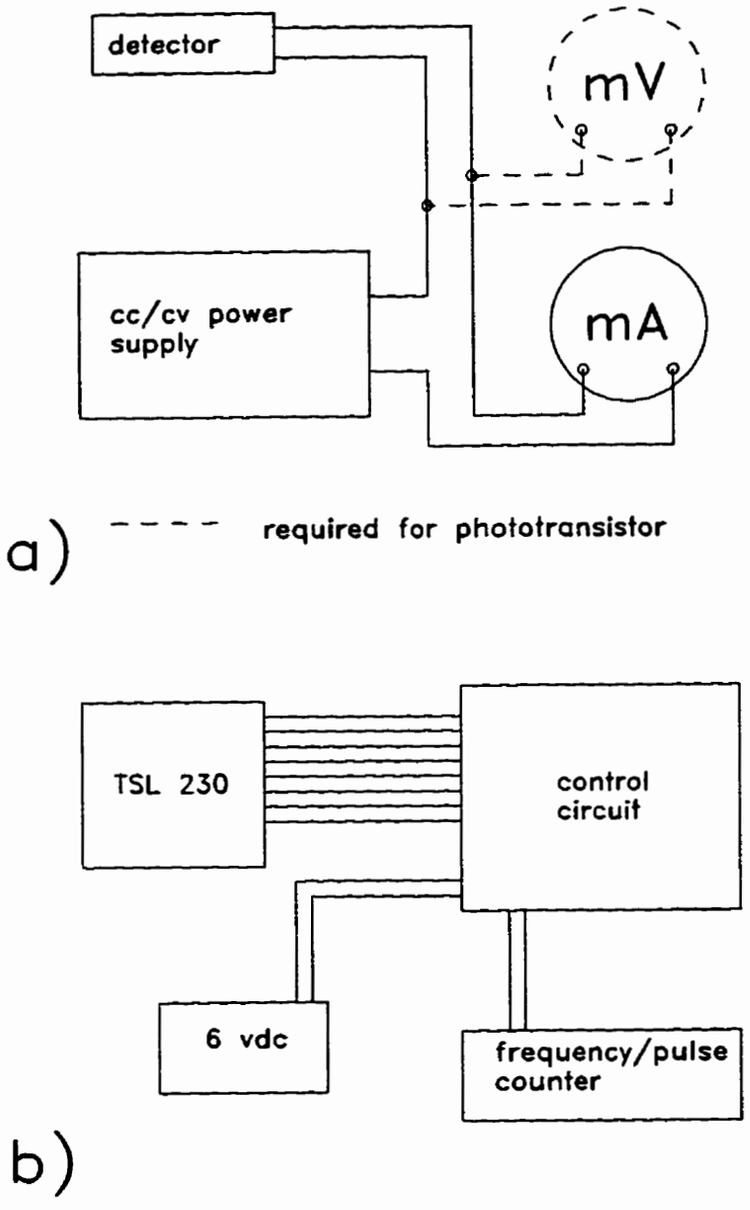

Figure 3.3: Block Diagram for Detector Circuits

a) Photodiode or phototransistor

b) TSL 230 Light- to-Frequency Converter

This LED had its spectral peak at 940 nm.

There were a number of problems associated with the L33007: this wavelength was absorbed by water, causing a weak signal; the beam was poorly collimated; the module leaked on occasion.

All but one of the incident light sources were initially tested using the same Skanamatic P33008 detector. The intent was to provide a common plane of reference in which the sources could be compared with respect to intensity and performance under various states of attenuation. The Skanamatic P33008 was very similar to the detector used in the Claritek SM8830 : the Skanamatic P33001. The difference was that the P33008 did not incorporate an infrared-passing, visible light blocking filter, which would have prevented the testing of visible light sources.

3.3.1.1 Infrared Light Emitting Diode

The original incident light source, the Skanamatic L33007 (7), was tested to provide a baseline of performance against which the other sources could be judged. The Skanamatic L33007 consisted of an infrared light emitting diode (with a spectral peak of 940 nm), encased within a threaded aluminum (or stainless steel, model L33014) barrel with a collimating lens.

3.3.1.2 Visible Light Emitting Diode

The visible light emitting diode module used was the Skanamatic L33008 (7). It consisted of a LED with collimating lens fixed within a threaded barrel. The spectral peak of the

L33008 output occurred at 660 nm. This incident light source was the visible light analog of the IR-emitting L33007.

3.3.1.3 Visible Laser Diode

To determine the viability of using laser sources, two laser diode modules were tested. Both were nominally 3 mW output; the Alpec (Quarton) was collimated, while the Imatronic had a variable focus lens. Both of these light sources produced substantially greater detector signals than LED sources.

In testing the laser sources it became apparent that the detector suffered an optical defect analogous to that observed with the Skanamatic LED sources: the highest signals were measured when the incident beam struck the detector focusing lens obliquely and approximately 1 mm off-centre.

3.3.2 Photodetectors

Three types of photodetectors were tested: a phototransistors, photodiodes, and an integrated light-to-frequency converter. Phototransistors offer the advantage of built-in amplification, but the output is dependent on the bias voltage and is inherently non-linear. Photodiodes have a broad operating range. The output is bias insensitive and inherently linear, but the output signal is relatively small. The integrated light-to-frequency converter was a new device with no application history; the features integral to this device make it highly desirable in our application.

3.3.2.1 Phototransistor

The Skanamatic P33008 (7) module was taken as representative of this type of detector which consisted of a phototransistor with integral lens, encased within a threaded aluminum (or stainless steel, model P33018) barrel with a separate focusing lens. This device was very similar to the detector used in the Claritek SM8830, utilizing the Skanamatic P33001. As stated previously, the difference between the P33008 and P33001 was that the former did not incorporates an IR band-pass filter, which allowed testing it with visible light sources.

3.3.2.2 Silicon Photodiodes

At the commencement of testing of the silicon photodiodes, the results of incident light source testing had produced a firm commitment to laser sources. Hence, all subsequent tests of detectors and light guides used laser sources for incident light.

Three photodiodes were acquired for testing: Antel Optronics AS7025, Mitsubishi PD2101, and E.G.& G. VACTEC VTB6061 (13). Of these only the VTB6061 was suitable for testing directly on the test cell, the others being designed for use with optical fiber only.

3.3.2.3 Integrated Light-to-Frequency Circuit

The Texas Instruments model TSL230 programmable light-to-frequency converter (54, 55) incorporated a 100-element silicon photodiode array into a single eight pin dual inline package (DIP) integrated circuit. This integrated circuit also included an analog current-to-

frequency converter, and temperature compensating circuitry. It was also designed to allow transistor-transistor logic (TTL) selectable sensitivity (100X, 10X, 1X), and TTL scalable output range (1, 1/2, 1/10, 1/100).

3.3.3 Fiber Optics

In framing the original proposal, three types of light guides were considered: multi-fiber bundles, large core optical fiber (greater than approximately 500 micrometers in diameter) and small core optical fibers (less than approximately 100 micrometers in diameter). Subsequent research revealed the "small core" criterion to be somewhat ill-defined, and it was further refined to singlemode optical fiber and multimode optical fiber.

Preliminary experiments with fiber bundle light guides resulted in the conclusion that the use of multi-fiber bundles in the incident light source assembly was inappropriate due to the large exit angle of the beam. Consequently, further use of this fiber bundle was limited to applications in detector subassemblies.

Large-core fiber, with a 500 micrometer core diameter, was too stiff to conform to the existing detector housing and was removed from further consideration. The requirements for fabrication of single-, and multi-mode fiber optic source and detector subassemblies from component parts was found to be beyond the capabilities of the facilities available. It was more expedient and cost-effective to specify the design requirements and have subassemblies constructed by a custom optical fabricator.

3.4 Subassemblies Tested

3.4.1 Incident Source Subassemblies

The consideration at this point was limited to laser source with single-, or multi-mode optical fiber guided assemblies. As noted previously, although it was relatively straightforward to launch the laser output into the fiber bundle, the resultant output from the fiber bundle was too divergent to be of use directly, and the large section of the bundle made optical collimation impractical.

3.4.1.1 Singlemode Fiber Collimator

Singlemode propagation (56) of light in an optical fiber occurs when the core diameter of the fiber is sufficiently small relative to the wavelength of light so that the light follows a single, preferred path through the fiber. This acts as a spatial filter for the laser diode, resulting in a near-Gaussian beam intensity profile from the collimating lens affixed to the output end of the optical fiber.

The advantage of using the singlemode fiber collimator in conjunction with the diode laser as the incident light source is the quality of the light beam: it is well-defined, stable, free of stray light, and has a very small angle of divergence.

The disadvantages of the singlemode source result from the same mechanism which produces its beam quality: the small core diameter (4 micrometers) of the optical fiber limits the coupling efficiency, thus reducing the optical output of the source. The small core diameter also reduces the available alignment tolerance, making alignment more difficult, thereby increasing the fabrication cost of this assembly. A singlemode

source, consisting of a Toshiba TOLD9211 laser diode (58) coupled to a fiber collimator was obtained from Oz Optics Ltd. The fiber collimator (56) consisted of four meters of 4/125 (4 micrometer core, 125 micrometer cladding OD) optical fiber, one end fitted with an FC-type connector, and terminated with a GRIN lens collimator. The laser diode was mounted in a proprietary alignment fixture which included a focusing lens for optically coupling the laser output to the fiber core, and an FC-type receptacle to mate with the fiber collimator.

3.4.1.2 Multimode Fiber Collimator

Multimode propagation (57) of light in an optical fiber occurs when the diameter of the fiber core is large relative to the wavelength of the propagated light, resulting in many possible paths for the light as it travels through the fiber. Both constructive and destructive interference occurs between the different "modes" due to the phase shift induced by the slightly different path lengths, producing an output beam profile of relatively uniform intensity macroscopically, but with a "speckled" appearance.

The multimode fiber collimator offered a practical advantage, as well as some technical/theoretical disadvantages with its use. The larger core diameter allows a greater portion of the source light to be launched into the fiber with a more liberal tolerance for alignment, resulting in a brighter source which would be easier to fabricate. The multimode propagation produces a beam which cannot be as tightly collimated as a singlemode beam, resulting in a more divergent beam. The spatial filtering provided by the multimode fiber is not as definitive as that provided by the singlemode fiber: flexing

or bending the fiber would change the conditions which favour certain propagation modes, and disfavour other modes, producing an incident beam with an intensity profile which would change in response to bending and vibration of the optical fiber.

A multimode fiber collimator (9) was obtained from NSG America Inc. This collimator consisted of three meters of 62.5/125 (62.5 micrometer core, 125 micrometer cladding) optical fiber, one end fitted with an FC-type connector (to mate with laser diode receptacle), and the other end terminated with GRIN collimating lens.

3.4.2 Detector Subassemblies

Preliminary experiments using single-, and multimode fiber collimators as detector light gathering optics, while somewhat encouraging, were judged to be impractical for the application in question. The nature of the fiber collimator as a detector optic requires that the incident light source be pointed at the detector collimator, *and be located within the beam that would come from the detector collimator, if a laser source were substituted for the detector*. In effect, the fiber collimators were too discriminating to use with the alignment mechanisms which could readily be installed in the Claritek Monitor sensing head.

3.4.2.1 Fiber Optic Light Guides

Fiber optic light guides consist of many optical fibers bundled together in a sheath. Generally, the ends of the bundle are fixed within ferrules and polished. Two one-eighth inch diameter light guides, 48 inches long, were obtained from Edmund Scientific Co.

(part no. D39366). One light guide was fitted with the E.G.&G. VTB6061 photodiode. The reduction in detector signal resulting from attenuation by the light guide mandated the use of an amplifier.

Another detector subassembly utilizing the fiber bundle light guide was constructed with the Texas Instruments TSL230 integrated circuit. It was not possible to exploit the TSL230 alone due to an interference phenomenon between the multimode beam (the preferred incident source) and the detector array. The use of the fiber light guide with the TSL230 reduced this interference. It was surmised that this was a result of the scrambling effect of the incoherent fiber arrangement within the light guide.

3.5 Test Procedure

One and one-half liters of deionized water would be allowed to degas, and come to room temperature, by standing overnight. The test cell and magnetic stirring bar were washed with detergent and water, repeatedly rinsed with deionized water, and allowed to dry.

For the test, the water was poured into the test cell containing the stirring bar. The cell was centered on the magnetic stirrer such that the stirring bar was free to rotate. The magnetic stirrer was set to provide maximum stirring without air entrainment. Beginning with the incident light source, the opto-electronic components were positioned on the cell. The incident light source was generally positioned 15 mm from, and normal to, the cell wall, 50 mm above the cell floor, and 50 mm from the nearer end wall. With the incident light source switched on, the detector or detection optic was positioned facing the incident light source such that the incident beam was well-centered in the detection optic after

passing through the test cell. The orientation and position of the detector or detection optic was then adjusted to achieve the maximum detector signal.

When a stable maximum detector signal was achieved, it was noted as such. The turbidity of the water was then increased by the addition of diatomaceous earth (DE). The initial weight increment used was to some extent determined by the resolution of the incident light source/detector combination being tested, but was generally in the range of 0.5 mg to 2.0 mg. The DE portions were weighed on an analytical balance and recorded with a precision of +/- 0.1 mg. The detector signal was recorded, when stable, with a precision of three significant figures. The mass of DE portions added to the test cell were increased to several hundred milligrams as a test progressed.

The background signal due to ambient light was determined by manually interrupting the incident light beam between the source and test cell with an opaque shutter. A test would be terminated when the detector became unresponsive to increased slurry concentration, or when the attenuated beam signal became indistinguishable from the background signal.

CHAPTER 4

Results and Discussion

4.1 Incident Light Sources

The incident light sources were initially tested using the same detector, the Skanamatic P33008. The intent was to provide a common plane of reference in which the sources could be compared with respect to intensity and performance under various states of attenuation. A summary of test results is presented in Table 4.1.

4.1.1 Infra Red Light Emitting Diode

The Skanamatic L33014 was the incident light source used in the production model of the Claritek turbidity monitor. It was tested as a representative of infrared light emitting diode-type sources and to provide a baseline of performance against which the other sources could be judged.

Initial testing produced very inconsistent results with regards to positioning of the detector within the source beam. Subsequent mapping of the source beam profile revealed that the beam intensity distribution was non-Gaussian. Instead of having an intensity maximum at or near the central axis of the detector body, the beam exhibited a local minimum surrounded by a ring of maximum intensity approximately 6 mm in diameter at the detector lens. (This result was further complicated by a similar sensitivity profile in the Skanamatic P33008 detector chosen as the "baseline standard" for photodetectors.) Performance testing of this source/detector combination gave maximum (zero-concentration) detector currents of 0.766 mA (with a LED current of 90 mA, 90% of

Table 4.1 Summary of Test Results

Incident Light Source	Incident Source Optic	Detector	Detector Optic	Maximum signal mA/Hz	Maximum concentration (linear) mg/l	Maximum concentration (non linear) mg/l
IRLED[1] •	Integral Lens[9]	Phototransistor[14]	Integral Lens[18]	0.766	~400	~1500
VisLED[2] •	Integral Lens	Phototransistor	Integral Lens	8.95	>450	N.A.
VisLED[2] •	Integral Lens	Phototransistor	Integral Lens	7.48	~1000	~1800
ALPEC DL[3] •	Integral Lens	Phototransistor	Integral Lens	54.7	~1000	~2600
IRLED[1]	Integral Lens	Phototransistor	Integral Lens	0.52	~600	~800
VisLED[2]	Integral Lens	Phototransistor	Integral Lens	9.56	~600	>1150
Imatronic DL[4]	Integral Lens	Phototransistor	Integral Lens	87.18	~880	~1700
TOLD 9211[5]	Single Mode[10]	Phototransistor	Integral Lens	73.09	~550	>1330
TOLD 9211[6]	Single Mode[11]	Phototransistor	Integral Lens	71.67	~610	>1570
TOLD 9211[7]	Single Mode[12]	Phototransistor	Integral Lens	74.48	~600	>1470
TOLD 9211[6]	Single Mode	Photodiode[15]	None	0.2837	~600	>1450
TOLD 9211[6]	Multi Mode[13]	Photodiode[15]	None	0.913	~500	~1600
TOLD 9211[8]	Multi Mode	Photodiode[15]	None	1.672	~500	>1530
TOLD 9211[8]	Multi Mode	Photodiode amplified	Fiber Bundle[19]	4290 mV	~500	>1200
TOLD 9211[6]	Single Mode	TSL 230[17]	Fiber Bundle	1173.7 kHz	~600	>1480
TOLD 9215[8]	Multi Mode	TSL 230	Fiber Bundle	1164.9 kHz	~1000	>1470
TOLD 9215[8]	Multi Mode	TSL 230	Fiber Bundle	943.5 kHz	>>400	>>400

[*] preliminary examinations
[1] Skanamatic L33014 Infrared light emitting diode
[2] Skanamatic L33008 visible red light emitting diode
[3] ALPEC 670 nm 3mW diode laser module
[4] Imatronic 670 nm 3 W diode laser module
[5] Toshiba TOLD 9211 670 nm 3mW diode laser in connectorized package
[6] New Toshiba TOLD 9211 670 nm 3 mW diode laser identical to [5]
[7] Connectorized package from 5 with replacement diode laser also Toshiba TOLD 9211
[8] Toshiba TOLD 9215 670 nm 10 mW diode laser in connectorized package
[9] Skanamatic L33014 was fitted with collimating lenses
[10] Singlemode fiber collimator fabricated by Oz Optics Ltd.
[11] Additional singlemode fiber collimator identical to [10] used with [6]
[12] Same collimator as [10], used on repaired package [5]
[13] Multimode fiber collimator fabricated by NSG Inc.
[14] Skanamatic P33008 phototransistor
[15] EG&G VTB6061 photodiode
[16] EG&G VTB6061 photodiode with amplifier
[17] Texas Instruments TSL230 light-to-frequency converter
[18] Skanamatic P33008 was fitted with focusing lens
[19] Edmund Scientific Co. Part no. D39366 fiber optic light guide

maximum input) and 0.520 mA (with a LED current of 45 mA, 90% of maximum for visible LED). At the lower source intensity, the maximum linear measurable concentration was 600 mg diatomaceous earth per liter of deionized water.

That the 940 nm wavelength of the IRLED was unsuited to aqueous applications was made apparent by the attenuation of the incident beam caused by deionized water alone. The addition of water to the otherwise empty cell reduced the detector signal from 2.17 mA to 0.766 mA, indicating that the wavelength in question is at least moderately absorbed by water (see Fig. 4.1, 4.2).

4.1.2 Visible Light Emitting Diode

The visible light emitting diode module used was the Skanamatic L33008. This incident light source was the visible light analogue of the IR-emitting L33007. This source was tested using the same P33008 detector used previously. During preliminary testing, the hollow, conical nature of the beam from this source became apparent.

Testing of this source with a drive current of 45 mA (90% of maximum) produced a maximum detector signal (zero solids concentration) ranging from 7.48 mA to 9.56 mA. The determination of maximum detectable concentration was somewhat subjective in this case. As described previously, the linear limit of LOG (signal current) occurred at about 600 mg/l. However, there was sufficient incident intensity available to judge concentrations greater than 1150 mg/l in the non-linear portion of the curve. Testing with this visible LED (660 nm) demonstrated the benefit of using an incident source less absorbed by water: little attenuation of the incident beam by water was detected (Fig.4.3).

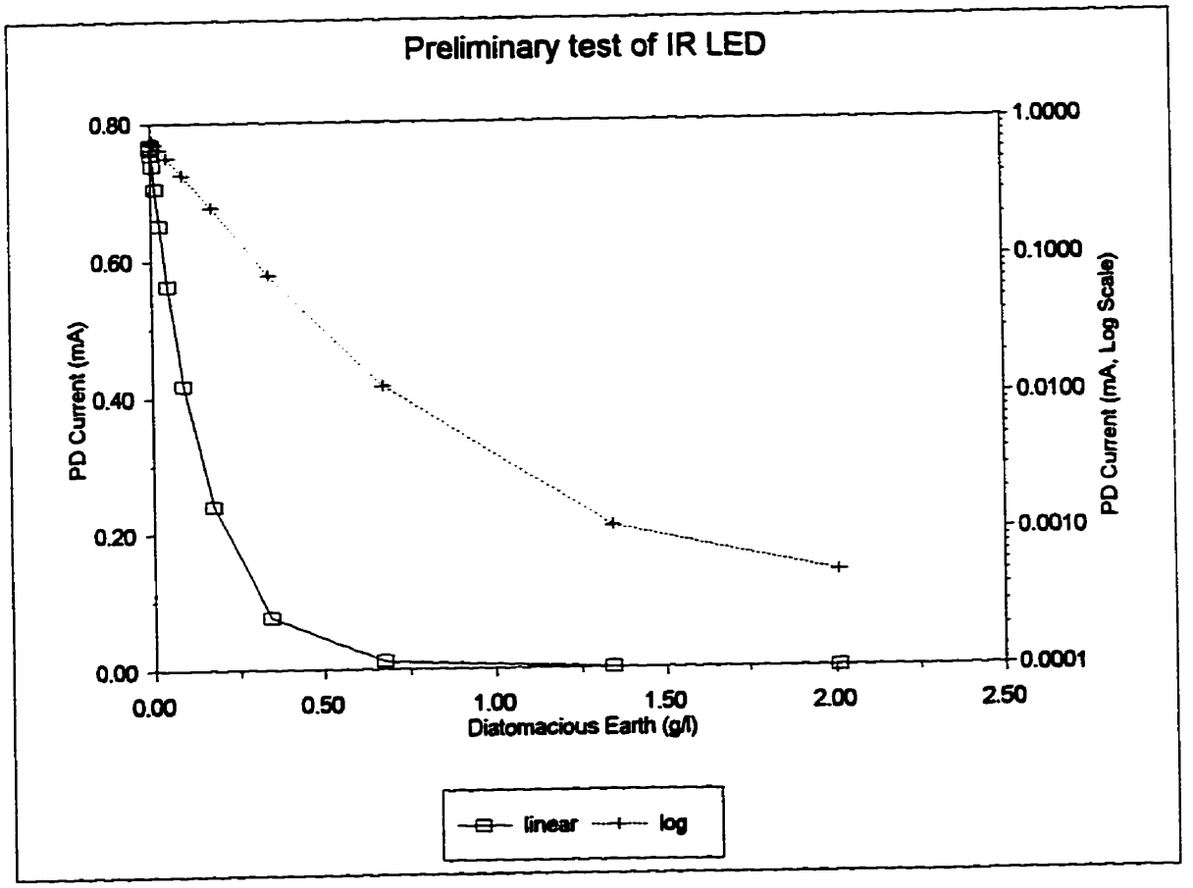

Figure 4.1: IR LED with Phototransistor

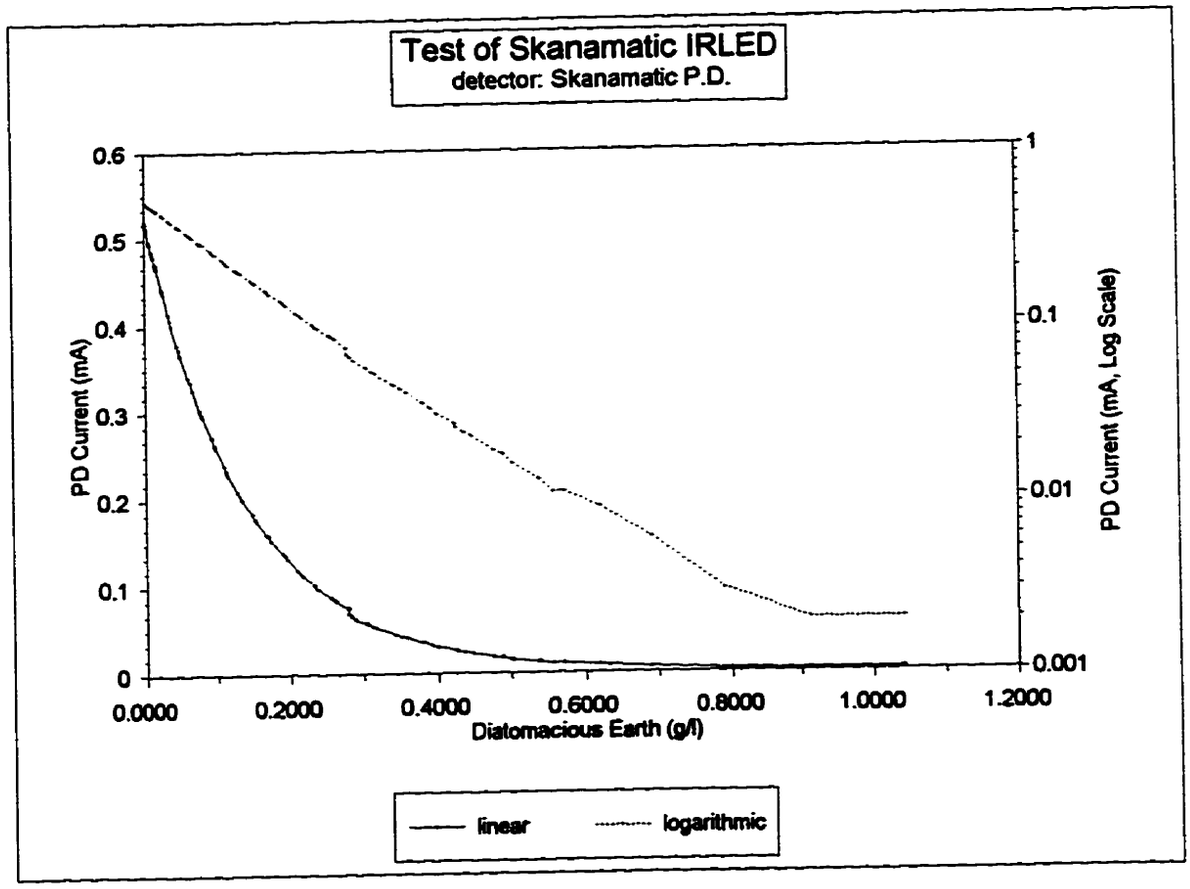

Figure 4.2: IR LED with Phototransistor

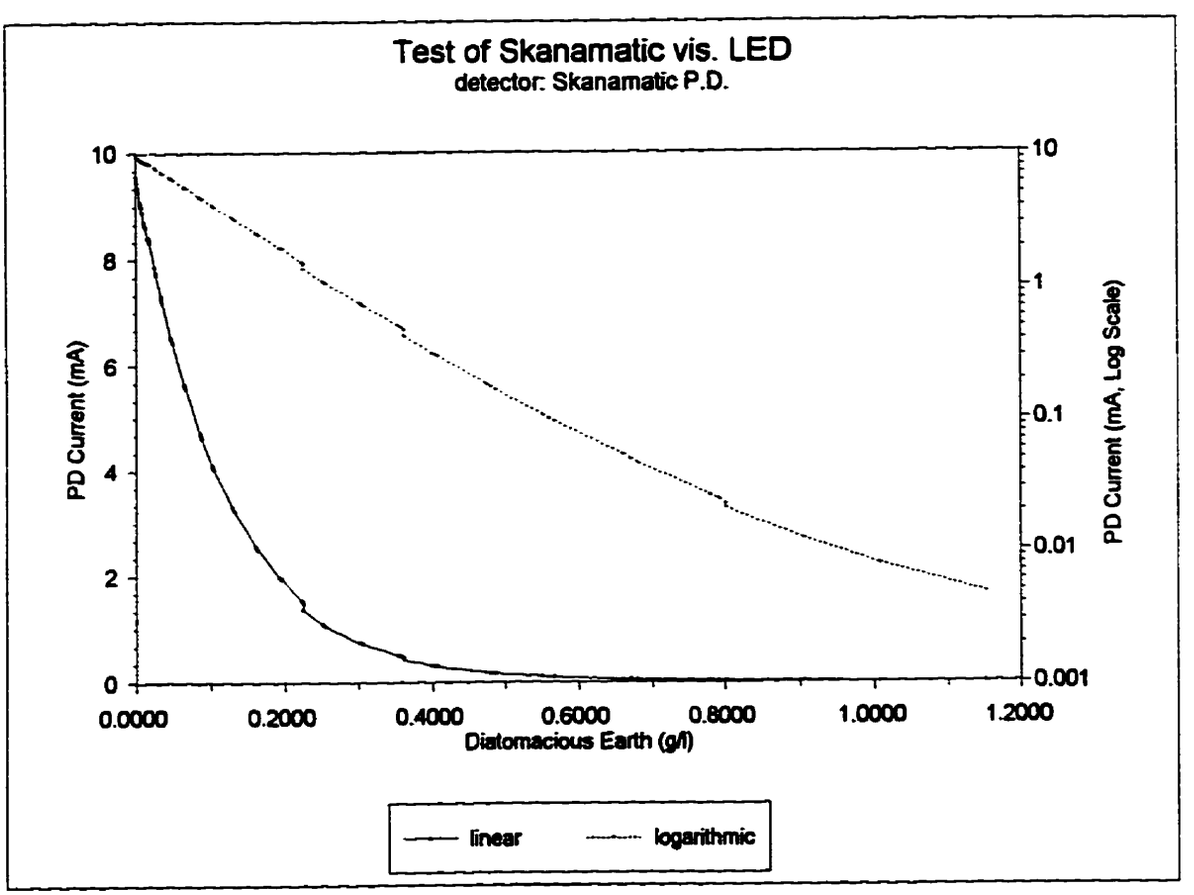

Figure 4.3: Visible LED with Phototransistor

4.1.3 Visible Diode Laser

To determine the viability of using laser sources, two laser diode modules were tested. Both were nominally 3 mW output; the Alpec (Quarton) was collimated, while the Imatronic had a variable focus lens. Both of these light sources produced substantially greater detector signals: the maximum detector current achieved using the Alpec (Quarton) module was 54.7 mA, with the Imatronic, 87.2 mA. The maximum concentration in the linear portion of the LOG (detector signal) curve obtained with the Imatronic module was approximately 880 mg/liter, in the nonlinear portion of the curve, the maximum concentration was approximately 1700 mg/liter.

The attenuation curve of these light sources using the Skanamatic detector was very irregular. This irregularity was most pronounced at low and very high solids concentrations. Both of these could be attributed to the intensity of these light sources relative to the operating range of the Skanamatic detector: at lower concentrations the incident intensity was sufficiently high to partially saturate the detector; at high solids concentrations, the scattered light was sufficiently intense to illuminate the detector by second and higher order reflections (59, 60, 61, 62, 63) (see Fig. 4.4).

In testing the laser sources it became apparent that the detector suffered an optical defect analogous to that observed with the Skanamatic LED sources: the highest signals were measured when the incident beam struck the focusing lens obliquely and approximately 1 mm off-center.

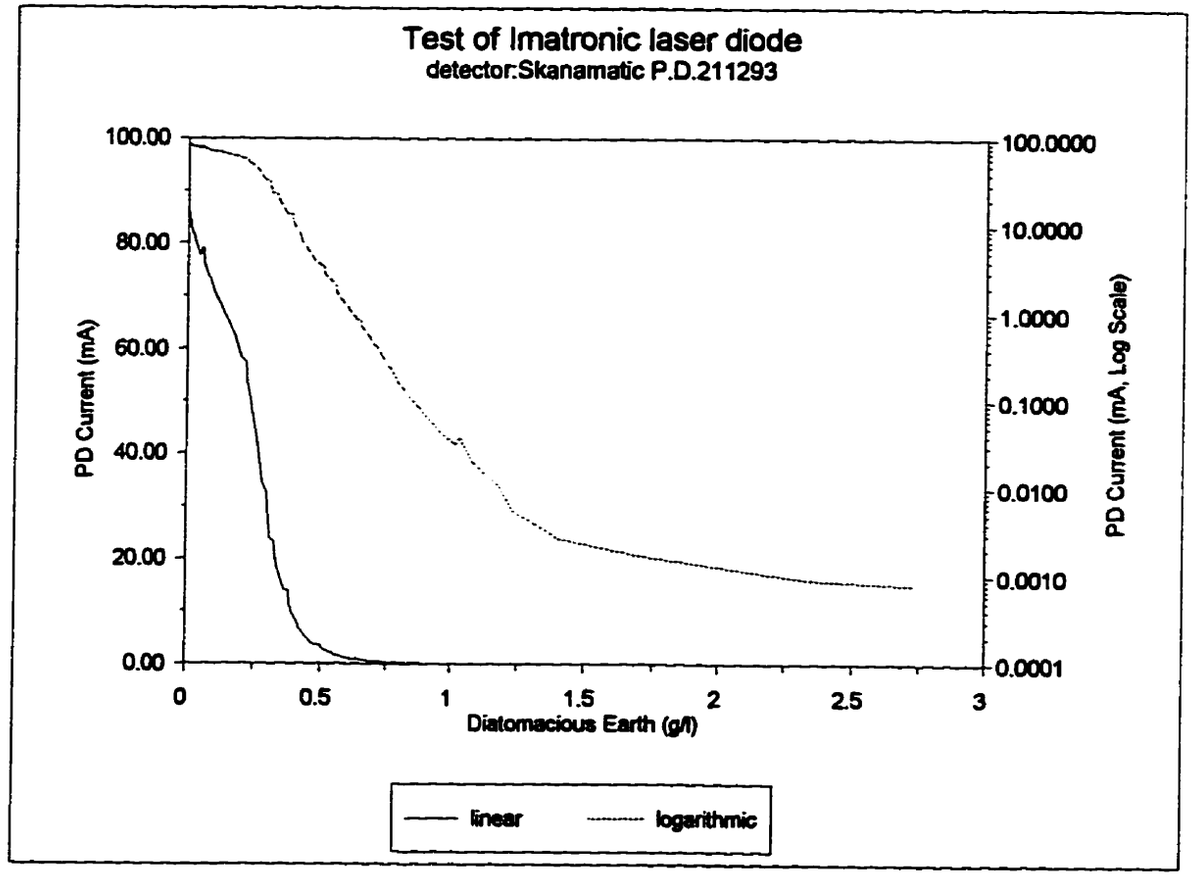

Figure 4.4: Diode Laser Module with Phototransistor

4.2 Photodetectors

Three types of photodetectors were tested: phototransistors, photodiodes, and an integrated light-to-frequency converter. To reiterate, phototransistors offer the advantage of built-in amplification, but the output is dependent on the bias voltage and is inherently non-linear. Photodiodes have a broad operating range, the output is bias-insensitive and inherently linear, but the output signal is relatively small. The integrated light-to-frequency converter was a new device with no application history; the features integral to this device make it highly desirable in our application.

4.2.1 Phototransistor

The Skanamatic P33008 module was taken as representative of this type of detector. As this detector was used in the preliminary evaluation of incident light sources, test results using this detector were presented in the previous section. This detector exhibited serious non-linearity of the LOG (signal)-solids concentration relationship at the lower and higher concentration extremes. This was most pronounced using the more intense laser incident light sources. The non-linearity exhibited was a symptom of saturation of the detector at lower solids concentrations. The non-linearity at higher solids concentrations was a product of the wide acceptance angle of the optical system used in this particular detector, resulting in high detection of scattered light with more intense incident light sources.

4.2.2 Silicon Photodiode

At the commencement of testing of the silicon photodiodes, the results of incident light

source testing had produced a firm commitment to laser sources. All subsequent tests of detectors and light guides used laser sources.

The VTB6061 (and the other photodiodes) produced very small signal currents relative to phototransistors; the zero concentration signal with the most intense source being considered was 1.68 mA; the "maximum detectable concentration" was approximately 500 mg diatomaceous earth per liter, although the non-linear range could be extended beyond 1530 mg per liter (see Fig. 4.5).

4.2.3 Integrated Light-to-Frequency Circuit

The Texas Instruments TSL230 programmable light-to-frequency converter was initially tested as the bare detector chip with the preferred incident light source (Toshiba TOLD9215, delivered via multimode fiber collimator). This test produced a widely varying, noisy signal. Subsequent testing with a multi-fiber light guide delivering the signal to the detector was quite successful.

4.3 Fiber Optic Subassemblies

Preliminary experiments with fiber samples resulted in the following conclusions. The use of multi-fiber bundles in the incident light source assembly was inappropriate due to the large exit angle of the beam. The "large core" fiber was too stiff to conform to the existing sensing head. The requirements for fabrication of fiber optic source and detector subassemblies with single- or multimode optical fiber were found to be beyond the capabilities of the facilities available. It was more expedient and cost effective to specify

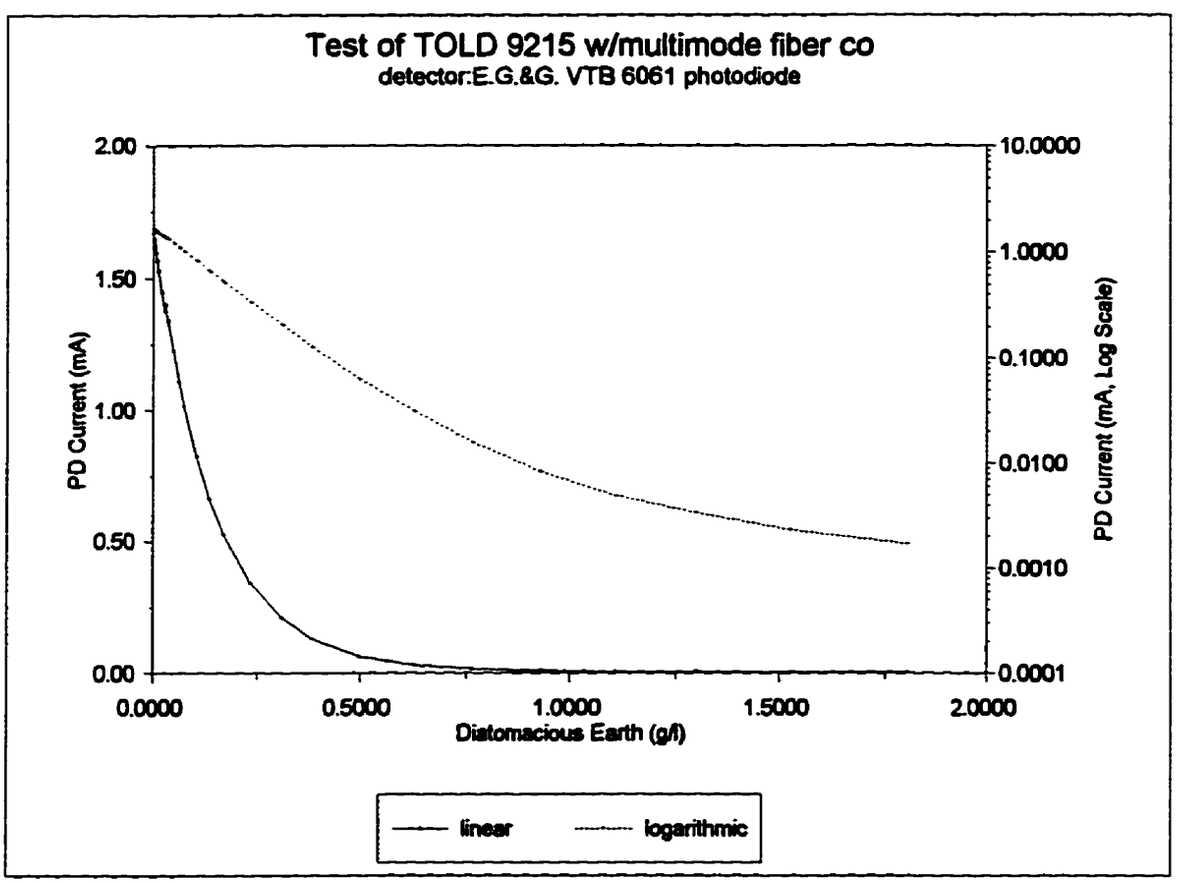

Figure 4.5: 10 mW Diode Laser - Fiber Collimator with Photodiode

the design requirements and have subassemblies constructed by a custom optical fabricator.

4.3.1 Source Assemblies

As noted previously, although it was relatively straightforward to launch the laser light into the fiber bundle, the resultant output was too divergent to be of use directly, and the large section of the bundle made optical collimation impractical.

4.3.1.1 Singlemode Optical Fiber

A singlemode source, consisting of a Toshiba TOLD9211 laser diode coupled to four meters of 4/125 (4 micrometer core, 125 micrometer cladding) optical fiber, terminated with a GRIN lens collimator, was obtained.

A test of this single mode source with the Skanamatic detector produced a maximum signal of 71.7 mA (the low concentration portion of this graph was also nonlinear, indicating saturation of the detector) and a maximum measurable concentration (linear) of approximately 610 mg/l; the nonlinear maximum concentration was in excess of 1570 mg/l (see Fig. 4.6).

Testing this source against E.G.&G. VTB6061 photodiode produced a maximum signal of 0.29 mA (no saturation), with maximum measurable concentrations (linear) and (nonlinear) of approximately 600 mg/l and greater than 1450 mg/l, respectively (see Fig. 4.7).

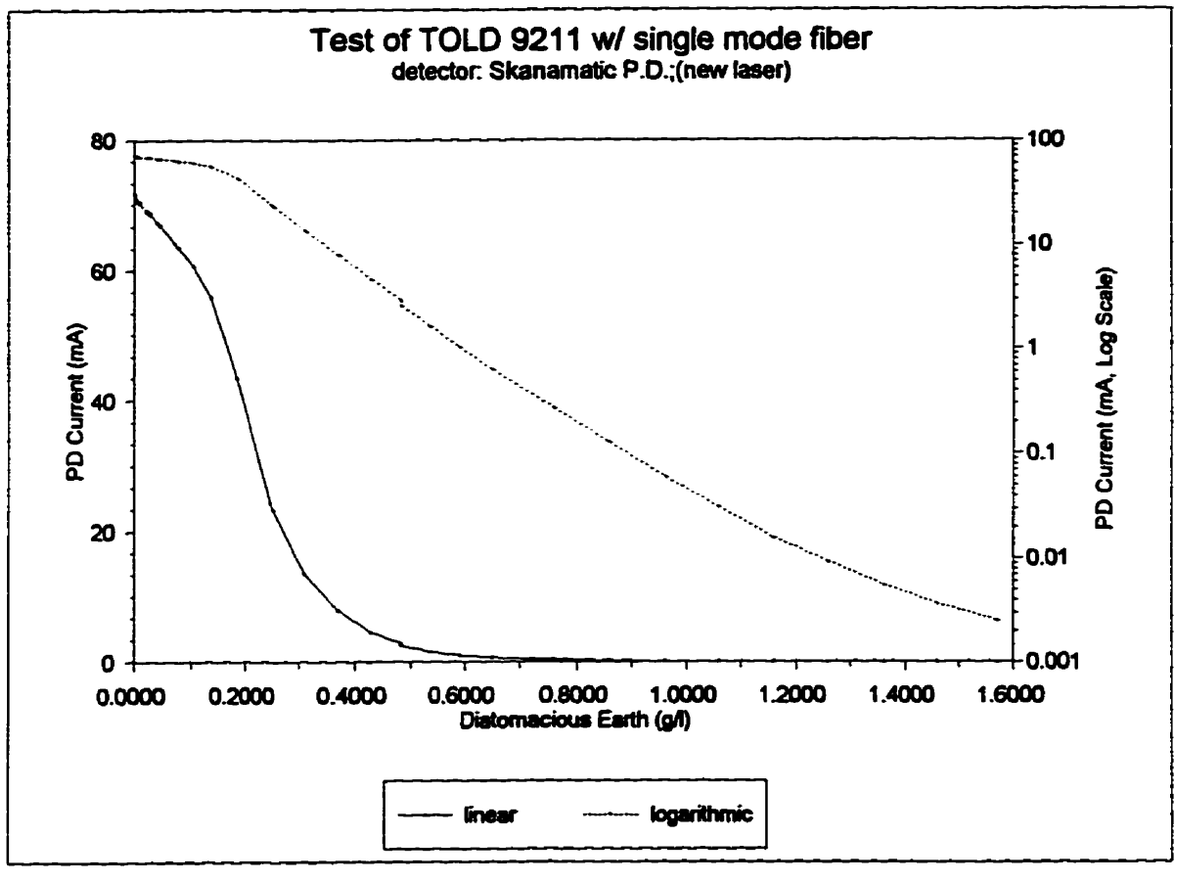

Figure 4.6: 3 mW Diode Laser - Fiber Collimator with Phototransistor

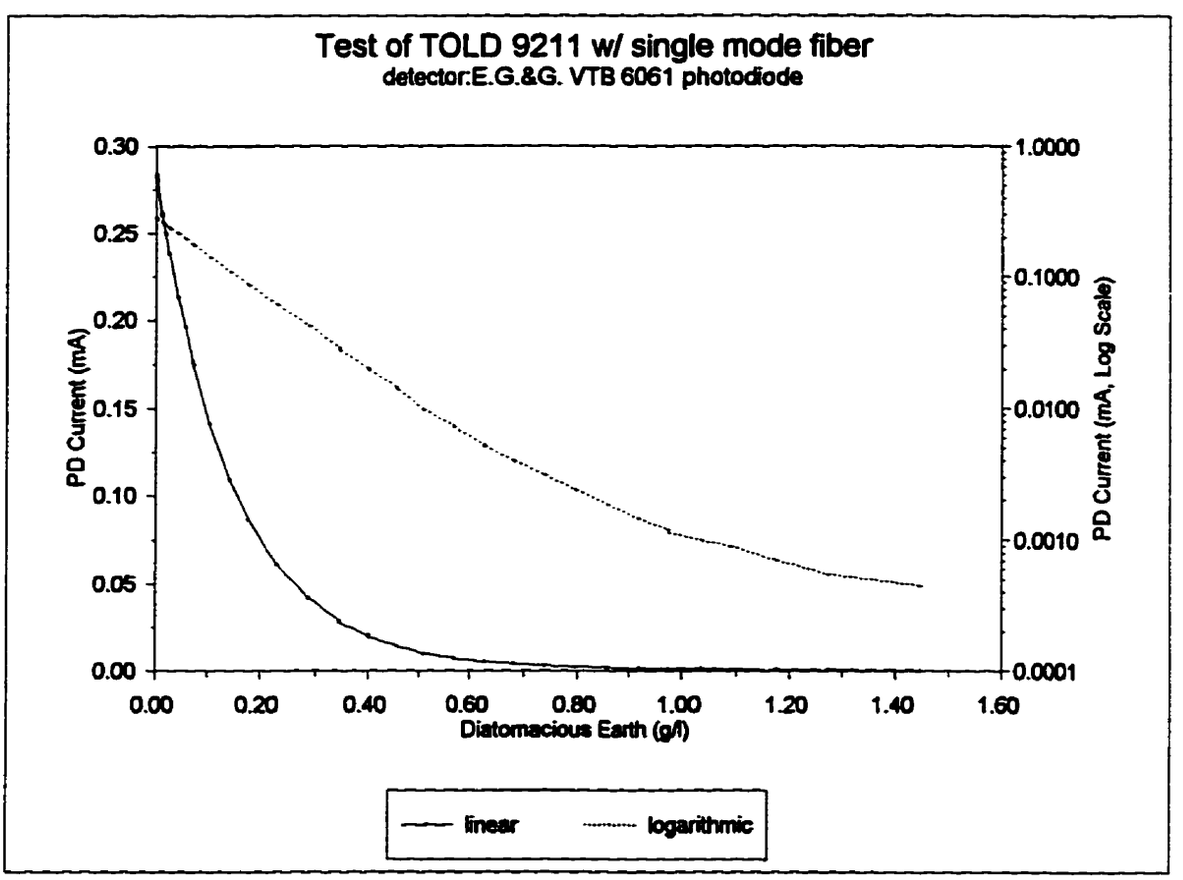

Figure 4.7: 3 mW Diode Laser - Fiber Collimator with Photodiode

4.3.1.2 Multimode Optical Fiber

A multimode fiber collimator was obtained from NSG America Inc. This collimator consisted of three meters of 62.5/125 (62.5 micrometer core, 125 micrometer cladding OD) optical fiber, one end fitted with an FC-type connector (to mate with laser diode receptacle), and the other end terminated with GRIN collimating lens.

This fiber collimator, fitted with the Oz Optics laser source (Toshiba TOLD9211, 3mW (nom.)) was tested with the E.G.&G. VTB6061 photodiode. This combination produced a maximum detector current of 0.913 mA, a maximum linear measurable concentration of approximately 500 mg/l, and a maximum nonlinear measurable concentration of approximately 1600 mg/l (see Fig. 4.8).

When fitted with a laser source obtained from Seastar Optics (Toshiba TOLD9215, 10mW (nom.)), the above combination produced a maximum detector current of 1.67 mA, a maximum linear measurable concentration of approximately 500 mg/l, and a maximum nonlinear measurable concentration of greater than 1530 mg/l (see Fig. 4.5).

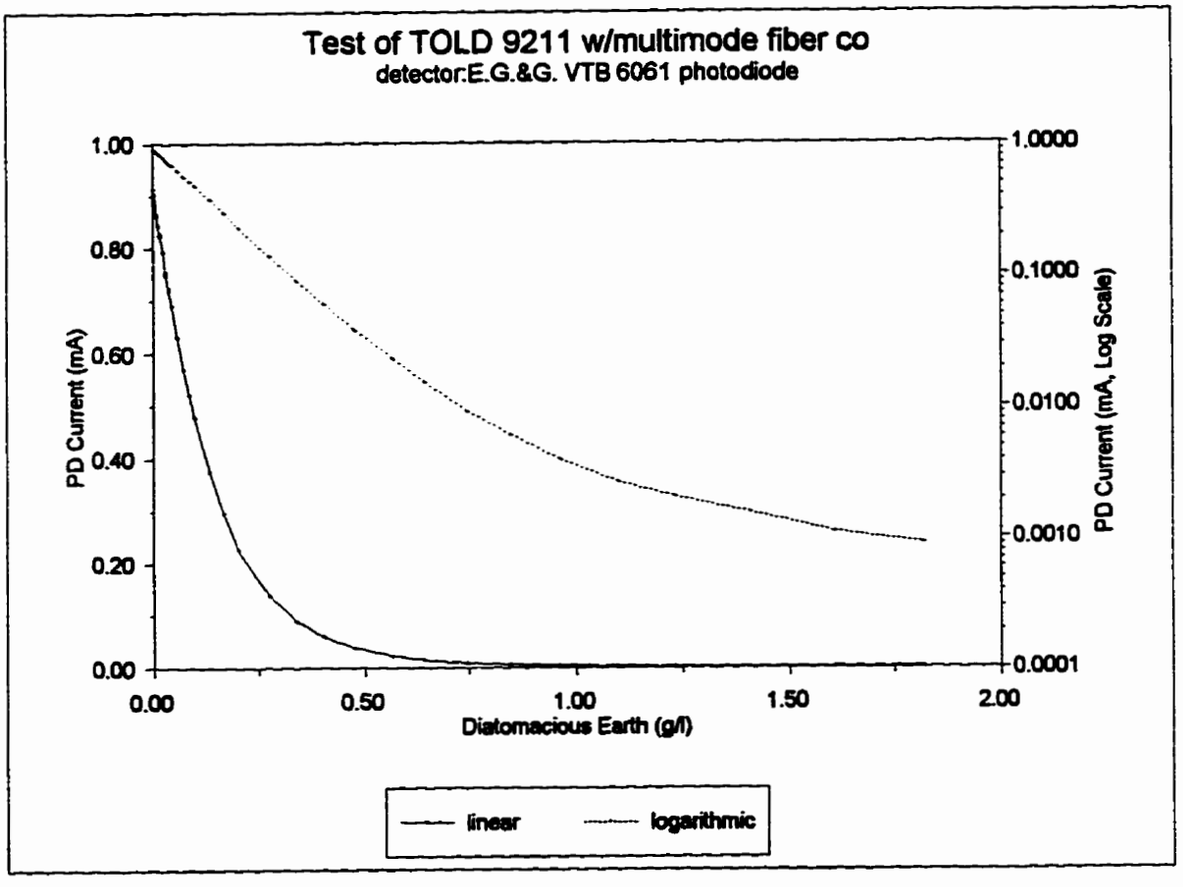

Figure 4.8: Diode Laser - Multimode Fiber Collimator with Photodiode

4.3.2 Detector Subassemblies

Preliminary experiments using single-, and multimode fiber collimators as detector light gathering optics, while somewhat encouraging, were judged to be impractical for the application in question.

4.3.2.1 Multi-fiber Light Guides

One detector subassembly was constructed by fitting the E.G.&G. VTB6061 photodiode to one end of the light guide, with the other end positioned on the test cell in place of a detector. Testing this detector assembly with TOLD9215/ NSG multimode fiber source assembly produced a maximum detector signal of 0.83 mA, a maximum linear measurable concentration of approximately 500 mg/l, and a maximum nonlinear measurable concentration greater than 1200 mg/l. Due to the reduction in detector signal resulting from attenuation by the light guide, this test was conducted with the use of an amplifier. The amplifier introduced another source of nonlinearity, as shown by an inflection in the detector response curve not seen previously (see Fig. 4.9).

A second detector subassembly was constructed with the Texas Instruments TSL230 integrated circuit. As mentioned previously, it was not possible to exploit the TSL230 directly due to interference between the multimode beam (the preferred source) and detector array. The use of the fiber light guide reduced this interference, most likely a result of the scrambling effect of the incoherent fiber arrangement within the light guide.

Testing the TSL230 detector subassembly with the TOLD9211/Oz Optics singlemode source produced sufficient intensity at the detector to require that the arrangement be "detuned" slightly (by increasing the distance between the end of the light guide and the detector surface) to prevent saturation of the detector at low concentrations. The maximum detector signal was set to 1.16 MHz at zero solids concentration. The maximum linear measurable concentration was approximately 600 mg/l, with a maximum nonlinear measurable concentration greater than 1470 mg/l (see Fig. 4.10).

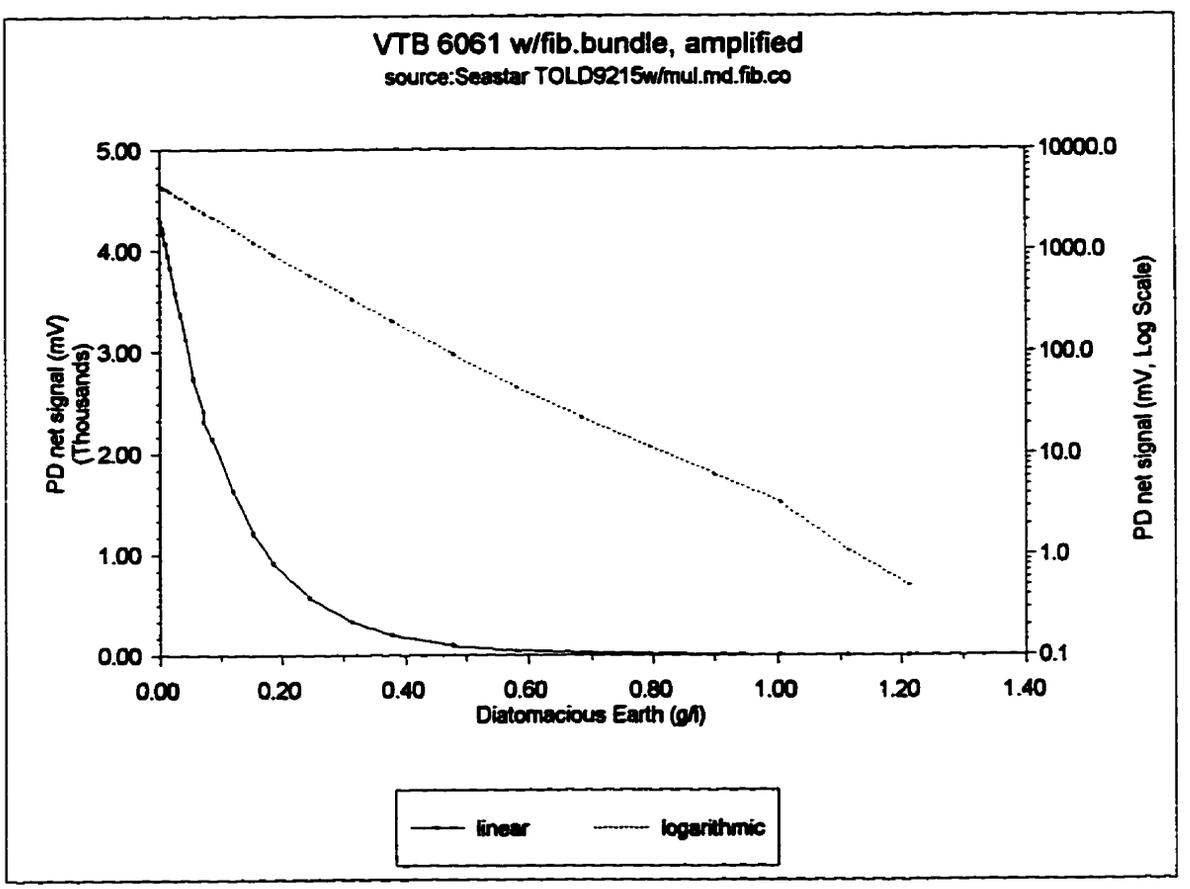

Figure 4.9: 10 mW Diode Laser - Fiber Collimator with

Amplified Photodiode - Light Guide

Testing TSL230 detector subassembly with the TOLD9215/NSG multimode source subassembly produced a maximum linear measurable concentration of approximately 1000 mg/l, and a maximum nonlinear measurable concentration greater than 1470 mg/l (see Fig. 4.11).

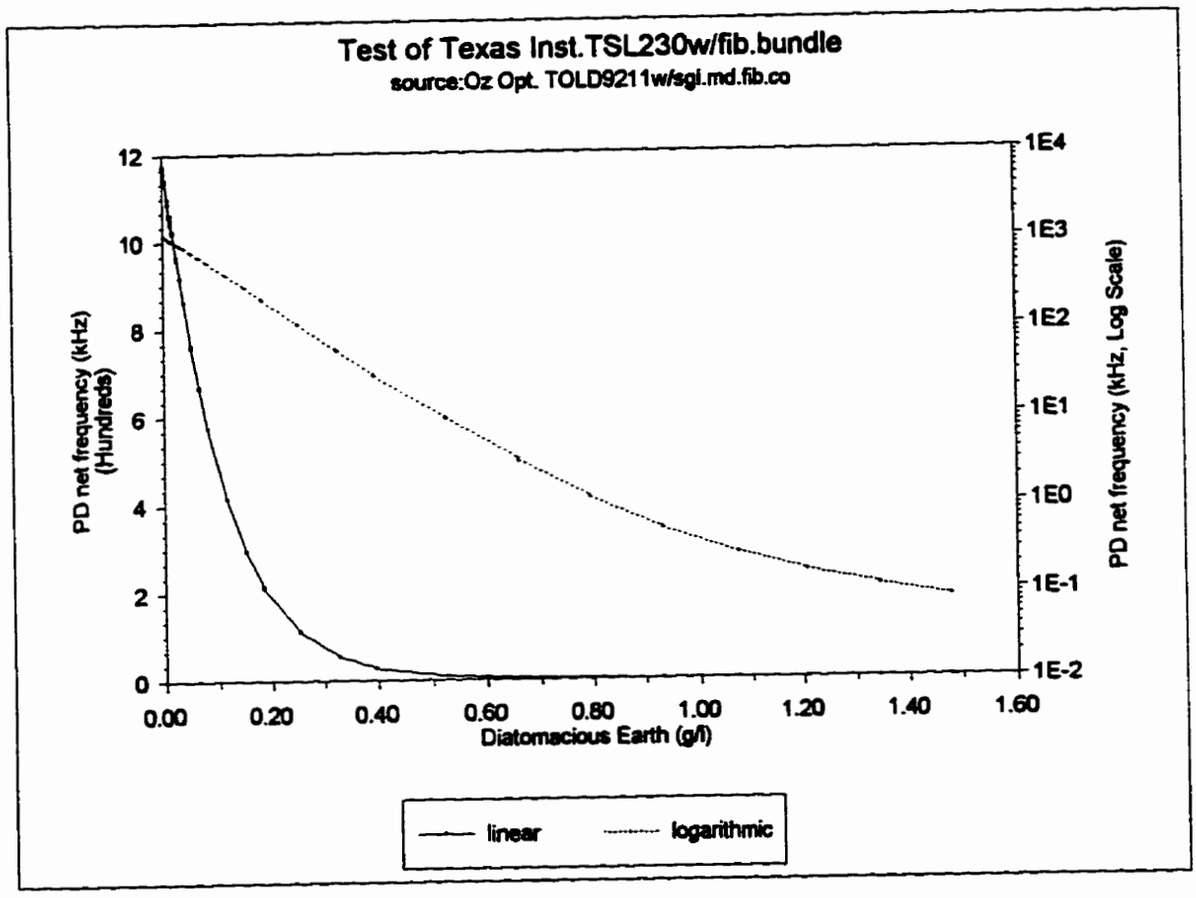

Figure 4.10: 3mW Diode Laser - Fiber Collimator with Integated Circuit

Detector - Light Guide

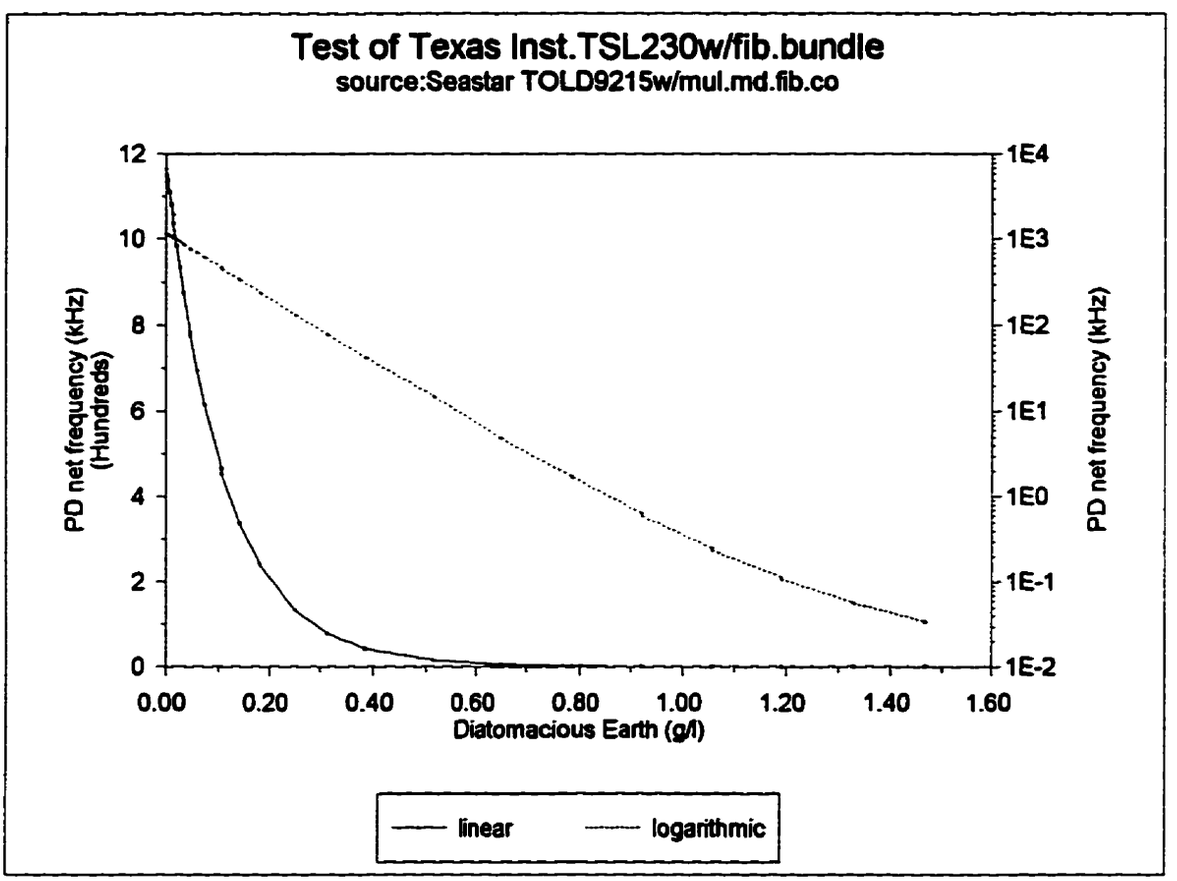

Figure 4.11: 10 mW Diode Laser - Fiber Collimator with Integrated Circuit Detector - Light Guide

CHAPTER 5

Component Selection and Adaptation

Testing of the candidate source and detection components produced well-defined, although contextually sensitive, selection parameters for choosing those components which would ultimately be used to construct the prototype turbidimeter head. The opto-electronic assemblies selected on a cost/benefit basis were the Toshiba TOLD 9215 laser source fitted with the NSG multimode fiber collimator, and the Texas Instruments TSL 230 integrated light-to-frequency converting circuit fitted with a multi-fiber light guide.

5.1 Incident Light Sources

The 980 nM infrared LED was unsuitable since this wavelength is apparently absorbed by water. Although the 660 nM visible LED produced an order of magnitude increase in maximum signal strength, the output beam divergence resulted in an unacceptable degree of non-linearity in the detector response at higher solids concentrations. The poorly defined output beam of light emitting diodes in general made them less adaptable for use with optical fiber. The superior beam quality of the visible laser diode produced a substantial increase in the maximum signal intensity at the detector. The well-defined output of the diode laser is imminently suitable for launching into optical fiber.

The use of fiber optic collimators had a mixed impact. There was a negligible reduction in incident light intensity at low concentrations. However, a definite reduction in the concentration range of the system occurred. This was the result of "spatial filtering" at the laser-fiber interface which significantly reduced the amount of stray, off-axis light

produced by the fiber collimator.

The Toshiba TOLD 9211 diode laser, singlemode fiber collimator assembled by Oz Optics Ltd. performed well, but achieved its performance through the the use of relatively sophisiticated and expensive optics. This light source design would not benefit significantly from the economies of increased production and as such was considered too expensive. The Toshiba TOLD 9215 with an NSG multimode fiber collimator was the most intense incident light source tested. Although the beam quality of the multimode fiber collimator was inferior to that of the singlemode fiber collimator, the difference was insignificant when weighed against the fact that the multimode design benefits from the economies of volume production. Thus the Toshiba TOLD 9215 with the NSG multimode fiber colimator was chosen as the incident light source subassembly for the prototype.

5.2 Photodetectors

The Skanamatic P33008 phototransistor was found to be generally unsuitable in the current application. Aside from its mechanical shortcomings, its performance was limited by its high intensity saturation response, and its nonlinear response curve at lower concentrations.

The photodiode had better operating characteristics than the phototransistor. It did not saturate with even the most intense source under test and exhibited a broader linear range (LOG (signal) vs. concentration-relationship). However, it produced a much smaller output signal. This required amplification, which introduced a nonlinearity.

Fiber collimators (in the detection application, this optic is properly termed a "focuser", since it collects a light beam and focuses it onto the end of an optical fiber) were too alignment-sensitive for the testing apparatus and therefore the alignment tolerance was likely too critical for economical manufacturing.

The fiber bundle light guide with photodiode produced a viable subassembly, although it suffered from the photodiode's shortcomings.

The light-intensity-to-frequency converter, the TSL 230, in combination with the fiber bundle light guide, resulted in the most cost effective, functional detector assembly. This assembly would require the fabrication of a custom adapter/mount linking the fiber light guide to the detector chip.

5.3 The Design and Construction of the Prototype:

To complete the prototype required the fabrication of a detection subassembly, and the fitting of the fiber end of the detection and incident light assemblies to the sensing head.

The detection subassembly was completed with the design and fabrication of an interfacing connector to join the fiber bundle to the detector. This connector (see Fig. 5.1) rigidly secured the fiber bundle to the chip while allowing the fiber bundle end to be "aimed" at the photo-sensitive area of the detector.

The fitting of the opto-electronic components to the sensing head required the design and fabrication of two mechanical adapters, one to fit the output end of the fiber collimator to sensing head, and one to fit the input end of fiber light guide to sensing head. These adapters took the form of brass bushings externally threaded to 3/8 X 24

UNF (to mate with threads in sensing head) and bored to mate with the exterior contours of the fiber collimator and fiber bundle (see Fig. 5.2 and Fig. 5.3).

The only modification to the sensing head required to allow completion was increasing the diameter of the wiring channel from 1/4 inch to 3/8 inch to accommodate the additional thickness of the fiber optic bundle (see Fig. 5.4 for sketch of modified sensing head showing fiber optic components installed).

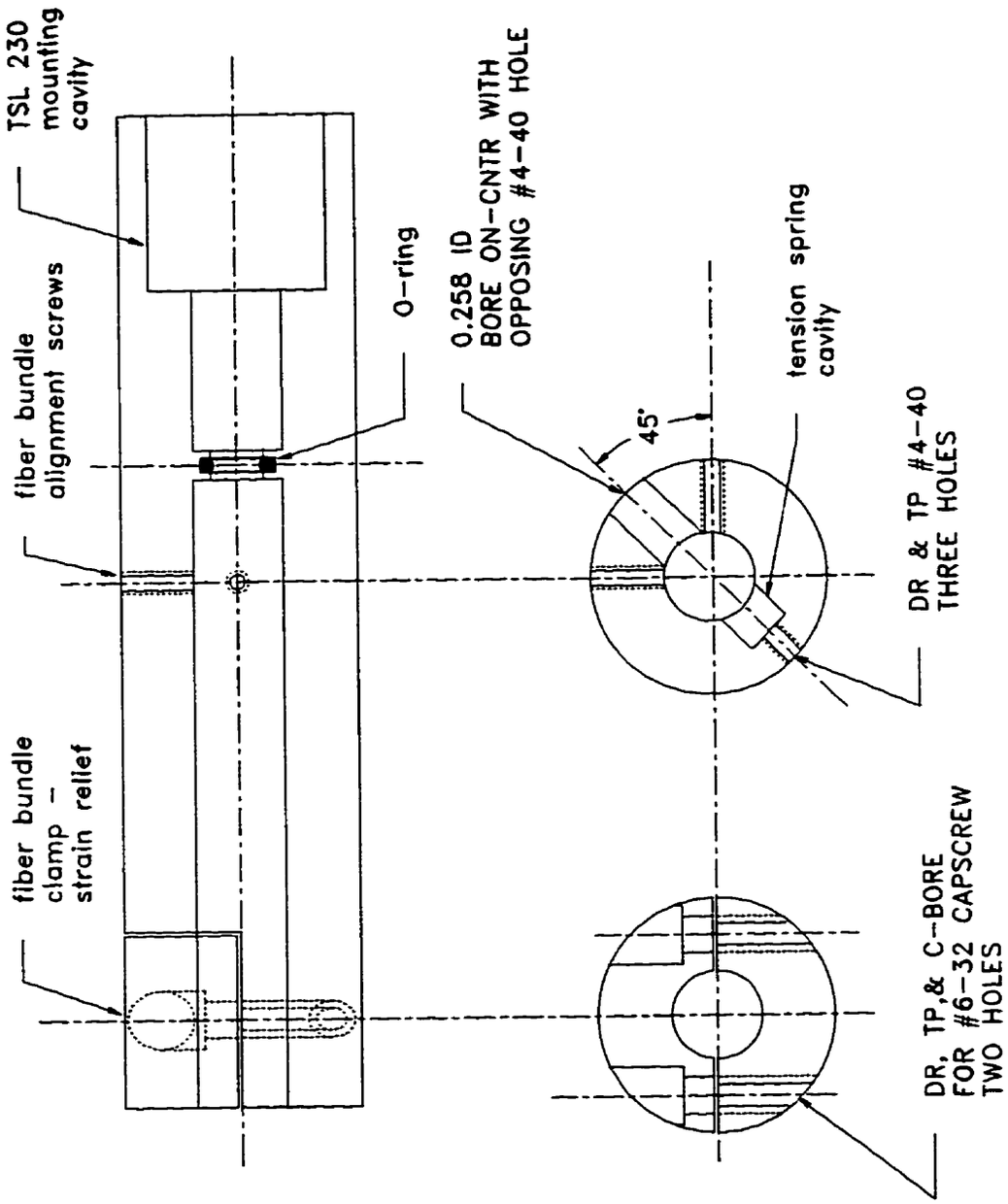

Figure 5.1a: Fiber Bundle - TSL230 Detector Adapter

a) Sectioned View Through Centre Line

b) Sectioned View Through Clamping and Alignment Sections

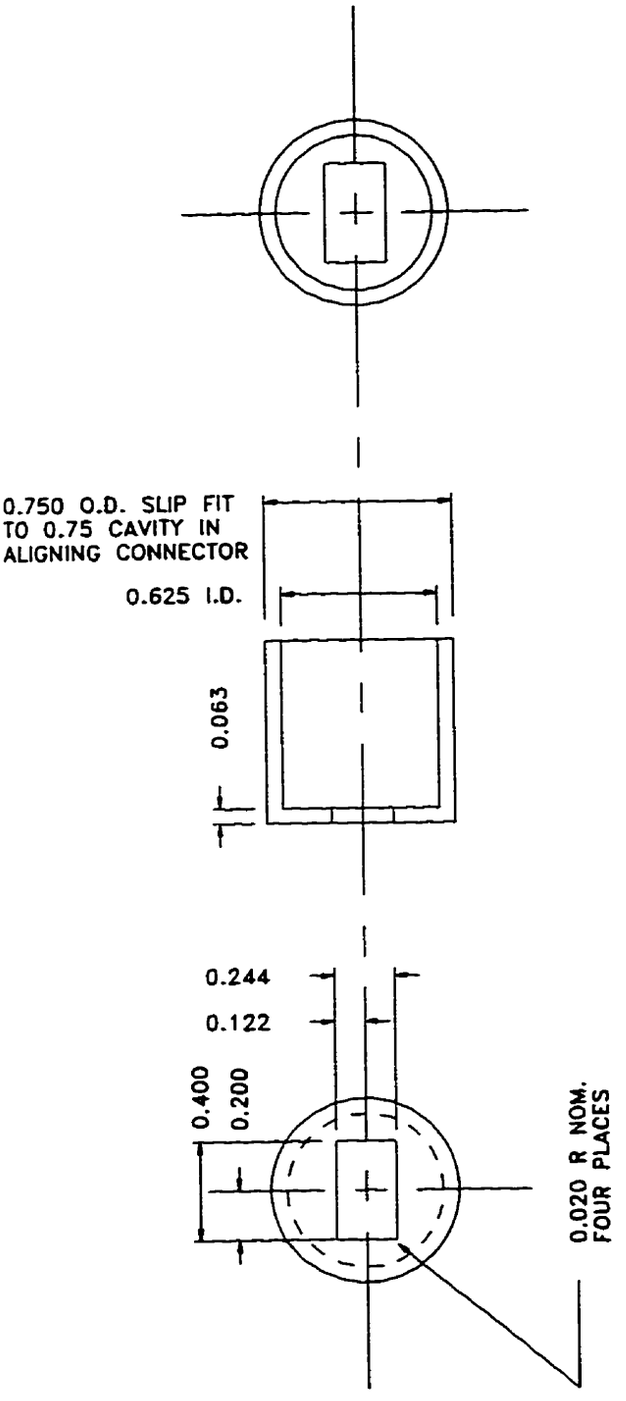

Figure 5.1b: Mount for TSL230 (Dimensions in Inches)

End and Sectional Views Through Centreline

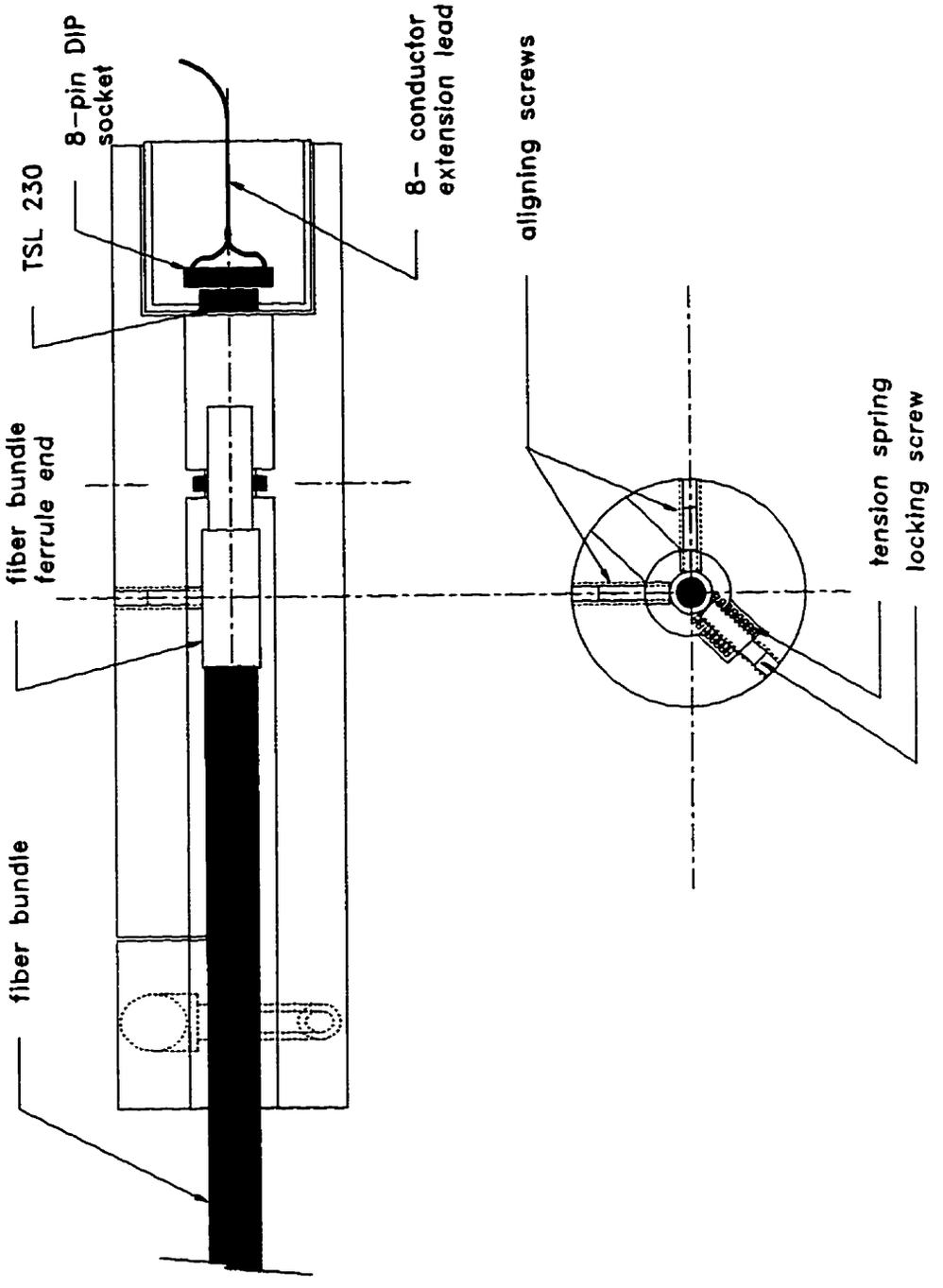

Figure 5.1c: Fiber Bundle - Detector Adapter

Sectioned Views Showing Fiber Bundle and TSL230 Location

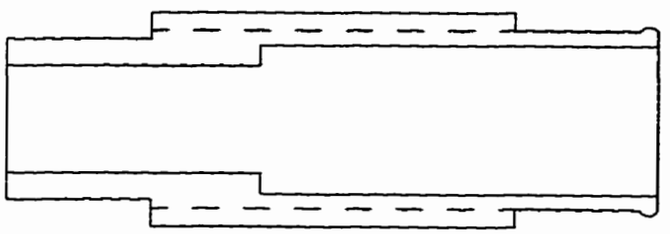

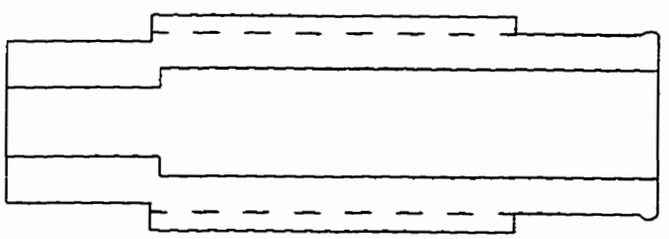

Figure 5.2 Fiber Bundle - Flushing Insert Adapter

Figure 5.3 Fiber Collimator - Flushing Insert Adapter

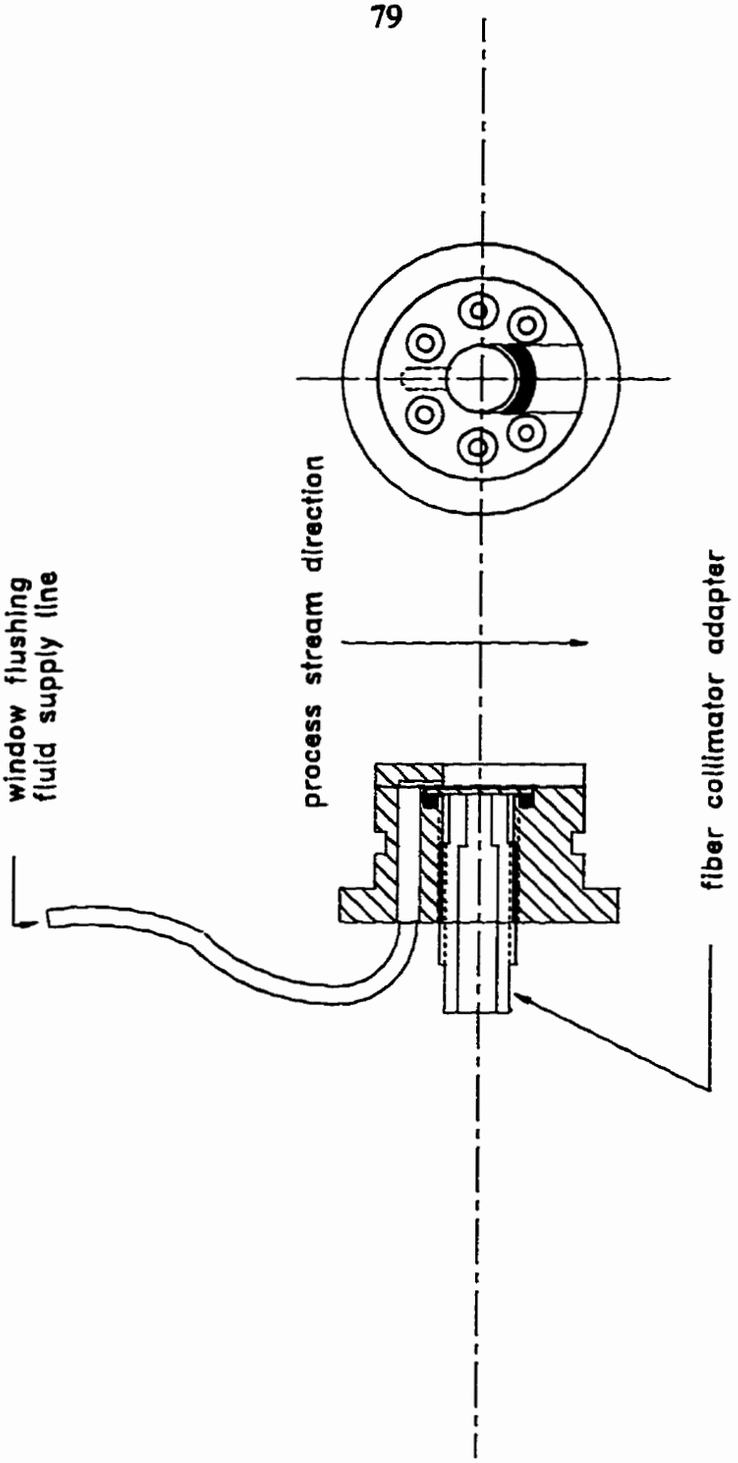

Figure 5.4a: Fiber Collimator Adapter Installed in Flushing Insert

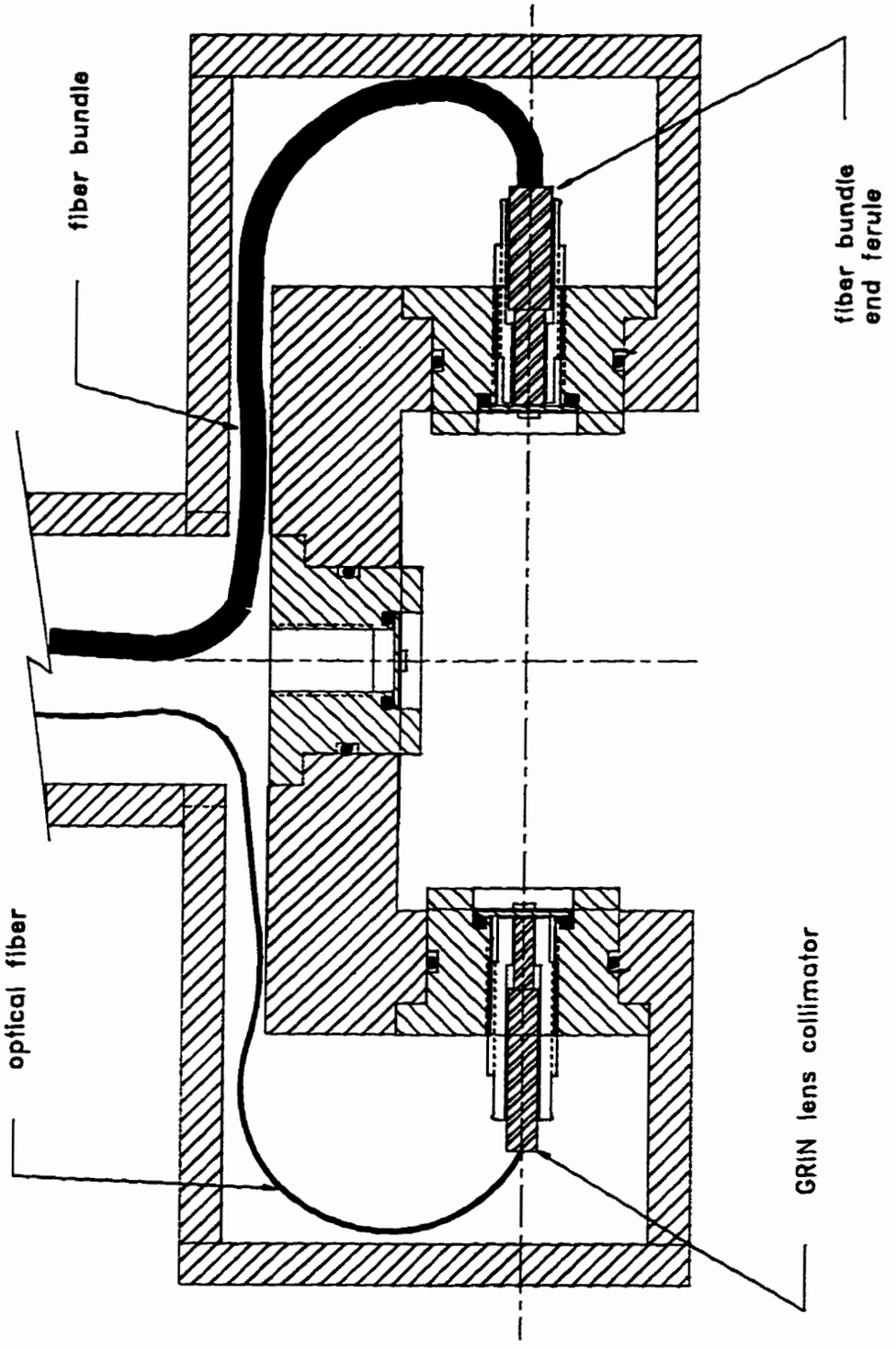

Figure 5.4b: Optical Fiber Source and Detection Components Installed in Sensing Head

5.4 Design Recommendations

In the course of creating the prototype, certain concessions and compromises were made. This was done to allow for the greatest possible flexibility in component selection, and to conform with the requirement that modifications to existing sensing head be kept to a minimum. By fixing the opto-electronic subassembly components, and allowing for the redesign of the sensing head, the manufacturing processes could be greatly simplified.

5.4.1 Incident Light Source

The diode laser and fiber collimator of the prototype subassembly are mechanically connectorized and therefore separable. This feature was adopted to allow for the convenient replacement of the laser at the circuit board. However, since current laser diodes have expected lifetimes in excess of 20,000 hours, failure of the laser diode becomes an unlikely event. Fixing, or "pigtailing" the fiber collimator directly to the laser diode eliminates the connector, and one alignment step. A secondary benefit would be the reduction of the losses associated with launching light through the connector, which would allow the use of a lower powered laser diode.

5.4.2 Detector

The interfacing adapter used to join the fiber bundle to the TSL 230 could be radically simplified to a plastic bushing with alignment and strain-relief provided by a rigid adhesive. The detector chip is so inexpensive that in the event of damage or failure of the fiber bundle, the entire optical subassembly could be discarded.

5.4.3 Sensing Head

The bulk and complexity of the sensing head could easily be reduced by the elimination of several redundant fixtures. On the incident beam side, the flushing insert could be modified to accept the collimator ferrule without an intervening adapter. Since the collimator was specified to be waterproof, the window could also be eliminated.

On the detector side, similar modifications could be made. The elimination of the window would require a fiber bundle with a fused end since the light guide currently used is not specified as being waterproof.

Fabricating the sensor body to include the optical aperture flushing function would eliminate the flushing inserts. This would permit a sufficiently close tolerance to be applied to bore locations for the incident beam collimator and detection fiber bundle that alignment between these components would become intrinsic to the sensor body.

CHAPTER 6

CONCLUSIONS

At the outset of this research, four technical objectives were to be met: 1) the range of the instrument was to be increased from 5 - 200 Jackson Turbidity Units to 0 - 2000 Jackson Turbidity Units; 2) the accuracy of the instrument was to be improved from 5% of calibrated range to 1 % of calibrated range; 3) the incident light source would be a semiconductor laser of less than 750 nanometer wavelength; and, 4) the light signal would be transmitted to and from the sensing head using optical fiber. All four technical objectives were met with some degree of success. A 680 nanometer diode laser was used as an incident light source, and the incident light and attenuated signal were transmitted to and from the sensing head with optical fiber. The objective of increasing the operating range to 0 - 2000 JTU with 1% accuracy was not realized. However, a range of 0 - 1000 JTU with 1% accuracy was achieved.

CHAPTER 7

Recommendations for Further Study

During the process of upgrading the Claritek SM8830 to a more current technological standard, questions and problems regarding various system components beyond the scope of this thesis remain unaddressed. In addition, other novel applications of the technology to real-world problems were frequently suggested.

7.1 Claritek SM8830 System Components

The fiber collimators were ordered from the fabricators with the stipulation that they be suitable for submerged applications, in other words, that the collimating GRIN lens and the lens-fiber interface be "waterproof". It would be useful to research the stability of the sealing and bonding compounds in various system liquids. Accelerated life testing of fiber collimators would provide information regarding anticipated lifespans, modes of failure, and symptoms of failure or incipient failure. Similarly, such research and testing could be applied to the GRIN lens, the optical fiber, and the fiber bundle. In the latter case, finding the end face of the fiber bundle to be inert to some, or most system fluids would eliminate the need for a window, simplifying the design of the sensing head.

Another area which would benefit from further investigation is the mechanism of achieving and maintaining alignment during assembly and use, (respectively), between the incident collimator and detection fiber bundle. At present, this alignment is achieved by allowing a liberal tolerance in the collimator mount to permit the incident beam to be manually centred on the end face of the fiber bundle. By specifying the maximum

deviation between the optical output axis and the mechanical axis of the collimator, in combination with a suitable tolerance for the collimator mounting bore in the sensing head, the need for manual alignment of the incident beam with the detection fiber bundle could be eliminated.

7.2 Other Applications of System Components

The system components used in the turbidity meter could be readily adapted to the detection or measurement of gas -, or air-borne suspended particles. Such a device could be applied to the measurement of engine particulate emissions, fog or visibility detectors, and smokestack-or duct-mounted particulate detectors.

One novel application of the system components was a single-ended turbidimeter or nephelometer. This device would measure particle concentrations by the amount of light reflected back to a detector (or light guide) near the incident light source. Since such a device requires no alignment, it would be mechanically quite simple.

REFERENCES

1. Allen, T. "Particle Size Measurement" 3rd ed., 1981, Chapman and Hall.
2. Gulari, E., Annaprogada, A., Jaward, B., In "Particle Size Distribution" Theodore Provder, ed., ACS Symposium Series 332, 1987, p. 133-145.
3. Frock, H.N. - ibid - p. 146-160.
4. Whipple G.C., D.D. Jackson, Mass. Inst. Technol. Quart. vol. 13, 1900, pp 274.
5. (-) "Claritek Model SM8830 Suspend Solids Transmitter User Manual" 1992, Revision 2.1, Claritek Instruments Ltd.
6. (-) "Suspended Solids and Turbidity Monitor" Application Notes, 1990, Claritek Instruments Ltd.
7. (-) "Skanamatic Product Catalog", 1988, Electro Corporation
8. (-) "IRAP Research Development Proposal", 1993, Arjay Engineering.
9. (-) "SELFOC Product Guide", 1989, NSG America Inc.
10. (-) "Optics Guide 5", 1990, Melles Griot Inc.
11. (-) "Optoelectronics Device Data" 3rd Revision, 1989, Motorola Inc.
12. Zelinger, G., Electronic Product News, Apr. 1986, p. 42-48.
13. (-) "Optoelectronics Data Book - Silicon Photodiodes", 1990 EG&G VACTEC.
14. (-) "Photodiodes, 1990-1991 Catalog", 1991, Hamamatsu Photonics K.K. Solid State Division.
15. Zelinger, G., Electronic Product News, July 1986, p. 22-25
16. Ilett, T., Canadian Electronics Engineering, Nov. 1985, p. 32-36.
17. Siegmund, W.P., Holliday, C.T. "Fiber Optics Comes of Age", Proceedings of

Society of Photo-optical Instrumentation Engineers, vol. 31, 1972.

18. Weast, R.C., Handbook of Chemistry and Physics, 56th ed., 1975-1976, CRC Press

19. Matsushita, K., Ideda, K., Proc. SPIE, vol 31, 1972, p. 23-35

20. Perlicki, K., Beblowska, M., Kruszewski, J. Proc. Soc. Photo Optical Instrum. Eng., Vol 2634, pp. 186-190, 1994.

21. Jarnstuom, L., Lasan, L, Rigdahl, M., Colloids and Surfaces A: Physico chemical and Engineering Aspects v. 104, n2-3 1995, pp. 191-205, 207-216.

22. Feng, L., Fan M., Hongwas Jishu/ Infrared Technology, v 15, n 3, 1993, p. 35-36

23. Crowther, J.M., J.F. Dalrymple, Ibid, pp. 229-235.

24. Werner P., Hambech, B. Water Supply v4, n3, 1986 p. 227-232.

25. Kleizen H.N., et al. Filtration and Separation v 32, n9, 1995 p. 897-901.

26. Chu, B., "Laser Light Scattering", 2nd ed., 1991, Academic Press Inc.

27. Miran H.H., et al., Measurement Science & Technology, V5, n6, 1994,p. 685-693.

28. Ortmanis, A. et al., Enzyme and Microbial Technology V13, n6, 1991, p. 450-455.

29. Brown, C.M. et al, J. of Crystal Growth, v 108, n3-4, 1991, p. 455-464.

30. Roebeck, G.C., Jeffrey e.A., Proc. AWWA Seminar on minimizing and recycling water plant sludge, 1973 pp I1-I21.

31. Sangodoyin, A.Y., Int. J. Environmental Studies A/B V 48, n 3-4, 1995, p. 257-262.

32. Spencer, C.M., Collins, M.R., Journal American Water Works Assoc. V. 87, n 12, 1995, p. 71-82.

33. Riesenberg, F. et al., ibid p. 48-56.

34. Kuo, J.F. et al., Water Environment Research, V. 66, n7, 1994 p. 879-886.

35. Lin, S.H., Peng, C.F., Water Research, V 30, n3, 1996 p. 587-592.

36. Valeur, J.R. et al., Proc. 1995 Int. Conf. on Coastal Research in Terms of Large Scale Experiments, p. 951-962.

37. Bates, A.B., Proc. Institution of Civil Eng., Water, Maritime and Energy, V/18, n1, 1996, 1-9.

38. Rodger, A.J., Delisio, E., Proc. national Conference on Hydraulic Engineering, p. 865-869.

39. Effler, S.W., Johnson, D.L. Water Resources Bulletin, V23, n1, 1987, p. 73-79.

40. Yamane, T., Biotechnology Progress, V9, n1, 1993, p. 81-85.

41. Makoto, S. et al., J. Chem. Technol Biotechnol. V40, n3, 1987, p. 203-213.

42. McCormick, C.L. et al., Polymer, V27, n12, 1986 p. 1976-1980.

43. Tan, J.S., Handel, T.M., Polymer Science and Technology "Microdomains in Polymer Solution" Vol. 30 1985 p. 417-427.

44. Koetz, J. et al., Polymer V27, n10, 1986, p. 1574-1580.

45. Besombes, M. et al., J. Polymer Science, Part B: Polymer Physics V26, n9, 1988, p. 1881-1896.

46. Bottero, J.Y. et al., J. of Colloid and Interface Science, V124, n2, 1988, p. 515-527.

47. ASTM Standard

48. Amann, J.P., Papcosta, K., Proc. Water Quality Technology Conference, Houston, TX 1985, p. 575-581.

49. Pickering, R.J., U.S. Geological Survey, Report 76-153, pp. 1-7 (1976).

50. Ronald, J., Zeneveld, V., Spinrad, R.W., Barytz, R. Proc. Soc. Photo-Optical Instrum. Eng., Vol. 208, 1979, pp. 159-168.

51. Mack, Stephen, F. "Using Turbidity to predict total Suspended Solids and Mined Streams in Interior Alaska", 1988, State of Alaska Dept. of Natural Resources, Division of Geological and Geophysical Surveys.

52. Yamamoto, S., Sato, K., Hatono, Y., Nippon Kikai Gakkai Ronbunshu, C. Hen, V 53, n491, 1987 p. 1450-1453.

53. Garcia-Rubio, L.H., ACS Symposium Series V332, p. 161-178.

54. Weiss, S., Photonics Spectra, Vol. 28, Issue 9, 1994, p. 39-40

55. (-), "TSL230, TSL230A, TSL230B Programmable Light-to-Frequency Converters, Product Data Information Sheet, Texas Instruments Inc. SOES007B, 1994.

56. (-) Application Notes, 1992, Oz Optics Ltd.

57. (-) "Optical Devices and Laser Diode Instrumentation, Product Catalog" Revision 3, 1993, Seastar Optics Inc.

58. (-) "Visible Laser Product Guide 650 nm to 690 nm", 1992, Toshiba America Electronic Components Inc.

59. Milburn, D.I., Hollands, K.G.T., Solar Energy, Vol. 55, No. 2, (1995) p. 85-91.

60. -Ibid- Solar Energy, Vol. 52, No. 6 (1994) p. 497-507.

61. -Ibid- Proceedings, Windows Innovation '95 Conference, June 1995, p. 60-71.

62. -Ibid- Optics Communications, v. 115, p. 158-169.

63. -Ibid- Optics Communications, v. 118, p. 1-8.

APPENDIX

Contents **Page**

Glossary: The following terms and descriptions apply to the tables of experimental data contained in this appendix

weight add'n (g) : the weighed increment of diatomaceous earth, in grams, added to the slurry

weight sum (g) : the sum total of weighed increments of diatomaceous earth in the slurry

concent. (g/l) : the sum total of diatomaceous earth in the slurry divided by the volume volume of slurry (generally 1.5 liters) yielding concentration in grams per liter

current (mA) : the total signal of a reverse-biased phototransistor or photodiode including that attributed to ambient light, in milliamperes; - generally directly related to the light intensity impinging on the detector, or, inversly related to the attenuating slurry concentration

P.D. signal (mV) : the signal of an amplified photodiode, in millivolts; as above

frequency (kHz) : the signal of the light intensity -to- frequency converter integrated circuit, in thousands of cycles per second; as above

current LED off : the background signal from a reverse-biased phototransistor or photodiode with the incident light source blocked or turned off, in milliamperes; attributed to ambient light scattering onto the detector

P.D. signal LD off (mV) : as above, from amplified photodiode, in millivolts

frequency LD off (kHZ) : as above, from light intensity-to-frequency converter

net current : the result of subtracting the background signal (current LED off) from the total signal (current (mA)) yielding the attenuated light intensity signal of a reverse-biased phototransistor or photodiode, in milliamperes

net signal (mv) : as above, from amplified photodiode, in millivolts

net frequency : as above, from light intensity-to-frequency converter, in thousands of cycles per second

air only : refers to attenuating condition at start of some tests; allows the measurement of light intensity with minimum attenuation and measurement of ambient scattered onto detector by nearby objects and equipment

tank only : refers to attenuating condition produced by empty test cell (tank), allows measurement of attenuation of incident light beam, and scattering of ambient light onto detector attributable to cell walls

tank/water : as above with only deionized water in cell

Preliminary test of IR LED
09/15/93

weight add'n (g)	concent. (g/l)	current (mA)
0	0	0.766
0.0017	0.0011333	0.762
0.0049	0.0032667	0.754
0.0097	0.0064667	0.738
0.0198	0.0132	0.704
0.0375	0.025	0.651
0.0715	0.0476667	0.562
0.136	0.0906667	0.417
0.263	0.1753333	0.24
0.5154	0.3436	0.077
1.0152	0.6768	0.0119
2.0159	1.3439333	0.0011
3.0139	2.0092667	0.0005

Preliminary test of visible LED
09/09/93

weight (g)	concent. (g/l)	current (mA)
0	0	8.95
0.0057	0.0038	8.68
0.0095	0.0063333	8.48
0.0193	0.0128667	8.04
0.0293	0.0195333	7.57
0.0765	0.051	5.8
0.1274	0.0849333	4.42
0.2261	0.1507333	2.58
0.326	0.2173333	1.5
0.8279	0.5519333	0.116

Preliminary test of visible LED
09/15/93

weight (g)	concent. (g/l)	current (mA)
0	0	7.48
0.0023	0.0015333	7.38
0.0058	0.0038667	7.28
0.0117	0.0078	7.07
0.0222	0.0148	6.61
0.0422	0.0281333	5.98
0.0838	0.0558667	4.78
0.1626	0.1084	3.18
0.3258	0.2172	1.39
0.6471	0.4314	0.292
1.657	1.1046667	0.0055
2.1638	1.4425333	0.0019
2.6607	1.7738	0.0012
3.6519	2.4346	0.0007
4.1613	2.7742	0.0006

Preliminary test of ALPEC laser
10/09/93

weight add'n (g)	concent. (g/l)	current (mA)
0	0	54.7
0.0017	0.0011333	54.55
0.0047	0.0031333	54.6
0.0093	0.0062	54.5
0.0195	0.013	54.45
0.039	0.026	54.3
0.0795	0.053	54.05
0.1606	0.1070667	53.35
0.3217	0.2144667	38.85
0.6436	0.4290667	5.965
1.2917	0.8611333	0.212
2.5856	1.7237333	0.0041
3.088	2.0586667	0.0025
4	2.6666667	0.0015
5	3.3333333	0.0011

Test of infrared LED
Dec1295
Light source: Skanamatic L33014 IRLED
Detector: Skanamatic P33008 phototransistor
Source current: ~45%; 45.0mA
P.D. bias voltage: 10 vDC

weight add'n (g)	weight sum (g)	concent. (g/l)	current (mA)	current LEDoff	net current
air only		0	1.734	0.009	
tank/water		0	0.529	0.009	0.52
0.0012	0.0012	0.0008	0.528	0.008	0.52
0.0009	0.0021	0.0014	0.526	0.008	0.518
0.0013	0.0034	0.00227	0.52	0.007	0.513
0.0007	0.0041	0.00273	0.519	0.007	0.512
0.0007	0.0048	0.0032	0.518	0.007	0.511
0.0054	0.0102	0.0068	0.504	0.007	0.497
0.0005	0.0107	0.00713	0.503	0.006	0.497
0.0007	0.0114	0.0076	0.502	0.007	0.495
0.0051	0.0165	0.011	0.493	0.007	0.486
0.0008	0.0173	0.01153	0.49	0.007	0.483
0.0011	0.0184	0.01227	0.487	0.006	0.481
0.0047	0.0231	0.0154	0.478	0.006	0.472
0.0015	0.0246	0.0164	0.476	0.006	0.47
0.0014	0.026	0.01733	0.473	0.006	0.467
0.0102	0.0362	0.02413	0.45	0.006	0.444
0.0022	0.0384	0.0256	0.447	0.006	0.441
0.0022	0.0406	0.02707	0.443	0.006	0.437
0.011	0.0516	0.0344	0.421	0.006	0.415
0.0036	0.0552	0.0368	0.414	0.006	0.408
0.0023	0.0575	0.03833	0.408	0.006	0.402
0.013	0.0705	0.047	0.385	0.006	0.379
0.0031	.0.0736	0.04907	0.38	0.006	0.374
0.0027	0.0763	0.05087	0.375	0.007	0.368
0.0166	0.0929	0.06193	0.349	0.007	0.342
0.0051	0.098	0.06533	0.343	0.006	0.337
0.0044	0.1024	0.06827	0.333	0.006	0.327
0.0153	0.1177	0.07847	0.309	0.007	0.302
0	0.1177	0.07847	0.316	0.012	0.304

0.0026	0.1203	0.0802	0.311	0.013	0.298
0.0029	0.1232	0.08213	0.309	0.014	0.295
0.0196	0.1428	0.0952	0.284	0.012	0.272
0.0049	0.1477	0.09847	0.275	0.012	0.263
0.0019	0.1496	0.09973	0.272	0.012	0.26
0.0177	0.1673	0.11153	0.251	0.011	0.24
0.0041	0.1714	0.11427	0.246	0.011	0.235
0.0018	0.1732	0.11547	0.242	0.011	0.231
0.002	0.1752	0.1168	0.241	0.012	0.229
0.0193	0.1945	0.12967	0.222	0.012	0.21
0.005	0.1995	0.133	0.218	0.012	0.206
0.0045	0.204	0.136	0.213	0.012	0.201
0.0205	0.2245	0.14967	0.199	0.014	0.185
0.0051	0.2296	0.15307	0.19	0.011	0.179
0.0036	0.2332	0.15547	0.187	0.011	0.176
0.0203	0.2535	0.169	0.172	0.011	0.161
0.004	0.2575	0.17167	0.169	0.01	0.159
0.0043	0.2618	0.17453	0.164	0.01	0.154
0.0237	0.2855	0.19033	0.15	0.01	0.14
0.0045	0.29	0.19333	0.148	0.011	0.137
0.0053	0.2953	0.19687	0.144	0.011	0.133
0.0254	0.3154	0.21027	0.129	0.01	0.119
0.0066	0.322	0.21467	0.126	0.01	0.116
0.0056	0.3276	0.2184	0.123	0.01	0.113
0.0226	0.3502	0.23347	0.112	0.01	0.102
0.0052	0.3554	0.23693	0.107	0.009	0.098
0.0042	0.3596	0.23973	0.106	0.009	0.097
0.0242	0.3838	0.25587	0.097	0.009	0.088
0.0054	0.3892	0.25947	0.095	0.009	0.086
0.0059	0.3951	0.2634	0.093	0.009	0.084
0.0257	0.4208	0.28053	0.084	0.009	0.075
0	0.4208	0.28053	0.099	0.03	0.069
0.0057	0.4265	0.28433	0.096	0.03	0.066
0.0073	0.4338	0.2892	0.094	0.031	0.063
0.0246	0.4584	0.3056	0.088	0.031	0.057
0.0106	0.469	0.31267	0.085	0.031	0.054
0.0073	0.4763	0.31753	0.084	0.031	0.053
0.0387	0.515	0.34333	0.076	0.031	0.045

0.0135	0.5285	0.35233	0.074	0.031	0.043
0.0108	0.5393	0.35953	0.072	0.031	0.041
0.0318	0.5711	0.38073	0.067	0.031	0.036
0.0159	0.587	0.39133	0.064	0.031	0.033
0.0124	0.5994	0.3996	0.062	0.031	0.031
0.0376	0.637	0.42467	0.058	0.031	0.027
0	0.637	0.42467	0.048	0.022	0.026
0.017	0.654	0.436	0.046	0.022	0.024
0.0162	0.6702	0.4468	0.044	0.021	0.023
0.0449	0.7151	0.47673	0.04	0.021	0.019
0.0192	0.7343	0.48953	0.039	0.021	0.018
0.0204	0.7547	0.50313	0.037	0.021	0.016
0.0538	0.8085	0.539	0.034	0.021	0.013
0.0272	0.8357	0.55713	0.032	0.021	0.011
0.0213	0.857	0.57133	0.031	0.02	0.011
0.072	0.929	0.61933	0.029	0.02	0.009
0.106	1.035	0.69	0.026	0.02	0.006
0.1479	1.1829	0.7886	0.023	0.02	0.003
0.1863	1.3692	0.9128	0.021	0.019	0.002
0.1947	1.5639	1.0426	0.021	0.019	0.002

Test of visible LED
111194
Light source: Skanamatic L33008 vis. LED
Detector: Skanamatic P33008 phototransistor
LED current: 90% 45.0 mA
P.D. bias voltage: 10 vdc

weight add'n (g)	weight sum (g)	concent. (g/l)	current (mA)	current LEDoff m	net current
air only		0	8.01		
tank only		0	6.1	0.019	6.081
tank/water		0	9.58	0.007	9.573
tank/water		0	9.55	0.016	9.534
tank/water		0	9.58	0.016	9.564
0.0011	0.0011	0.0007333	9.52	0.016	9.504
0.0007	0.0018	0.0012	9.47	0.016	9.454
0.0015	0.0033	0.0022	9.39	0.016	9.374
0.0008	0.0041	0.0027333	9.35	0.0102	9.3398
0.001	0.0051	0.0034	9.3	0.0102	9.2898
0.0044	0.0095	0.0063333	9.1	0.0102	9.0898
0.001	0.0105	0.007	9.06	0.0102	9.0498
0.0012	0.0117	0.0078	9.01	0.0074	9.0026
0.0013	0.013	0.0086667	8.92	0.0074	8.9126
0.0037	0.0167	0.0111333	8.73	0.0074	8.7226
0.0011	0.0178	0.0118667	8.67	0.0081	8.6619
0.0014	0.0192	0.0128	8.63	0.0081	8.6219
0.0048	0.024	0.016	8.42	0.0081	8.4119
0.0006	0.0246	0.0164	8.44	0.0079	8.4321
0.0009	0.0255	0.017	8.41	0.0079	8.4021
0.0014	0.0269	0.0179333	8.35	0.0075	8.3425
0.0102	0.0371	0.0247333	7.88	0.0075	7.8725
0.0021	0.0392	0.0261333	7.78	0.0075	7.7725
0.0014	0.0406	0.0270667	7.73	0.0069	7.7231
0.0096	0.0502	0.0334667	7.34	0.0069	7.3331
0.0012	0.0514	0.0342667	7.27	0.0065	7.2635
0.0015	0.0529	0.0352667	7.21	0.0065	7.2035
0.0174	0.0703	0.0468667	6.54	0.0065	6.5335
0.0012	0.0715	0.0476667	6.5	0.0064	6.4936
0.0015	0.073	0.0486667	6.44	0.0064	6.4336

0.0227	0.0957	0.0638	5.66	0.0064	5.6536
0.0017	0.0974	0.0649333	5.61	0.0066	5.6034
0.0018	0.0992	0.0661333	5.57	0.0066	5.5634
0.0297	0.1289	0.0859333	4.75	0.0066	4.7434
0.0009	0.1298	0.0865333	4.71	0.0077	4.7023
0.0021	0.1319	0.0879333	4.66	0.0077	4.6523
0	0.1319	0.0879333	4.64	0.0054	4.6346
0.0204	0.1523	0.1015333	4.14	0.0054	4.1346
0.0014	0.1537	0.1024667	4.1	0.0054	4.0946
0.001	0.1547	0.1031333	4.08	0.0071	4.0729
0.0015	0.1562	0.1041333	4.06	0.0071	4.0529
0.0371	0.1933	0.1288667	3.33	0.0071	3.3229
0.0017	0.195	0.13	3.28	0.0073	3.2727
0.0035	0.1985	0.1323333	3.25	0.0073	3.2427
0.0416	0.2401	0.1600667	2.58	0.0073	2.5727
0.0034	0.2435	0.1623333	2.53	0.0076	2.5224
0.0016	0.2451	0.1634	2.51	0.0076	2.5024
0.0439	0.289	0.1926667	1.99	0.0076	1.9824
0.0027	0.2917	0.1944667	1.96	0.0079	1.9521
0.002	0.2937	0.1958	1.94	0.0079	1.9321
0	0.2937	0.1958	1.96	0.0099	1.9501
0.0402	0.3339	0.2226	1.56	0.0099	1.5501
0.0022	0.3361	0.2240667	1.53	0.0174	1.5126
0.0022	0.3383	0.2255333	1.5	0.0174	1.4826
0	0.3361	0.2240667	1.39	0.024	1.366
0.0408	0.3769	0.2512667	1.12	0.024	1.096
0.0027	0.3796	0.2530667	1.1	0.025	1.075
0.0031	0.3827	0.2551333	1.08	0.025	1.055
0.0702	0.4529	0.3019333	0.77	0.025	0.745
0.0032	0.4561	0.3040667	0.76	0.0265	0.7335
0.004	0.4601	0.3067333	0.73	0.0203	0.7097
0.069	0.5291	0.3527333	0.53	0.02	0.51
0.0071	0.5362	0.3574667	0.51	0.02	0.49
0.0056	0.5418	0.3612	0.49	0.021	0.469
0	0.5418	0.3612	0.435	0.011	0.424
0.0574	0.5992	0.3994667	0.322	0.0112	0.3108
0.0047	0.6039	0.4026	0.315	0.0112	0.3038
0.006	0.6099	0.4066	0.309	0.0113	0.2977

0.1014	0.7113	0.4742	0.194	0.0118	0.1822
0.0085	0.7198	0.4798667	0.186	0.0115	0.1745
0.0097	0.7295	0.4863333	0.177	0.0115	0.1655
0.0977	0.8272	0.5514667	0.118	0.0115	0.1065
0.0133	0.8405	0.5603333	0.112	0.0111	0.1009
0.0106	0.8511	0.5674	0.106	0.0111	0.0949
0.1384	0.9895	0.6596667	0.065	0.0112	0.0538
0.016	1.0055	0.6703333	0.06	0.0112	0.0488
0.0147	1.0202	0.6801333	0.057	0.0114	0.0456
0.1492	1.1694	0.7796	0.038	0.0119	0.0261
0	1.1694	0.7796	0.0345	0.009	0.0255
0.0194	1.1888	0.7925333	0.0336	0.009	0.0246
0.014	1.2028	0.8018667	0.0321	0.01	0.0221
0	1.2028	0.8018667	0.0348	0.0141	0.0207
0.1546	1.3574	0.9049333	0.0455	0.0334	0.0121
0.1541	1.5115	1.0076667	0.0251	0.0173	0.0078
0.2147	1.7262	1.1508	0.0323	0.0276	0.0047

Test of visible laser diode
+21/12/95
Light source: Imatronic 670/3 laser diode
Detector: Skanamatic P33009 photodetector
Source current: 75.0'mA (~4.8vdc)
P.D. bias voltage: 10 vDC

weight add'n(mg)	weight sum (g)	concent. (g/l)	current (mA)	current LEDoff m	net current
air only		0	92.1	0.0258	92.1
tank/water		0	87.2	0.0232	87.1768
2.7	0	0	87.1	0.0232	87.0768
0	0	0	87	0.0245	86.9755
2.6	0	0	86.6	0.0237	86.5763
2.1	0.0027	0.0018	86.4	0.0185	86.3815
1.8	0.0027	0.0018	86.2	0.0175	86.1825
1.3	0.0053	0.003533	85.9	0.016	85.884
1.2	0.0074	0.004933	85.8	0.016	85.784
0	0.0092	0.006133	86	0.0155	85.9845
1.2	0.0105	0.007	85.8	0.0155	85.7845
4.5	0.0117	0.0078	85.3	0.0165	85.2835
0	0.0117	0.0078	85	0.0195	84.9805
2.2	0.0129	0.0086	84.8	0.0195	84.7805
1.7	0.0174	0.0116	84.6	0.0195	84.5805
8.9	0.0174	0.0116	83.6	0.0195	83.5805
3.9	0.0196	0.013067	83.2	0.0195	83.1805
2.7	0.0213	0.0142	83	0.0195	82.9805
10.4	0.0302	0.020133	81.9	0.0195	81.8805
2.8	0.0341	0.022733	81.7	0.0175	81.6825
3.2	0.0368	0.024533	81.3	0.016	81.284
12.5	0.0472	0.031467	80.1	0.0148	80.0852
2.7	0.05	0.033333	79.9	0.0148	79.8852
3.2	0.0532	0.035467	79.6	0.0148	79.5852
14.3	0.0657	0.0438	78.4	0.0148	78.3852
3.2	0.0684	0.0456	78	0.015	77.985
4.1	0.0716	0.047733	77.7	0.0155	77.6845
0	0.0859	0.057267	79.2	0.0155	79.1845
3.4	0.0891	0.0594	78.8	0.0155	78.7845
21	0.0932	0.062133	76.7	0.0155	76.6845

3.9	0.0932	0.062133	76.3	0.0155	76.2845
4.2	0.0966	0.0644	75.8	0.0155	75.7845
19.1	0.1176	0.0784	74	0.0155	73.9845
4.7	0.1215	0.081	73.7	0.0155	73.6845
4.2	0.1257	0.0838	73.5	0.0155	73.4845
21.8	0.1448	0.096533	71.6	0.0155	71.5845
5.4	0.1495	0.099667	71.2	0.0155	71.1845
5.3	0.1537	0.102467	70.8	0.0155	70.7845
23.6	0.1755	0.117	69	0.0155	68.9845
5.4	0.1809	0.1206	68.7	0.155	68.545
5.1	0.1862	0.124133	68.3	0.0155	68.2845
24.5	0.2098	0.139867	66.5	0.012	66.488
6.6	0.2152	0.143467	66.1	0.0088	66.0912
5	0.2203	0.146867	65.6	0.0088	65.5912
23.3	0.2448	0.1632	63.8	0.0088	63.7912
6.5	0.2514	0.1676	63.3	0.0088	63.2912
6.4	0.2564	0.170933	62.8	0.0088	62.7912
29.9	0.2797	0.186467	60.2	0.0088	60.1912
9.3	0.2862	0.1908	59.2	0.0088	59.1912
9.1	0.2926	0.195067	58.3	0.0088	58.2912
6	0.3225	0.215	57.4	0.0088	57.3912
27.2	0.3318	0.2212	53.4	0.0088	53.3912
6	0.3409	0.227267	52.3	0.0088	52.2912
4.7	0.3469	0.231267	51.2	0.0088	51.1912
28	0.3741	0.2494	45.9	0.0088	45.8912
4.1	0.3801	0.2534	44.9	0.0089	44.8911
5.9	0.3848	0.256533	43.4	0.0089	43.3911
27.2	0.4128	0.2752	36.7	0.0089	36.6911
5.4	0.4169	0.277933	35.5	0.0089	35.4911
5.2	0.4228	0.281867	34.3	0.0089	34.2911
0	0.45	0.3	32.5	0.0092	32.4908
27.4	0.4554	0.3036	27.1	0.0092	27.0908
9.9	0.4606	0.307067	25	0.0092	24.9908
8.1	0.4606	0.307067	24	0.0092	23.9908
5.1	0.488	0.325333	23.2	0.0092	23.1908
21.2	0.4979	0.331933	20	0.0092	19.9908
7.3	0.506	0.337333	18.9	0.0092	18.8908
7.2	0.5111	0.340733	17.9	0.0092	17.8908

25.3	0.5323	0.354867	15.4	0.0093	15.3907
5.6	0.5396	0.359733	14.8	0.0093	14.7907
7.7	0.5468	0.364533	13.9	0.0094	13.8906
0	0.5721	0.3814	13.9	0.0313	13.8687
27	0.5777	0.385133	11.3	0.0313	11.2687
7.8	0.5854	0.390267	10.5	0.00313	10.49687
6.7	0.5854	0.390267	10	0.0292	9.9708
0	0.6124	0.408267	8.4	0.0185	8.3815
7.1	0.6202	0.413467	8	0.0185	7.9815
17.7	0.6269	0.417933	7.35	0.0185	7.3315
7.9	0.6269	0.417933	6.95	0.0185	6.9315
5.8	0.634	0.422667	6.7	0.0185	6.6815
20.2	0.6517	0.434467	5.85	0.0185	5.8315
6.9	0.6596	0.439733	5.65	0.0185	5.6315
7.1	0.6654	0.4436	5.3	0.0185	5.2815
20.2	0.6856	0.457067	4.65	0.0185	4.6315
9.2	0.6925	0.461667	4.4	0.0185	4.3815
6	0.6996	0.4664	4.18	0.0185	4.1615
19.1	0.7198	0.479867	3.75	0.0185	3.7315
0	0.729	0.486	3.75	0.0095	3.7405
5.9	0.735	0.49	3.61	0.0095	3.6005
5.6	0.7541	0.502733	3.48	0.0095	3.4705
21.8	0.7541	0.502733	3.08	0.0094	3.0706
6.1	0.76	0.506667	2.88	0.0092	2.8708
5	0.7656	0.5104	2.81	0.0092	2.8008
20.1	0.7874	0.524933	2.52	0.0092	2.5108
5.5	0.7935	0.529	2.44	0.0092	2.4308
5.4	0.7985	0.532333	2.34	0.0092	2.3308
0	0.8186	0.545733	2.1	0.0092	2.0908
21.1	0.8241	0.5494	1.85	0.0092	1.8408
7.4	0.8295	0.553	1.78	0.0092	1.7708
5.5	0.8295	0.553	1.72	0.0092	1.7108
26.9	0.8506	0.567067	1.49	0.0092	1.4808
6.4	0.858	0.572	1.43	0.0092	1.4208
6.9	0.8635	0.575667	1.39	0.0092	1.3808
25.3	0.8904	0.5936	1.21	0.0092	1.2008
6.7	0.8968	0.597867	1.17	0.0092	1.1608
5.8	0.9037	0.602467	1.11	0.0092	1.1008

27.1	0.929	0.619333	0.95	0.0092	0.9408
0	0.9357	0.6238	0.93	0.0109	0.9191
8	0.9415	0.627667	0.87	0.0109	0.8591
5.3	0.9686	0.645733	0.84	0.0109	0.8291
25.1	0.9686	0.645733	0.75	0.0109	0.7391
7.9	0.9766	0.651067	0.71	0.0109	0.6991
4.8	0.9819	0.6546	0.68	0.0109	0.6691
25	1.007	0.671333	0.59	0.0113	0.5787
5.5	1.0149	0.6766	0.57	0.0117	0.5583
5.3	1.0197	0.6798	0.53	0.0117	0.5183
25.9	1.0447	0.696467	0.45	0.0113	0.4387
6.5	1.0502	0.700133	0.44	0.0113	0.4287
7.2	1.0555	0.703667	0.43	0.0113	0.4187
29	1.0814	0.720933	0.37	0.0112	0.3588
14.3	1.0879	0.725267	0.345	0.0112	0.3338
13.2	1.0951	0.730067	0.325	0.0112	0.3138
39.4	1.1241	0.7494	0.265	0.0112	0.2538
15.8	1.1384	0.758933	0.25	0.0112	0.2388
18.7	1.1516	0.767733	0.225	0.0112	0.2138
51.1	1.191	0.794	0.175	0.0121	0.1629
20.6	1.2068	0.804533	0.16	0.0121	0.1479
14.6	1.2255	0.817	0.152	0.0119	0.1401
68.9	1.2766	0.851067	0.113	0.0121	0.1009
19.8	1.2972	0.8648	0.104	0.0124	0.0916
18.2	1.3118	0.874533	0.095	0.0109	0.0841
78	1.3807	0.920467	0.068	0.0114	0.0566
22	1.4005	0.933667	0.0625	0.0113	0.0512
25.2	1.4187	0.9458	0.0585	0.0113	0.0472
76	1.4967	0.9978	0.0455	0.0113	0.0342
30.7	1.5187	1.012467	0.0429	0.0113	0.0316
25.4	1.5439	1.029267	0.039	0.00112	0.03788
95.5	1.6199	1.079933	0.0312	0.0113	0.0199
37.2	1.6506	1.1004	0.0288	0.0112	0.0176
32.9	1.676	1.117333	0.027	0.0112	0.0158
127	1.7715	1.181	0.0215	0.0107	0.0108
138	1.8087	1.2058	0.019	0.0112	0.0078
209	1.8416	1.227733	0.0169	0.0113	0.0056
267.3	1.9686	1.3124	0.0154	0.0114	0.004

407	2.1066	1.4044	0.0143	0.0116	0.0027
530.3	2.3156	1.543733	0.0137	0.0115	0.0022
571.6	2.5829	1.721933	0.0132	0.0115	0.0017
1064.5	2.9899	1.993267	0.0126	0.0113	0.0013
1307.2	3.5202	2.3468	0.0122	0.0113	0.0009
1654.5	4.0918	2.727867	0.0117	0.0109	0.0008

Test of visible laser diode
10/27/94
Light source: Oz subassembly:TOLD 9211 w/ singlemode fi
Detector: Skanamatic P33008 photodetector
Source current: 44 mA
P.D. bias voltage: 10.43 vDC

weight add'n (g)	weight sum (g)	concent. (g/l)	current (mA)	current LEDoff m	net current
air only		0	75.8	0.0133	
tank/water		0	73.1	0.0112	73.0888
0.0007	0.0007	0.0004667	73	0.0104	72.9896
0.0006	0.0013	0.0008667	72.9	0.0124	72.8876
0.0006	0.0019	0.0012667	72.9	0.0139	72.8861
0.0023	0.0042	0.0028	72.8	0.0146	72.7854
0	0.0042	0.0028	72.9	0.0158	72.8842
0.0035	0.0077	0.0051333	72.6	0.0162	72.5838
0.0014	0.0091	0.0060667	72.5	0.0147	72.4853
0.0023	0.0114	0.0076	72.2	0.0158	72.1842
0.0012	0.0126	0.0084	72.2	0.0158	72.1842
0.0163	0.0289	0.0192667	70.8	0.0138	70.7862
0.001	0.0299	0.0199333	70.8	0.0138	70.7862
0.0029	0.0328	0.0218667	70.6	0.0148	70.5852
0.0048	0.0376	0.0250667	70.3	0.0152	70.2848
0.015	0.0526	0.0350667	69.2	0.0152	69.1848
0.0138	0.0664	0.0442667	68.25	0.0144	68.2356
0.0015	0.0679	0.0452667	68.05	0.0144	68.0356
0.0019	0.0698	0.0465333	67.85	0.0144	67.8356
0.0016	0.0714	0.0476	67.8	0.0125	67.7875
0	0.0714	0.0476	67.7	0.0166	67.6834
0.0168	0.0882	0.0588	66.3	0.0325	66.2675
0.0025	0.0907	0.0604667	66.2	0.0325	66.1675
0.0036	0.0943	0.0628667	65.95	0.0325	65.9175
0.0041	0.0984	0.0656	65.4	0.0325	65.3675
0.028	0.1264	0.0842667	63.05	0.0285	63.0215
0	0.1264	0.0842667	63.3	0.0285	63.2715
0.0019	0.1283	0.0855333	63.1	0.0168	63.0832
0.0025	0.1308	0.0872	62.95	0.0168	62.9332
0.004	0.1348	0.0898667	62.65	0.0168	62.6332

0.0332	0.168	0.112	59	0.0124	58.9876
0	0.168	0.112	59.35	0.0175	59.3325
0.0399	0.2079	0.1386	53.25	0.0175	53.2325
0.005	0.2129	0.1419333	52.3	0.0175	52.2825
0.0042	0.2171	0.1447333	51.5	0.0175	51.4825
0.0036	0.2207	0.1471333	50.75	0.0175	50.7325
0.0481	0.2688	0.1792	39.05	0.0095	39.0405
0.0409	0.3097	0.2064667	27.1	0.0099	27.0901
0.0032	0.3129	0.2086	27	0.0099	26.9901
0.0033	0.3162	0.2108	26.35	0.0099	26.3401
0.0027	0.3189	0.2126	25.8	0.0099	25.7901
0.0363	0.3552	0.2368	19.85	0.0079	19.8421
0.0343	0.3895	0.2596667	15.4	0.0079	15.3921
0.0369	0.4264	0.2842667	11.65	0.0087	11.6413
0.0393	0.4657	0.3104667	8.79	0.0087	8.7813
0.0466	0.5123	0.3415333	6.23	0.0087	6.2213
0.0818	0.5941	0.3960667	3.73	0.0134	3.7166
0.0968	0.6909	0.4606	1.88	0.0095	1.8705
0.0991	0.79	0.5266667	1.045	0.0087	1.0363
0.1354	0.9254	0.6169333	0.494	0.0083	0.4857
1.0762	2.0016	1.3344	0.0145	0.0093	0.0052

Test of visible laser diode fiber collimator
mar2495
Light source: Oz sbasbly:TOLD 9211 (new) w/single
Detector: Skanamatic P33008 phototransitor
Source current: 44 mA
P.D. bias voltage: 10.33 Vdc

weight add'n (g)	weight sum (g)	concent. (g/l)	current (mA)	current LEDoff	net current
air only		-	-	-	-
tank/water		0	71.7	0.0248	71.6752
0.0059	0.0059	0.00393	71	0.0248	70.9752
0	0.0059	0.00393	70.8	0.0248	70.7752
0.0028	0.0087	0.0058	70.6	0.0248	70.5752
0	0.0087	0.0058	70.7	0.0248	70.6752
0.0022	0.0109	0.00727	70.6	0.0248	70.5752
0	0.0109	0.00727	70.7	0.0248	70.6752
0.0019	0.0128	0.00853	70.6	0.0248	70.5752
0	0.0128	0.00853	70.5	0.0273	70.4727
0.0192	0.032	0.02133	69.1	0.0273	69.0727
0.0042	0.0362	0.02413	68.9	0.0273	68.8727
0.006	0.0422	0.02813	68.5	0.0273	68.4727
0	0.0422	0.02813	68.7	0.0174	68.6826
0.0179	0.0601	0.04007	67.4	0.0174	67.3826
0.0072	0.0673	0.04487	67	0.0174	66.9826
0.0394	0.1067	0.07113	64.2	0.0174	64.1826
0.0088	0.1155	0.077	63.6	0.0174	63.5826
0.0394	0.1549	0.10327	60.7	0.0174	60.6826
0.0475	0.2024	0.13493	55.9	0.0134	55.8866
0.0745	0.2769	0.1846	43.5	0.0134	43.4866
0.0942	0.3711	0.2474	24.4	0.0134	24.3866
0.0087	0.3798	0.2532	23.4	0.0134	23.3866
0.0874	0.4672	0.31147	13.5	0.0134	13.4866
0.0897	0.5569	0.37127	7.85	0.0083	7.8417
0.0861	0.643	0.42867	4.63	0.0083	4.6217
0.0804	0.7234	0.48227	2.87	0.0076	2.8624
0	0.7234	0.48227	2.54	0.0069	2.5331
0.0804	0.8038	0.53587	1.63	0.0069	1.6231
0.0829	0.8867	0.59113	1.03	0.0069	1.0231

0.0925	0.9792	0.6528	0.62	0.0069	0.6131
0.1578	1.137	0.758	0.273	0.0068	0.2662
0.1522	1.2892	0.85947	0.132	0.0069	0.1251
0.1527	1.4419	0.96127	0.0653	0.0068	0.0585
0.1469	1.5888	1.0592	0.0374	0.0069	0.0305
0.1509	1.7397	1.1598	0.0224	0.0068	0.0156
0.1487	1.8884	1.25893	0.0159	0.0068	0.0091
0.1539	2.0423	1.36153	0.0122	0.0068	0.0054
0.1502	2.1925	1.46167	0.0104	0.0068	0.0036
0.1657	2.3582	1.57213	0.0093	0.0068	0.0025

Performance test of visible laser diode
feb0695
Light source: Oz sbasbly:TOLD 9211 (repaired) w/si
Detector: Skanamatic P33008 photodetector
Source current: 41.4 mA
P.D. bias voltage: 10.43 vDC

weight add'n (g)	weight sum (g)	concent. (g/l)	current (mA)	current LEDoff	net current
air only		0	74.4	0.034	74.366
tank/water		0	74.5	0.0211	74.4789
0.014	0.014	0.00933	73.5	0.0264	73.4736
0.013	0.027	0.018	73	0.0251	72.9749
0.0127	0.0397	0.02647	72.1	0.0261	72.0739
0.0205	0.0602	0.04013	70.5	0.0282	70.4718
0	0.0602	0.04013	71	0.0193	70.9807
0.0227	0.0829	0.05527	69.3	0.0185	69.2815
0.034	0.1169	0.07793	66.8	0.0184	66.7816
0.0365	0.1534	0.10227	63.8	0.0183	63.7817
0.0611	0.2145	0.143	57	0.0182	56.9818
0.0604	0.2749	0.18327	46.4	0.0182	46.3818
0.0595	0.3344	0.22293	33.6	0.0182	33.5818
0.0618	0.3962	0.26413	22.7	0.0142	22.6858
0.064	0.4602	0.3068	15.5	0.0142	15.4858
0.0718	0.532	0.35467	9.81	0.0146	9.7954
0.0765	0.6085	0.40567	6.08	0.0146	6.0654
0.1064	0.7149	0.4766	3.22	0.0135	3.2065
0.1132	0.8281	0.55207	1.74	0.0135	1.7265
0.122	0.9501	0.6334	0.885	0.0118	0.8732
0	0.9501	0.6334	0.685	0.0061	0.6789
0.1211	1.0712	0.71413	0.364	0.0066	0.3574
0.1728	1.244	0.82933	0.149	0.0066	0.1424
0.2482	1.4922	0.9948	0.0505	0.0069	0.0436
0.2909	1.7831	1.18873	0.0195	0.0068	0.0127
0.4307	2.2138	1.47587	0.0105	0.0069	0.0036

Test of visible laser diode fiber collimator
mar2895 with large area photodiode detector
Light source: Oz sbasbly:TOLD 9211 (new) w/single
Detector: E.G.&G. VTB 6061 photodiode
Source current: 44 mA
P.D. bias voltage: 10 Vdc

weight add'n (g)	weight sum (g)	concent. (g/l)	current (mA)	current LDoff(m	net current
air only		-	-	-	-
tank/water		0	0.29	0.0063	0.2837
0.0014	0.0014	0.00093	0.289	0.0062	0.2828
0.0015	0.0029	0.00193	0.287	0.0062	0.2808
0	0.0029	0.00193	0.285	0.006	0.279
0.002	0.0049	0.00327	0.283	0.0061	0.2769
0.0119	0.0168	0.0112	0.266	0.006	0.26
0	0.0168	0.0112	0.267	0.0059	0.2611
0.0105	0.0273	0.0182	0.255	0.0058	0.2492
0	0.0273	0.0182	0.256	0.0057	0.2503
0.0102	0.0375	0.025	0.244	0.00565	0.23835
0	0.0375	0.025	0.244	0.00545	0.23855
0.0017	0.0392	0.02613	0.2435	0.0055	0.238
0.0251	0.0643	0.04287	0.2185	0.00535	0.21315
0.02	0.0843	0.0562	0.201	0.00515	0.19585
0.0229	0.1072	0.07147	0.182	0.0051	0.1769
0.0026	0.1098	0.0732	0.18	0.005	0.175
0	0.1098	0.0732	0.179	0.0047	0.1743
0.0474	0.1572	0.1048	0.146	0.0048	0.1412
0.0581	0.2153	0.14353	0.114	0.00465	0.10935
0.053	0.2683	0.17887	0.0916	0.0046	0.087
0.0788	0.3471	0.2314	0.0656	0.0046	0.061
0.0861	0.4332	0.2888	0.0466	0.0046	0.042
0	0.4332	0.2888	0.0465	0.0045	0.042
0.0876	0.5208	0.3472	0.0333	0.0046	0.0287
0	0.5208	0.3472	0.0323	0.0045	0.0278
0.0833	0.6041	0.40273	0.0246	0.0045	0.0201
0	0.6041	0.40273	0.024	0.0045	0.0195
0.0806	0.6847	0.45647	0.0188	0.0044	0.0144
0	0.6847	0.45647	0.0187	0.00445	0.01425

0.0795	0.7642	0.50947	0.0143	0.00445	0.00985
0.0882	0.8524	0.56827	0.0118	0.00445	0.00735
0	0.8524	0.56827	0.0116	0.00435	0.00725
0.09	0.9424	0.62827	0.0096	0.00435	0.00525
0	0.9424	0.62827	0.00945	0.0043	0.00515
0.0803	1.0227	0.6818	0.0082	0.0042	0.004
0.0845	1.1072	0.73813	0.0073	0.0042	0.0031
0.0864	1.1936	0.79573	0.00655	0.00415	0.0024
0.0923	1.2859	0.85727	0.00605	0.0042	0.00185
0.0937	1.3796	0.91973	0.0056	0.00415	0.00145
0.0859	1.4655	0.977	0.0053	0.0041	0.0012
0	1.4655	0.977	0.0051	0.00395	0.00115
0.0882	1.5537	1.0358	0.00505	0.00405	0.001
0.0832	1.6369	1.09127	0.0048	0.0039	0.0009
0.1291	1.766	1.17733	0.0047	0.004	0.0007
0.146	1.912	1.27467	0.00455	0.004	0.00055
0.2589	2.1709	1.44727	0.00435	0.0039	0.00045
0	2.1709	1.44727	0.00435	0.0039	0.00045

Test of visible laser diode fiber collimator
with large area photodiode detector
Light source: Oz laser:TOLD 9211 w/NSG multimod
Detector: E.G.&G. VTB 6061 photodiode
Source current: 44 mA
P.D. bias voltage: 10 Vdc

weight add'n (g)	weight sum (g)	concent. (g/l)	current (mA)	current LDoff(m	net current
air only	0	0	1.1	0.0063	1.0937
tank/wat	0	0	0.918	0.0046	0.9134
0.0024	0.0024	0.0016	0.907	0.0047	0.9023
0.0024	0.0048	0.0032	0.8955	0.0046	0.8909
0.003	0.0078	0.0052	0.886	0.0046	0.8814
0	0.0078	0.0052	0.888	0.0046	0.8834
0.0054	0.0132	0.0088	0.867	0.0046	0.8624
0.005	0.0182	0.01213	0.848	0.0045	0.8435
0.005	0.0232	0.01547	0.829	0.00455	0.82445
0	0.0232	0.01547	0.8315	0.0045	0.827
0.0119	0.0351	0.0234	0.798	0.00455	0.79345
0.0096	0.0447	0.0298	0.7535	0.0046	0.7489
0	0.0447	0.0298	0.759	0.00635	0.75265
0	0.0447	0.0298	0.7595	0.0044	0.7551
0.0099	0.0546	0.0364	0.723	0.00435	0.71865
0	0.0546	0.0364	0.7285	0.0045	0.724
0.0098	0.0644	0.04293	0.6955	0.0045	0.691
0.019	0.0834	0.0556	0.6355	0.0045	0.631
0.0205	0.1039	0.06927	0.576	0.00465	0.57135
0.02	0.1239	0.0826	0.525	0.0046	0.5204
0.0188	0.1427	0.09513	0.4825	0.0046	0.4779
0.052	0.1947	0.1298	0.3805	0.00445	0.37605
0	0.1947	0.1298	0.3795	0.0039	0.3756
0.051	0.2457	0.1638	0.3005	0.0038	0.2967
0.0553	0.301	0.20067	0.232	0.00385	0.22815
0.1128	0.4138	0.27587	0.1425	0.0039	0.1386
0.0965	0.5103	0.3402	0.095	0.0039	0.0911
0.0983	0.6086	0.40573	0.06395	0.0038	0.06015
0.1086	0.7172	0.47813	0.04215	0.00375	0.0384
0.1347	0.8519	0.56793	0.02685	0.00375	0.0231

Test of visible laser diode fiber collimator

mar3095	with large area photodiode detector
Light source:	Seastar:TOLD 9215 w/NSG multimode fiber c
Detector:	E.G.&G. VTB 6061 photodiode
Source current:	44 mA
P.D. bias voltage:	10 Vdc

weight add'n (g)	weight sum (g)	concent. (g/l)	current (mA)	current LDoff(mA)	net current
air only	0	0	2.23	0.0062	2.2238
tank/water	0	0	1.677	0.00515	1.67185
0.0033	0.0033	0.0022	1.6515	0.00515	1.64635
0	0.0033	0.0022	1.6505	0.00515	1.64535
0.0023	0.0056	0.0037333	1.633	0.00515	1.62785
0	0.0056	0.0037333	1.6335	0.00515	1.62835
0.002	0.0076	0.0050667	1.62	0.00515	1.61485
0	0.0076	0.0050667	1.6255	0.00505	1.62045
0	0.0076	0.0050667	1.6235	0.00565	1.61785
0.0031	0.0107	0.0071333	1.602	0.00575	1.59625
0.0047	0.0154	0.0102667	1.5715	0.0057	1.5658
0.0055	0.0209	0.0139333	1.532	0.0057	1.5263
0.012	0.0329	0.0219333	1.4515	0.00565	1.44585
0.0106	0.0435	0.029	1.3815	0.00555	1.37595
0	0.0435	0.029	1.405	0.00495	1.40005
0	0.0435	0.029	1.408	0.00465	1.40335
0.0099	0.0534	0.0356	1.348	0.0049	1.3431
0.0194	0.0728	0.0485333	1.234	0.00495	1.22905
0.0202	0.093	0.062	1.113	0.00505	1.10795
0.0191	0.1121	0.0747333	1.0195	0.0045	1.015
0.0455	0.1576	0.1050667	0.8295	0.0046	0.8249
0.0468	0.2044	0.1362667	0.6695	0.0047	0.6648
0.0502	0.2546	0.1697333	0.531	0.0044	0.5266
0.0966	0.3512	0.2341333	0.347	0.00425	0.34275
0.1122	0.4634	0.3089333	0.2155	0.0042	0.2113
0.1121	0.5755	0.3836667	0.1325	0.0042	0.1283
0.1718	0.7473	0.4982	0.0679	0.0046	0.0633
0.1914	0.9387	0.6258	0.03555	0.00465	0.0309
0.2081	1.1468	0.7645333	0.01995	0.0043	0.01565
0.2505	1.3973	0.9315333	0.0125	0.0042	0.0083

0.2611	1.6584	1.1056	0.009	0.00415	0.00485
0.2881	1.9465	1.2976667	0.00755	0.0042	0.00335
0.3447	2.2912	1.5274667	0.00645	0.00415	0.0023
0.4172	2.7084	1.8056	0.00545	0.00375	0.0017

Performance test of VTB 6061 with amplifier and fiber bundle
04/17/95

Light source: Seastar:TOLD 9215 w/NSG multimode fib. coll.
Detector: E.G.&G. VTB6061 photodiode via fiber bundle
Source current: 44mA
Amplifier gain resistor: 5.17 kOhms

weight add'n (g)	weight sum (g)	concent. (g/l)	P.D. signal (mV)	P.D. signal LDoff(mV)	net signal (mV)
air only		-	-	-	-
tank/water		0.00000	4295.0	2.3	4292.7
0.0030	0.0030	0.00200	4220.0	2.3	4217.7
0.0000	0.0030	0.00200	4225.0	2.3	4222.7
0.0023	0.0053	0.00353	4210.0	2.3	4207.7
0.0000	0.0053	0.00353	4230.0	2.3	4227.7
0.0024	0.0077	0.00513	4180.0	2.3	4177.7
0.0000	0.0077	0.00513	4190.0	2.3	4187.7
0.0000	0.0077	0.00513	4170.0	2.3	4167.7
0.0053	0.0130	0.00867	4070.0	2.3	4067.7
0.0000	0.0130	0.00867	4075.0	2.3	4072.7
0.0059	0.0189	0.01260	3945.0	2.3	3942.7
0.0000	0.0189	0.01260	3955.0	2.3	3952.7
0.0058	0.0247	0.01647	3830.0	2.3	3827.7
0.0000	0.0247	0.01647	3845.0	2.3	3842.7
0.0125	0.0372	0.02480	3590.0	2.3	3587.7
0.0000	0.0372	0.02480	3580.0	2.3	3577.7
0.0109	0.0481	0.03207	3360.0	2.3	3357.7
0.0000	0.0481	0.03207	3380.0	2.3	3377.7
0.0133	0.0614	0.04093	3120.0	2.3	3117.7
0.0000	0.0614	0.04093	3125.0	2.3	3122.7
0.0206	0.0820	0.05467	2750.0	2.3	2747.7
0.0000	0.0820	0.05467	2730.0	2.3	2727.7
0.0238	0.1058	0.07053	2420.0	2.3	2417.7
0.0000	0.1058	0.07053	2320.0	2.3	2317.7
0.0227	0.1285	0.08567	2145.0	2.3	2142.7
0.0000	0.1285	0.08567	2155.0	2.3	2152.7
0.0529	0.1814	0.12093	1630.0	2.3	1627.7
0.0000	0.1814	0.12093	1635.0	2.3	1632.7
0.0496	0.2310	0.15400	1225.0	2.3	1222.7

0.0000	0.2310	0.15400	1205.0	2.3	1202.7
0.0494	0.2804	0.18693	920.0	2.3	917.7
0.0000	0.2804	0.18693	909.5	2.3	907.2
0.0868	0.3672	0.24480	579.0	2.3	576.7
0.0000	0.3672	0.24480	571.0	2.3	568.7
0.1044	0.4716	0.31440	334.0	2.3	331.7
0.0000	0.4716	0.31440	327.5	2.3	325.2
0.0961	0.5677	0.37847	202.5	2.3	200.2
0.0000	0.5677	0.37847	200.0	2.3	197.7
0.1506	0.7183	0.47887	97.5	2.3	95.2
0.0000	0.7183	0.47887	96.0	2.3	93.7
0.1527	0.8710	0.58067	48.0	2.3	45.7
0.0000	0.8710	0.58067	47.4	2.3	45.1
0.1558	1.0268	0.68453	25.3	2.3	23.0
0.0000	1.0268	0.68453	24.8	2.3	22.5
0.1663	1.1931	0.79540	13.9	2.3	11.6
0.0000	1.1931	0.79540	13.8	2.3	11.5
0.1560	1.3491	0.89940	8.6	2.3	6.3
0.0000	1.3491	0.89940	8.4	2.3	6.1
0.1583	1.5074	1.00493	5.6	2.3	3.3
0.0000	1.5074	1.00493	5.5	2.3	3.2
0.1599	1.6673	1.11153	3.4	2.3	1.1
0.0000	1.6673	1.11153	3.4	2.3	1.1
0.1536	1.8209	1.21393	2.8	2.3	0.5
0.0000	1.8209	1.21393	2.8	2.3	0.5

Performance test of TSL230 light-to-frequency chip
04/18/95
Light source: Oz Optics:TOLD 9211 w/sgl.md.fib.coll.
Detector: Texas Inst.Light intensity-to-frequency chip
Source current: 44 mA
Frequency counter: 1.0 sec. refresh rate

weight add'n (g)	weight sum (g)	concent. (g/l)	frequency (kHz)	frequency LDoff(kHz)	net frequency
air only		-	-	-	-
tank/water		0.00000	1174.000	0.260	1173.740
0.0025	0.0025	0.00167	1171.000	0.262	1170.738
0.0000	0.0025	0.00167	1165.500	0.262	1165.238
0.0023	0.0048	0.00320	1157.500	0.250	1157.250
0.0000	0.0048	0.00320	1156.500	0.250	1156.250
0.0028	0.0076	0.00507	1137.500	0.244	1137.256
0.0000	0.0076	0.00507	1142.000	0.244	1141.756
0.0074	0.0150	0.01000	1099.500	0.251	1099.249
0.0000	0.0150	0.01000	1088.500	0.259	1088.241
0.0046	0.0196	0.01307	1056.500	0.264	1056.236
0.0000	0.0196	0.01307	1061.000	0.262	1060.738
0.0046	0.0242	0.01613	1038.000	0.256	1037.744
0.0000	0.0242	0.01613	1047.000	0.232	1046.768
0.0000	0.0242	0.01613	1063.000	0.241	1062.759
0.0000	0.0242	0.01613	1053.500	0.246	1053.254
0.0053	0.0295	0.01967	1021.000	0.248	1020.752
0.0000	0.0295	0.01967	1026.000	0.244	1025.756
0.0097	0.0392	0.02613	960.000	0.240	959.760
0.0000	0.0392	0.02613	966.500	0.240	966.260
0.0100	0.0492	0.03280	918.000	0.262	917.738
0.0000	0.0492	0.03280	917.000	0.271	916.729
0.0101	0.0593	0.03953	862.000	0.268	861.732
0.0000	0.0593	0.03953	862.500	0.270	862.230
0.0194	0.0787	0.05247	766.000	0.281	765.719
0.0000	0.0787	0.05247	759.500	0.270	759.230
0.0214	0.1001	0.06673	670.000	0.284	669.716
0.0000	0.1001	0.06673	665.500	0.290	665.210
0.0236	0.1237	0.08247	578.000	0.297	577.703
0.0000	0.1237	0.08247	577.500	0.297	577.203

0.0520	0.1757	0.11713	417.000	0.308	416.692
0.0000	0.1757	0.11713	416.000	0.305	415.695
0.0524	0.2281	0.15207	301.000	0.311	300.689
0.0000	0.2281	0.15207	299.000	0.303	298.697
0.0501	0.2782	0.18547	218.000	0.319	217.681
0.0000	0.2782	0.18547	213.500	0.328	213.172
0.1015	0.3797	0.25313	115.000	0.346	114.654
0.0000	0.3797	0.25313	112.500	0.332	112.168
0.1110	0.4907	0.32713	57.350	0.333	57.017
0.0000	0.4907	0.32713	56.500	0.323	56.177
0.1036	0.5943	0.39620	30.400	0.335	30.065
0.0000	0.5943	0.39620	29.050	0.324	28.726
0.1939	0.7882	0.52547	9.960	0.336	9.624
0.0000	0.7882	0.52547	9.675	0.341	9.334
0.2017	0.9899	0.65993	3.620	0.356	3.264
0.0000	0.9899	0.65993	3.440	0.365	3.075
0.2011	1.1910	0.79400	1.580	0.381	1.199
0.0000	1.1910	0.79400	1.560	0.385	1.175
0.2049	1.3959	0.93060	0.920	0.385	0.535
0.0000	1.3959	0.93060	0.884	0.365	0.519
0.2126	1.6085	1.07233	0.644	0.374	0.270
0.0000	1.6085	1.07233	0.645	0.372	0.273
0.2032	1.8117	1.20780	0.544	0.372	0.172
0.0000	1.8117	1.20780	0.528	0.358	0.170
0.2024	2.0141	1.34273	0.478	0.361	0.117
0.0000	2.0141	1.34273	0.453	0.340	0.113
0.2032	2.2173	1.47820	0.444	0.360	0.084
0.0000	2.2173	1.47820	0.447	0.364	0.083

Performance test of TSL230 light-to-frequency chip
04/12/95
Light source: Seastar:TOLD 9215 w/NSG multimode fib. coll.
Detector: Texas Inst.Light intensity-to-frequency chip
Source current: 42 mA
Frequency counter: 1.0 sec. refresh rate

weight add'n (g)	weight sum (g)	concent. (g/l)	frequency (kHz)	frequency LDoff(kHz)	net frequency
air only		-	-	-	-
tank/water		0.00000	1165.000	0.131	1164.869
0.0025	0.0025	0.00167	1151.000	0.132	1150.868
0.0000	0.0025	0.00167	1149.000	0.129	1148.871
0.0018	0.0043	0.00287	1142.500	0.129	1142.371
0.0000	0.0043	0.00287	1143.000	0.121	1142.879
0.0017	0.0060	0.00400	1139.000	0.116	1138.884
0.0000	0.0060	0.00400	1136.500	0.120	1136.380
0.0050	0.0110	0.00733	1110.500	0.130	1110.370
0.0000	0.0110	0.00733	1112.500	0.126	1112.374
0.0044	0.0154	0.01027	1081.000	0.123	1080.877
0.0000	0.0154	0.01027	1085.000	0.122	1084.878
0.0049	0.0203	0.01353	1057.000	0.168	1056.832
0.0000	0.0203	0.01353	1037.500	0.143	1037.357
0.0090	0.0293	0.01953	983.500	0.157	983.343
0.0000	0.0293	0.01953	985.500	0.170	985.330
0.0101	0.0394	0.02627	934.500	0.238	934.262
0.0000	0.0394	0.02627	934.000	0.252	933.748
0.0097	0.0491	0.03273	876.000	0.200	875.800
0.0000	0.0491	0.03273	873.500	0.186	873.314
0.0188	0.0679	0.04527	785.000	0.187	784.813
0.0000	0.0679	0.04527	777.000	0.186	776.814
0.0203	0.0882	0.05880	695.500	0.226	695.274
0.0000	0.0882	0.05880	696.500	0.231	696.269
0.0219	0.1101	0.07340	615.500	0.221	615.279
0.0000	0.1101	0.07340	616.500	0.226	616.274
0.0494	0.1595	0.10633	468.000	0.218	467.782
0.0000	0.1595	0.10633	465.500	0.171	465.329
0.0000	0.1595	0.10633	454.000	0.159	453.841
0.0000	0.1595	0.10633	452.500	0.159	452.341

0.0519	0.2114	0.14093	338.000	0.160	337.840
0.0000	0.2114	0.14093	336.000	0.160	335.840
0.0594	0.2708	0.18053	241.500	0.160	241.340
0.0000	0.2708	0.18053	238.500	0.161	238.339
0.1052	0.3760	0.25067	133.000	0.162	132.838
0.0000	0.3760	0.25067	132.500	0.162	132.338
0.0946	0.4706	0.31373	79.200	0.162	79.038
0.0000	0.4706	0.31373	78.700	0.162	78.538
0.1090	0.5796	0.38640	42.600	0.163	42.437
0.0000	0.5796	0.38640	42.250	0.162	42.088
0.1920	0.7716	0.51440	15.100	0.163	14.937
0.0000	0.7716	0.51440	14.750	0.162	14.588
0.2017	0.9733	0.64887	5.075	0.163	4.912
0.0000	0.9733	0.64887	4.945	0.163	4.782
0.2045	1.1778	0.78520	1.890	0.164	1.726
0.0000	1.1778	0.78520	1.840	0.161	1.679
0.2033	1.3811	0.92073	0.798	0.162	0.636
0.0000	1.3811	0.92073	0.754	0.160	0.594
0.2044	1.5855	1.05700	0.391	0.143	0.248
0.0000	1.5855	1.05700	0.380	0.145	0.235
0.2031	1.7886	1.19240	0.252	0.139	0.113
0.0000	1.7886	1.19240	0.240	0.133	0.107
0.2062	1.9948	1.32987	0.189	0.132	0.057
0.0000	1.9948	1.32987	0.188	0.132	0.056
0.2066	2.2014	1.46760	0.164	0.130	0.034
0.0000	2.2014	1.46760	0.162	0.129	0.033

Test of TSL230 light-to-frequency chip
08/08/95

Light source: Seastar Optics TOLD9215 w/NSG m.m. fib coll
Detector: Texas Inst.Light intensity-to-frequency chip
w/ optical fiber bundle light guide
sensitivity X10; freq.div. /1
Source current: 42 mA
Frequency counter: 1.0 sec. refresh rate
Notes: collimator and bundle "index-matched" to cell
incident beam blocked inside cell

weight addition (g)	weight sum (g)	concent. (g/l)	frequency (kHz)	frequency LD blocked (kHz)	net frequency (kHz)
tank/water	0.0000	0.00000	943.500	0.025	943.475
0.0051	0.0051	0.00340	914.500	0.029	914.471
0.0000	0.0051	0.00340	915.000	0.022	914.978
0.0051	0.0102	0.00680	875.000	0.028	874.972
0.0000	0.0102	0.00680	843.000	0.028	842.972
0.0000	0.0102	0.00680	907.500	0.019	907.481
0.0086	0.0188	0.01253	872.500	0.019	872.481
0.0000	0.0188	0.01253	872.500	0.019	872.481
0.0000	0.0188	0.01253	842.000	0.020	841.980
0.0071	0.0259	0.01727	816.000	0.020	815.980
0.0000	0.0259	0.01727	804.500	0.023	804.477
0.0103	0.0362	0.02413	757.500	0.023	757.477
0.0000	0.0362	0.02413	745.500	0.024	745.476
0.0150	0.0512	0.03413	676.500	0.024	676.476
0.0000	0.0512	0.03413	686.000	0.023	685.977
0.0210	0.0722	0.04813	601.500	0.023	601.477
0.0000	0.0722	0.04813	589.500	0.023	589.477
0.0301	0.1023	0.06820	490.500	0.023	490.477
0.0000	0.1023	0.06820	485.000	0.024	484.976
0.0425	0.1448	0.09653	375.500	0.024	375.476
0.0000	0.1448	0.09653	375.000	0.025	374.975
0.0603	0.2051	0.13673	260.500	0.025	260.475
0.0000	0.2051	0.13673	259.000	0.029	258.971
0.0694	0.2745	0.18300	172.500	0.029	172.471

0.0000	0.2745	0.18300	170.500	0.029	170.471
0.0756	0.3501	0.23340	108.500	0.029	108.471
0.0000	0.3501	0.23340	107.500	0.030	107.470
0.0730	0.4231	0.28207	70.000	0.030	69.970
0.0000	0.4231	0.28207	68.850	0.033	68.817
0.0787	0.5018	0.33453	43.250	0.033	43.217
0.0000	0.5018	0.33453	42.700	0.036	42.664
0.0789	0.5807	0.38713	26.800	0.036	26.764
0.0000	0.5807	0.38713	26.520	0.035	26.485